The role of host and microbial factors in the pathogenesis of chronic schistosomiasis in mice

Thabo Rantanta Victor Mpotje

Thesis submitted to the University of Cape Town in fulfilment of the degree of Doctor of Philosophy.

Department of Pathology

Division of Immunology (Cytokine and Disease Group)

International Centre for Genetic Engineering and Biotechnology

Institute of Infectious Disease and Molecular Medicine

Faculty of Health Science

University of Cape Town

April 2021

Declaration

I, Thabo Rantanta Victor Mpotje, hereby declare that the work on which this thesis is based, is my original work and that neither the whole work nor any part thereof is being, has been, or is to be submitted for another degree in this or any other University.

This thesis/dissertation has been submitted to the Turnitin module (or equivalent similarity and originality checking software) and I hereby confirm that my supervisor has seen my report and any concerns revealed by such have been resolved with my supervisor.

Signature: Signed by candidate

Date: 16 April 2021

Acknowledgements

I would humbly like to acknowledge and show my genuine gratitude to everyone who has been part of my PhD journey. I am grateful to everyone who has taken part.

I thank all my funders, National Research Foundation, Merck, ICEB, UCT financial aid through Doctoral Research Scholarship award, Frank Forman Grant, and Harry Crossley Foundation.

I thank my supervisors, Prof. Frank Brombacher and Dr. Justin K. Nono, for their insightful and expert advice towards my project. They have brilliantly guided me with patience throughout my degree.

I thank, Ms Paballo Mosala, Dr. Nada Abdel Aziz, Mr Fungai Musaigwa, and Dr. Donald S. Kamdem, for the friendship and support they have granted me. They have extended their helping hands to assist me with some of my experiments.

I thank Dr. Donald Nyangahu for his expertise and assistance on 16S rRNA sequencing which enabled for a better characterisation of the Batf2 mice.

I thank Wendy Green, Zarinah Sonday, Munadia Ansarie, for all their technical and administrative support. Lizette Fick for helping with the histology work, and Rodney Lucas for animal work training.

I thank my fellow mentors and lab mates from the Brombacher group for their friendship and encouragement when I needed it the most.

I thank all my friends who have always been there for me when I needed it. They have helped me when I was feeling down and saw me through my struggles.

To my mother, Sarah Mofokeng and all my sister back home in QwaQwa for their patience and support throughout my studies. They have been my pillars throughout my entire journey.

A special thank you to my second family, the D'Altons, Robert, Lynnet, my best friend Jerrard, Josh and Taylor. They have all seen me through my struggles and were there to help me carry on without wavering.

I dedicate this work most specifically to Robert & Lynnet D'Alton, and my mother Sarah Mofokeng for all they have done for me. I am forever grateful.

Publications contributed.

Guler, R*., **Mpotje, T*.**, Ozturk, M., Nono, J. K., Parihar, S. P., Chia, J., Aziz, N. A., Hlaka, L., Kumar, S., Penn-Nicholson, A., Hanekom, W. A., Zak, D. E., Scriba, T. J., Suzuki, H., Brombacher, F. 2018. Batf2 differentially regulates tissue immunopathology in type 1 and type 2 diseases. Mucosal Immunology. **12**: 390 – 402.

Brombacher, T. M. Scibiorek, M., Berkiks, I., Moses, B. O. Ajonijebu, D. C., **Mpotje, T**., Brombacher, F. 2020. IFN-y of myeloid cells contributes to differentially modulate spatial learning and memory in the absence of interleukin-4 receptor alpha (IL-4Rα). *Brain, Behaviour, and Immunity*. **92**: 157–164. doi: 10.1016/j.bbi.2020.12.003.

Aziz, N. A*., Nono, J. K*., **Mpotje, T.,** Brombacher, F. 2018. The Foxp3+ regulatory T cell population Requires an intact IL-4Rα signaling to control inflammation during helminth infections. PLoS Biol. **16**(10): e2005850

Nono. J. K., Fu, K., **Mpotje, T**., Varrone, G., Aziz, N. A., Mosala, P., Hlaka, L., Kamdem, S. D., Daigen, Xu, Spangenberg, T., Brombacher, F. 2020. Investigating the antifibrotic effect of the antiparasitic drug Praziquantel in in vitro and in vivo preclinical models. *Scientific Reports*. **10**: 10638

Nono, J. K., Ndlovu, H., Aziz, N. A, **Mpotje, T.**, Hlaka, L., Brombacher, F. 2017. Host regulation of liver fibroproliferative pathology during experimental schistosomiasis via interleukin-4 receptor alpha. *PLOS Neglected Tropical Diseases*. **11**(8): e0005861.

Nono, J. K., Ndlovu, H., Aziz, N. A., **Mpotje**, T., Hlaka, L., Brombacher, F. 2017. Interleukin-4 receptor alpha is still required after Th2 polarization for the maintenance and the recall of protective immunity to Nematode infection. *PLOS Neglected Tropical Diseases*. **11**(6): e0005675.

Nono, J. K*., **Mpotje, T***., Mosala, P. Aziz, N. A., Musaigwa, F., Hlaka, L., Spangenberg, T., Brombacher, F. 2020. Effect of successive *Schistosoma mansoni* infection and praziquantel treatment cycles on susceptibility to reinfection and protection against pathology in the mouse model. Manuscript submitted for publication.

Hlaka, L., Ozturk, M., Chia, J. E., **Mpotje, T**., Nono, J. K., Jones, S., Simelane, S., Parihar, S. P., Roy, S., Suzuki, H., Brombacher, F., Guler, R. 2020. IL-4i1 regulates immune protection during Mycobacterium tuberculosis infection. Manuscript submitted for publication.

***equal contribution**

Table of contents

List of figures

List of tables

List of Abbreviations

Abx	**Antibiotic**
AP-1	**Activator protein 1**
AP	**Alkaline phosphatase**
APC	**Antigen presenting cell**
AST	**Aspartate aminotransferase**
Batf2	**Basic Leucine Zipper ATF-Like Transcription Factor 2**
BCA	**Bicinchoninic Acid Protein Estimation**
BSA	**Bovine serum albumin**
CAB	**Chromotrope 2R and aniline blue solution**
cDNA	**complementary DNA**
CD	**Cluster of differentiation**
CH	**Co-housing**
DC	**Dendritic cell**
ELISA	**Enzyme-linked Immunosorbent Assay**
Eosin	**Eosinophils**
FACS	**Fluorescent-activated cell sorter**
FITC	**Fluorescein isothiocyanate**
FCS	**Foetal calf serum**
FoxP3	**Forkhead box P3**
GATA3	**GATA-binding protein 3**
GAPDH	**Glyceraldehyde 3-phosphate dehydrogenase**
GM-CSF	**Granulocyte macrophage-colony stimulating factor**
H & E	**Hematoxylin and eosin**
HPRT	**Hypoxanthine-guanine phosphoribosyl-transferase**
IL	**Interleukin**
iFBS	**Inactivated fetal bovine serum**
IFN-γ	**Interferon-gamma**
iMat. Neut.	**Immature neutrophils**
IMDM	**Iscove's Modified Dulbecco's Medium**
mAbs	**Monoclonal antibodies**
MNV	***Murine norovirus***
MLN	**Mesenteric Lymph Node**
MHC	**Major histocompatibility complex**
Mph	**Macrophages**

Mt. Neut.	**Mature Neutrophils**
PBS	**Phosphate buffered saline**
PE	**Phycoerythrin**
PCR	**Polymerase chain reaction**
PMA	**Phorbol 12-myristate 13-acetate**
PNP	**4-Nitrophenylphosphate**
qRT-PCR	**Real-time reverse transcription PCR**
RBCs	**Red blood cells**
RNA	**Ribonucleic acid**
S. mansoni	***Schistosoma mansoni***
SEA	**Soluble egg antigen**
SPF	**Specific pathogen free**
T-bet	**T-box expressed in T cells**
TNF-α	**Tumour necrosis factor alpha**
Th	**T helper**
TGF-β	**Transforming growth factor beta**
TLR	**Toll-like receptors**
T-reg	**Regulatory T cell**
TSA	**Tryptic soy ager**
TSB	**Tryptic soy broth**
WT	**Wild type**

Abstract

There is burgeoning interest in the complex tripartite interplays between the commensal microbiota, host's genetic factors, and immune response during helminth infections which are still poorly understood. The study explores this relationship in the context of chronic schistosomiasis-driven pathology. In the first part of the thesis, removal of the host Basic Leucine Zipper ATF-Like Transcription Factor 2 (Batf2) gene in **129Sv** (**Batf2**$^{-/-}$) mice resulted in alteration of the intestinal microbial composition and reduced granulomatous inflammatory immune response. These changes associated with rescue from pre-mature mortality and improved fitness of **Batf2**$^{-/-}$ mice during chronic experimental schistosomiasis in relation to control wild type mice. The prolonged survival and reduced immunopathology were diminished by treatment with α-CD8 antibody highlighting the significance of CD8-expressing immune mediators during chronic Schistosomiasis. Transfer of the altered intestinal microbiota from **Batf2**$^{-/-}$ mice to wild type mice by co-housing was enough to rescue the latter from exacerbated granulomatous inflammation and prolonged their survival during chronic schistosomiasis. These observations suggest, for the first time, a central role of the host gut microbiota in decisively regulating the tissue immune response, the elicited pathology and host survival during schistosomiasis. To validate the robustness of this tripartite interaction during chronic schistosomiasis around the gut microbiota, the second part of the present work analysed two genetically identical murine models (C57BL/6) housed under two different specific Pathogen free environments (SPF1 and SPF2) and presenting differential susceptibility to chronic schistosomiasis. Our work revealed a higher susceptibility of **C57BL/6** mice from the SPF2 facility in relation to **C57BL/6** mice from the SPF1 facility. In confirmation with our first series of experiments, that demonstrated a central role of the host intestinal microbiota in regulating the immune responses, the pathology, and the survival of the host during schistosomiasis, the second series of experiments further presented an ameliorated immunological, pathological and vital prognosis of vulnerable SPF2 **C57BL/6** mice receiving the intestinal microbiota of more resistant **SPF1 C57BL/6** mice. Therefore, the study demonstrates the genetic regulation of gut microbiota which in turn, and/or in concert with the genetic make-up, influence the immunological, pathological, and vital host response during chronic schistosomiasis. The present work expands the conventional knowledge on schistosomiasis disease regulation and presents the gene-microbiota-immune-response interactome as a core piece of the regulatory machinery of this infection as exploitable to alter disease progression in the context of drug and vaccine development.

1. Literature review

1.1. Introduction to helminth infections

Helminths are a group of large and multicellular invertebrates that are either free-living or parasitic to other large organisms such as humans. They are characterised by having elongated, flat, or rounded bodies (CDC, 2016; Castro et al., 1996). There are three main types of helminths which are of clinical relevance to humans, and these include flatworms or **Trematodes**, tapeworms or **Cestodes**, and roundworms or **Nematodes** (CDC, 2016; Castro et al., 1996). These parasites are highly neglected tropical infectious agents which affect both human and animal health, mainly in developing countries that have limited resources (Hotez et al., 2008; WHO, 2012). The infections have roamed and parasitized humans since the era of humans' earliest known history and have influenced the course of mammalian life forms (Cox et al., 2002; Hotez et al., 2008). The helminth infections result in a disease burden which parallels those caused by well-known diseases such as malaria and tuberculosis globally (Hotez et al., 2008). They affect over 2 billion people worldwide resulting in morbidities that contribute to poverty and inadequate socioeconomic development (Wright et al., 2018; WHO, 2012). Given that helminth infections are frequently co-endemic with other infections such as malaria and HIV/AIDS, they therefore pose an additional indirect global threat in that they potentiate these disease conditions as well as tuberculosis (WHO, 2012; Hotez et al., 2008). They even reduce the effectiveness of vaccines used a range of infectious diseases (WHO, 2012). It is therefore crucial to develop and provide more resources through research to combat and ultimately reduce the global burden caused by the helminth infections.

1.2. Burden of Helminth infections

Helminth studies have received little attention compared to other major disease-causing agents such as HIV and Mtb, in that only about 1% of global funding is dedicated to research on these infections (Hotez et al., 2008), even though they also contribute to the global burden of diseases through enhanced poverty and morbidity (Hotez et al., 2006). One of the major impacts of helminth infections is on school-aged and pre-school children who most often harbour high numbers of intestinal worms and schistosomes. These infections lead to growth impairments, reduced physical fitness as well as impairment of cognition and memory from an early age (Crompton et al., 2002). The most surprising and poverty-fuelling economic consequence of these helminths is poor childhood educational performances, as well as reduced labour outcome

leading to continued disadvantaged communities (Miguel et al., 2003). Hookworms and schistosomiasis further impact on pregnancy by causing reduced birth weight, neonatal prematurity, as well as increased maternal morbidity and mortality (Christian et al., 2004).

1.3. Life cycle

1.3.1. General life cycle of Helminth infections

Helminth infections are unique in relation to other agents that are infectious such as viruses, bacteria, protozoa, and fungi, in that they develop and complete their life cycle in more than one host, and most of them, in their adult form are unable to replicate within human hosts, other than the *Strongyloides stercoralis* (Hotez et al., 2008; Grove et al., 1986). It is because of this replication feature that the prevalence of helminths should be considered together with the worm intensity/burden to assess the epidemiology of helminths (Hotez et al., 2008). The worm burden measures the number of infectious agents that an individual is exposed to, such as the number of eggs per gram of faeces or tissue for intestinal helminths and schistosomes, which are largely the cause of pathology in infected individuals (Anderson et al., 1982; Grove et al., 1986; Hotez et al., 2008).

1.3.2. Life cycle of *Schistosoma mansoni*

The *Schistosoma mansoni* (*S. manosni*), which is the model of infection used in the current study, develops within the mammalian host as well as in intermediate snail host of the genera *Biomphalaria* so they can complete their life cycle (CDC, 2019). The parasite's eggs which are eliminated through the host's faeces, hatch into miracidia in favourable conditions in an aquatic environment. These miracidia swim around in search of an intermediary snail host and gain entry to develop into sporocysts and then into cercaria. The cercaria which are infective to mammals, are then released from the snails and swim around searching for a human host. They enter the human hosts through the skin and shed their tails once inside to develop into schistosomulae. The schistosomulae then migrate using venous circulation to the lungs, then to the heart, and to the portal veins of the liver where they further develop into mature worms. The adult worms then migrate to the mesenteric venules where the female and male worms copulate resulting in the release of pathogenic eggs that are deposited to small venules of the perivesical and portal systems. Lastly, the eggs migrate to the lumen of the intestine where they will be expelled in the faeces of the human host (CDC, 2019).

1.4. Immune responses

1.4.1. General host immune responses to Helminth infections

It is crucial to understand and have knowledge of the helminths that develop within a human host, especially their developmental stages which are responsible for pathological changes that lead to morbidity and potentially to mortality (Castro et al., 1996). This will improve on strategies employed to design more effective drug candidates for the control of helminth infections. Considering this, it is also vital to note that the helminth parasites differ in their ability to induce pathogenesis in infected hosts. The trematodes which are leaf-shaped, are pathogenic in their egg, larva, and adult form, while the tapeworms and nematodes are more pathogenic in their larval and adult forms (Castro et al., 1996).

The presence of the pathogenic forms of the parasites induces a more dominant type 2 immune response that is also accompanied by Th1 and Th17 responses which all help in clearing the parasites from the infected host (Hotez et al., 2008, Hams et al., 2013). The dominant helminth-induced type 2 immune response is characterized by innate (i.e. eosinophils) and adaptive dominant Th2 immune responses that produce key inflammatory cytokines including IL-4, IL-5, IL-13, and IL-9 in the infected host (Fort et al., 2001; Dillon et al., 2004; McSorley et al., 2012), while the Th1 and Th17 responses contribute IFN-g, IL-12, TNF-alpha, and IL-17 inflammatory mediators (McSorley et al., 2012). Additionally, the humoral response through the production of IgE, and IgGs, also plays a significant role through their ability to recognize helminth antigens and help in the killing and clearance of the parasites from the infected host (LoVerde et al., 2019; McSorley and Maizels, 2012).

The inflammatory responses are mainly responsible for the expulsion of adult worms, help mediate survival of the infected host upon failure to clear the worms, and mediate a wound-healing fibro-pathological response that helps the host during chronic infection in order to help repair damaged tissues (Wynn et al., 2004; Loke et al., 2007; Finkelman et al., 2004; Hotez et al., 2008). Furthermore, the type 2 inflammatory immune response can help prevent survival of secondary infecting parasites (Voehringer et al., 2006), although this is not normally effective given that the clearance of worms even with the use of drugs, results in a memory immune response that fails to protect against re-infection (McSorley et al., 2012). The production of the inflammatory immune mediators further contributes to tissue immunopathology that results in symptomatic features that are characteristic of helminth

infections such as abdominal pain, diarrhoea, malnutrition, and impaired physical development (Caldas et al 2008; McSorley et al., 2012; WHO, 2020).

1.4.2. Immune responses to *Schistosoma mansoni*

In the case of *S. mansoni*, the host induces a variety of immune responses which result in development of granulomatous inflammation around the trapped eggs ultimately leading to hepato-splenomegaly (Caldas et al 2008). The infection induces several phases of Schistosomiasis disease as demonstrated in figure 1 with various arms of the host immune responses: (i) the initial dormant phase characterized by dominant Th1 response, (ii) the acute phase characterized by dominant Th2 response, (iii) as well as the chronic phase that is characterized by regulated inflammatory immune response and production of tissue repairing fibrosis (McSorley et al., 2012; LoVerde et al., 2019; Dunne and Cooke, 2005).

The initial phase of the infection begins from as early as 1 to 2 weeks upon detection of the migrating *S. mansoni* cercariae and this induces a dominant Th1 response which is characterized by the release of INF-γ and IL-12, persisting up to 4- or 5-weeks post infection (LoVerde et al., 2019). However, the response is not strong enough to cause any observable immunopathology, thus leading to the host being asymptomatic during this phase of infection (Hams et al., 2013; LoVerde et al., 2019; McSorley et al., 2012). As the infection progresses with the parasites maturing, mating, and releasing eggs within the host, the disease results in a temporary increase of pro-inflammatory Th1 response (TNF-a, INF-γ and IL-12). This contributes to the development of granulomatous inflammation that is mediated by the recruitment and aggregation of multicellular immune mediators such as the eosinophils, macrophages, neutrophils, CD4+ T cells, and immunoglobulins as depicted in figure 2 (Hams et al., 2013; LoVerde et al., 2019). The presence of the parasite eggs also induces an increase in Th2 response with the release of regulatory IL-10 cytokine that causes a decrease in Th1 response, and also results in the release of inflammatory cytokines including IL-4, IL-5, IL-9, and IL-13 which further potentiate the granulomatous inflammation (LoVerde et al., 2019; Hams et al., 2013). Although the type 2 response is more dominant, the host also induces other inflammatory immune mediators such as the pathogenic Th17 responses with the release of IL-17 cytokines contributing to the development of granulomatous inflammation (LoVerde et al., 2019).

As the infection progresses, the host further recruits fibroblasts which contributes to a gradual increase of fibrosis in the affected tissues (Hams et al., 2013). During week 7 to 8 post infection when the dominant Th2 is at its peak, the disease becomes more acute with well-formed granulomatous inflammation that, together with the Th2 response, help protect the host against the toxic *S. mansoni* eggs logged into tissues (Hams et al., 2013; LoVerde et al., 2019; Dunne and Cooke, 2005). Failure to mount a dominant Th2 response at this phase of infection predisposes the host to develop hepatotoxicity, endotoxemia, as well as severe cachexia that may all lead to mortality as demonstrated using animal models (LoVerde et al., 2019). The acute phase of infection often occurs in tourists and immigrants coming into endemic areas for Schistosomiasis and this is due to it being their first exposure to the infecting parasite (Caldas et al. 2008; LoVerde et al., 2019). The patients suffering from acute Schistosomiasis develop symptoms including malaise, fever, myalgia, eosinophilia, headache, fatigue, as well as abdominal pain (Caldas et al. 2008; LoVerde et al., 2019).

As the infection persists in the infected host from week 8 to 12, the dominant Th2 inflammatory response is modulated leading to significantly reduced granulomatous immunopathology surrounding the parasite eggs (LoVerde et al., 2019). At this point of infection, the newly released eggs also induce smaller granulomatous inflammation compared to the ones forming during the peak of acute schistosomiasis, and this is driven by well controlled antigen-specific T helper cells (LoVerde et al., 2019). Furthermore, the infection also induces a pathogenic Th17 that contributes to the development of the granulomatous inflammation through the release of IL-17 cytokines (Mbow et al. 2013). The modulated inflammatory immune response which also leads to reduced immunopathology is mediated through the action of IL-10 that is produced by alternatively activated macrophages and T regulatory cells (Rutitzky and Stadecker, 2011; Singh et al., 2005). It has been previously demonstrated that the IL-10 cytokine is very crucial to allow the transition of the disease from acute to chronic Schistosomiasis through modulation of the inflammatory immune responses in an infected host (Sadler et al., 2003). However, other studies have also suggested other key immune mediators that contribute to regulation of the immunopathology during Schistosomiasis, and these include the B cells as well as the type 1 CD8+ T cells (CD8+ IFN-y+ T cells) of which in their absence, the host succumbs to exacerbated granulomatous immunopathology (Jankovic et al., 1998; Pancreâ et al., 1999; Pedras-Vasconcelo and Pearce, 1996). The chronic phase of schistosomiasis through infection intensity, leads to a variety of disease outcomes (LoVerde et al., 2019). One form of the disease is known as intestinal Schistosomiasis which causes

intermittent abdominal pain, rectal bleeding, and diarrhoea with the symptoms correlated to the infection intensity (LoVerde et al., 2019). The second form of the disease is called hepatosplenic schistosomiasis which is a life-threatening disease that results in portosystemic shunting of venous blood, portal hypertension, severe hepatic as well as periportal fibrosis that leads to cirrhosis (LoVerde et al., 2019).

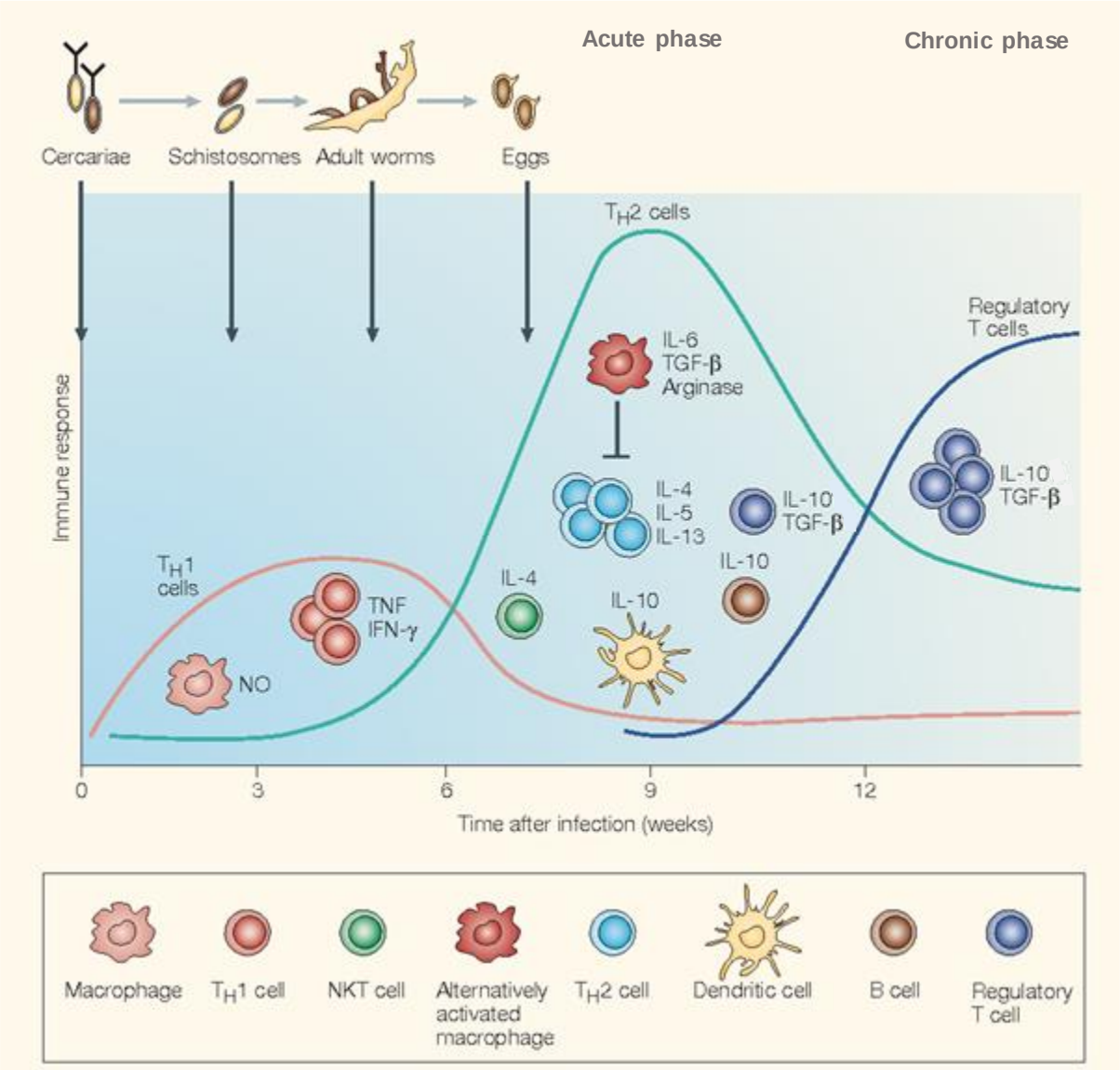

Figure 1: A graphical overview of the kinetics of the host immune response and *Schistosomiasis mansoni* disease. (Dunne & Cooke, 2005: Modified drawing by Dunne).

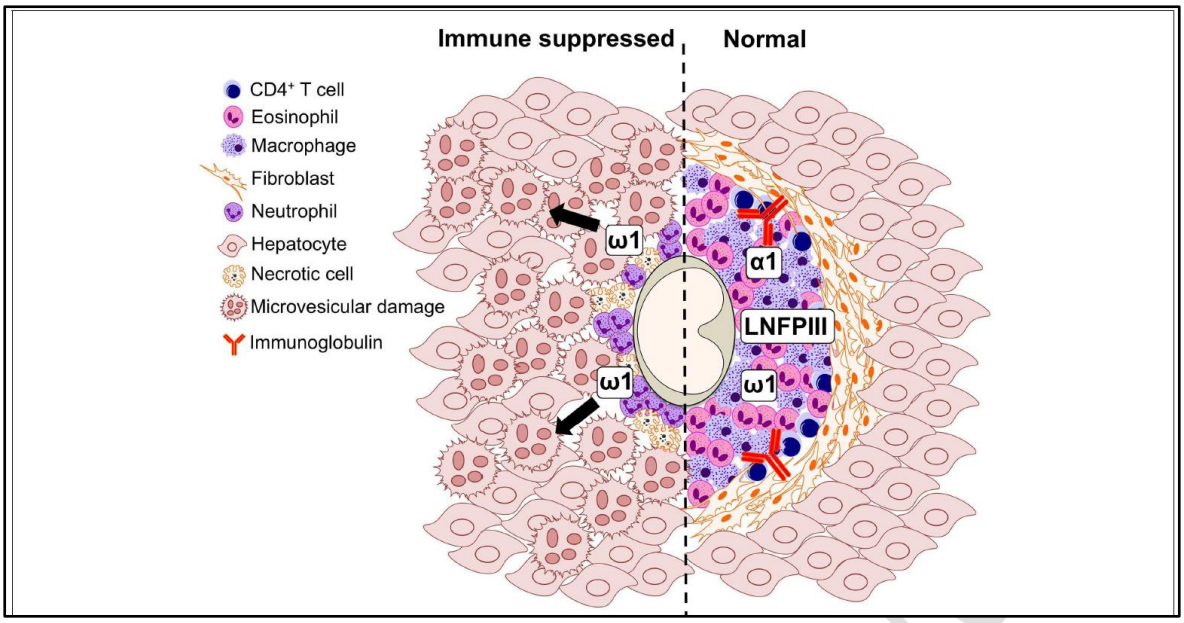

Figure 2: A graphical representation of type 2 granulomatous inflammation in response to *S mansoni* eggs. (Hams et al., 2013).

1.4.3. Development of immune tolerance during helminth infection

Immunosuppressive mediators which include IL-10, TGF-β, and the expansion of Foxp3+ T cells, all help keep the inflammatory immune responses in check to prevent exacerbated immunopathogenesis in an infected host (McSorley and Maizels, 2012). However, they also contribute a tolerogenic phenotype through their ability to suppress the pathogen-specific immunity resulting in prolonged survival of the infecting parasites within the host (McSorley and Maizels, 2012). The helminth infections have taken advantage of this feature to evade the immune response, favouring their survival in the infected host. The parasites modify the immune responses through their excretory and secretory products which interferes with the host's immunity from the point of pathogen recognition through to the end-stage effector mechanisms favouring a more suppressive Th2 response in the host leading to reduced Th1/Th17 responses (Hewitson et al., 2009). This feature of the helminths to manipulate immune responses predisposes the host to complications from other infectious pathogens that are normally controlled through the induction of Th1 immunity such as Mtb and HIV-1 which are also prevalent in disadvantaged areas where the helminths are present (Filbey et al., 2018; Hewitson et al., 2009; Walson and John-Stewart, 2012; Babu and Nutman, 2016). Therefore, the presence of helminths increases the susceptibility of the infected hosts to either HIV-1 or Mtb infection which further complicates conditions in already disadvantaged communities (Walson and John-Stewart, 2012; Babu and Nutman, 2016).

1.5. Control of helminth infections

1.5.1. General control of helminth infections

To overcome the complications caused by the helminths, global health systems such as the World Health Organization (WHO) have committed themselves to control and eradicate the parasites from endemic areas or in infected individuals through roadmaps and implementation of guidelines, policies and strategies that help combat these pathogens (WHO, 2012). Among the guidelines set out by the WHO, there are 6 key measures implemented for the control of helminth infections: 1, Intensified case-detection and case management - which focuses on principal strategies used for managing helminth infections that have no medicines to help prevent infection. This approach involves (i) early diagnosis of the pathogens, (ii) managing complications that are caused by the pathogen, (iii) providing treatment to reduce the infection and morbidity. 2, Vector and intermediate host control - which is one of the strategies employed using pesticides to control for insects or aquatic snails that serve as intermediary hosts that facilitate the transmission and persistence of the helminths in endemic areas. 3, Veterinary public health at the human-animal interface - this includes activities implemented at the human-animal interface which addresses human and animal health to help prevent, eliminate and control suffering as well as economic loss that is caused by the helminths. 4, Provision of safe water, sanitation, and hygiene – this includes programs aimed at providing safe and adequate water as well as ensuring appropriate sanitation in endemic areas since the helminths also thrive in poorly maintained environments. 5, Strengthening capacity to control helminths or rather neglected tropical diseases (NTD) - this focuses on providing essential skills that will help in effectively managing the national NTD control programmes that will address the limited expertise and knowledge needed in areas such as vector control, pesticide management, case management, as well as veterinary public health. 6, Preventative chemotherapy - which is aimed at using large-scale, single dose and safe medicines to significantly reduce extensive morbidities that result from the helminths infections. The approach makes use of larger scale administration of anti-helminthic medicines such as Praziquantel for use against Schistosoma and flukes (WHO, 2012; WebMD, 2019). Although this drug is widely used and effective at treating Schistosomiasis in infected individuals, it has limitations which include the induction of drug resistance in clinical settings, its mode of action is targeted at adult worms and not the pathogenic eggs which are responsible for the immunopathogenesis observed in infected individuals (Stelma et al., 1995; Ismail et al., 1999). The drug has also been reported to be ineffective in T or B cell deprived mice indicating that immunosuppressed individuals may be

at higher risk of succumbing to the Schistosomiasis-induced morbidity and potentially mortality especially in cases of co-infections (Sabah et al., 1985; Brindley et al., 1987). Furthermore, the individuals that are infected with helminths such Schistosoma develop chronic inflammatory disorders which result in delayed-onset pathology in infected hosts and unfortunately the drug treatment lacks the therapeutic potential to reverse schistosomiasis-induced pathology (Hotez et al., 2008; Nono et al., 2020). Therefore, complemental therapeutics or strategies aimed at reversing the helminth-induced pathology are required to enhance the protective mechanism against invading pathogens.

1.5.2. Host-directed-drug therapy for the control of helminth-induced immunopathology

The complementary strategies to deal with helminth-induced pathology are possible through host-directed therapy (HDT) which involves targeting of host molecules that are utilized by pathogens to survive in an infected host (Kaufmann et al., 2018). Such approaches have recently been more focused on research associated with bacterial and viral infections to overcome resistance against antimicrobial agents as well as to restrict host tissue damage (Kaufmann et al., 2018). There have also been recent advancements in the use of HDT in helminth infections targeting host factors to reverse and overcome helminth-induced pathology and protect the infected host (Nono et al., 2017; Andrews et al., 2006; Nono et al., 2017). Some of these advancements have extensively focused on understanding the role of the host IL-4Rα as a possible target for therapeutic invention in helminth infected individuals (Nono et al., 2017). This is because the IL-4Rα is an important mediator for type 2 immune responses that are critical to drive the control of helminth infections as well as associated immunopathology (Hams et al., 2013; LoVerde et al., 2019; Nono et al., 2017). The IL-4 and IL-13 are key cytokines which signals through this receptor to coordinate type 2 immune responses during helminth infections, and in the study by Nono et al., 2017, this receptor was demonstrated to be a crucial target for the regulation of liver fibroproliferative pathology as well as Th2 response in *Schistosoma mansoni* infected mice. Furthermore, the receptor was also demonstrated to be required to sustain and help recall the protective immunity to other helminth infections such as the Nematodes (Nono et al., 2017). Studies like these demonstrate the potential of using HDT as a complimentary strategy for the control of helminth infections and the resultant pathology.

Among the host factors with the potential to control *Schistosoma*-induced immunopathogenesis is the Basic leucine transcription factor 2 (Batf2). This transcription factor has recently gained

attention in both type 1 and type 2 diseases as a potential target for infectious diseases (Guler et al., 2018; Guler et al., 2015; Mpotje, 2017). The transcription factor belongs to a group of family members that contain basic leucine zipper domains which help them regulate and control the differentiation of immune cells and thus regulate various immunological functions (Guler et al., 2015). Furthermore, the Batf family members lack the transactivation domain and therefore need to form heterodimer with other transcription members that poses the transcription domain to be active (Murphy et al., 2013). They normally form heterodimers with members of the activator protein 1 (AP-1) regulatory domains such the JUN and FOS which have an additional carboxyterminal domain containing the transactivation domain that the Batf family members lack (Murphy et al., 2013).

The Batf2 is unique from the other Batf family members as it also has an additional carboxy terminal domain like other AP-1 family members (Murphy et al., 2013), hinting that the transcription factor may have more unexplored potential functions that may be crucial for therapeutic strategies against infections. The Batf2 was initially thought to be an AP-1 inhibitor given that it was demonstrated to prevent DNA binding of AP-1 complex molecules through the interaction with JUN protein leading to suppression of growth and apoptosis in tumour cells (Su et al., 2008; Liu et al., 2015). Furthermore, it was demonstrated to play a vital role of suppressing the expression of IL-23 leading to inhibited Th17 immunopathological response during *Trypanosoma cruzi* infection (Kitada et al., 2018). However, recent studies have also demonstrated the transcription factor to act as a transcriptional activator, especially in classically activated macrophages through interaction with IRF1 leading to increased inflammatory responses during mycobacterium infection (Roy et al., 2015). Given this role, the transcription was therefore, suggested as a potential biomarker and target for the development of host directed therapy against Mtb infections (Guler et al., 2015).

1.5.3. The role of Batf2 during acute Schistosomiasis

The study which preceded the current one, has also demonstrated the significance of Batf2 during acute Schistosomiasis (Mpotje, 2017). In the study, the transcription factor was shown to be crucial for the control of Schistosomiasis-induced inflammatory responses during the acute phase mainly in the small intestine leading to regulated small intestinal immunopathology that in turn promotes hosts survival during the infection. It was interesting to note that the absence of Batf2 resulted in increased fibro-granulomatous immunopathology in the small intestine but not the liver, and this indicated the potential of the transcription factor to have a

tissue specific role during Schistosomiasis (Mpotje, 2017). This phenomenon could potentially be attributed to a dimer it interacts with, either the JUN or IRF1 dimer which influences the batf2's role to act as either a suppressor or activator of transcription, depending on the disease (Guler et al., 2015; Murphy et al., 2013; Mpotje, 2017). Since the Batf2 plays a significant regulatory role during acute Schistosomiasis when the inflammatory immune response is more dominant and crucial to protect against the *S. mansoni* eggs (Hams et al., 2013; Mpotje, 2017), it is possible that the inflammatory response is regulated through the improved activity of Batf2 during chronic Schistosomiasis leading to reduced immunopathology. Considering what is known about the Batf2, the transcription factor could be a key target for therapeutic inventions for the control of infectious diseases, especially *Schistosoma mansoni* that has been demonstrated to be controlled through this transcription factor (Mpotje, 2017).

Since Batf2 acts as either an inhibitor or activator of transcription (Murphy et al., 2013), the choice of targeting the host factor will need to be disease specific. This means in the case of Mtb infection where the transcription factor is associated with inducing inflammatory responses against the bacteria (Roy et al., 2015), the design of a host-directed therapy based on Batf2 will be using drug candidates or compounds that bind to receptors such as Jak1/2, TLR2, or TLR4 which have been reported to induce activation of Batf2 (Roy et al., 2015). Alternatively, the Batf2 can be targeted using drug inhibitors which would block binding of the transcription to other heterodimers (IFR1 or JUN) to prevent transcriptional activation or suppression of a Batf2-target gene (Murphy et al., 2013) in diseases that are worsened by the presence of the transcription factor. Since Batf2 has dual roles during Schistosomiasis, the choice of targeting the transcription factor during the disease will need to be phase/time-dependent, i.e., Given that a previous study has demonstrated that the Batf2 is required during acute phase of Schistosomiasis (Guler et al., 2019) and not required during chronic Schistosomiasis, the drug inhibitors against Batf2 will need to be administered in hosts that have developed the chronic Schistosomiasis. On the other hand, hosts that have developed acute Schistosomiasis will need to be administered with drug inhibitors against natural competitors of Batf2 binding such as ATF-2 motif which would potentially allow for increased activity Batf2 (Guler et al., 2019; Kitada et al., 2017)

1.6. Commensal Microbiota

1.6.1. Introduction to microbiota

Mammalian hosts also harbour a variety of microorganisms comprised mainly of bacteria, viruses, fungi, and protozoans which all form the microbiota (Tlaskalová-Hogenová et al., 2011). This microbiota partakes to the induction of the immune response to protect from pathogens that invade hosts (Wu et al., 2012; Turnbaugh et al., 2006). The host develops a healthy relationship with the microbiota early in life leading to a well-maintained tissue homeostasis (Cardin et al., 2015). The bacteria, estimated to be around 3x 10^{13}, constitute a large number compared to other microbes and for this reason, most microbiome-wide association research studies (MWAS) have focused on understanding the composition and association of the bacteria in relation to disease within the host they inhabit (Sender, R. et al. 2016; Surana and Kasper, 2017). Furthermore, the microbiotas are generally symbiotic and help mediate metabolic functions which involves energy harvesting from food, therefore providing essential nutrients and vitamins such as amino acids and short-chain fatty acids to their hosts (Cardin et al., 2015). They also regulate physiological components such as the immune response as well as behaviour (Surana and Kasper, 2017).

1.6.2. Factors influencing microbiota composition.

The composition of microbial communities is believed to be initially shaped following maternal transmission during birth as foetuses are sterile *in utero*. However, there are studies which have reported the umbilical cord blood (Jime´nez et al., 2005), the placenta tissue (Aagaard et al., 2014), and amniotic fluid (Jime´nez et al., Bearfield et al., 2002; 2008; Rautava et al., 2012) as well as in foetal membranes (Steel et al., 2005; Rautava et al., 2012) to contain bacteria which all suggest that the *in utero* is not as sterile as previously believed (Martinez-Guryn et al., 2018; Rodrı´guez et al. 2015). The microbial community is therefore pioneered from the foetal development and is further influenced during birth, infancy, adult, and old age as depicted in figure 3 (Martinez-Guryn et al., 2018; Rodrı´guez *et al.* 2015). Moreover, during infancy the microbiota is influenced by several factors which include geographical location, environment, breastfeeding vs formula, genetics, complementary food, and duration of lactation (Rodrı´guez et al. 2015). In adults the composition of the intestinal microbiota is largely influenced by diet and lifestyle which, once established, remain relatively stable (Rodrı´guez et al. 2015). In elders, the composition is also influenced by diet and lifestyle, as well as medication as depicted in figure 3. However, the intestinal microbiota can be altered

by several factors which include lifestyle, infections, long-term changes in diet, as well as antibiotic treatment and medication (Rodrı´guez et al. 2015).

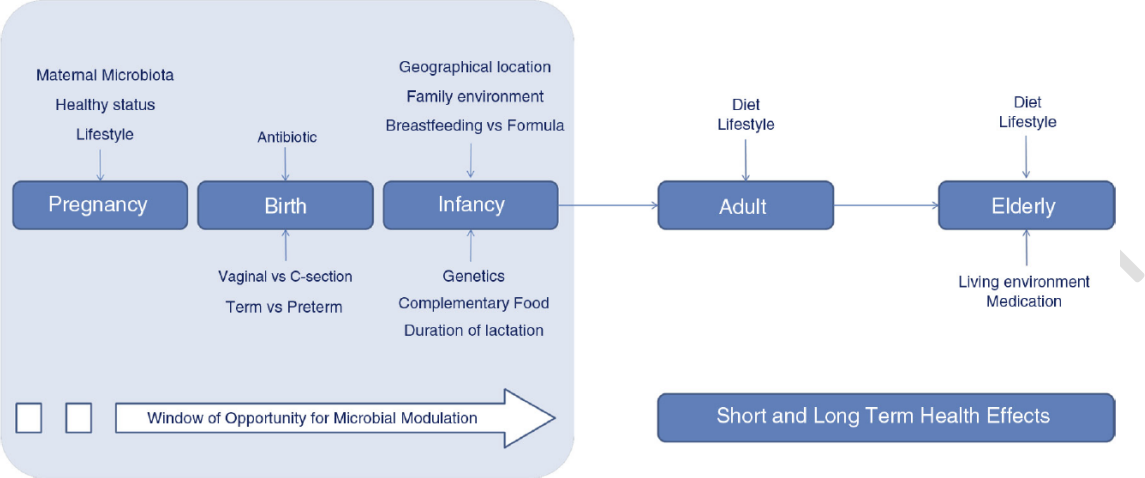

Figure 3. Development of intestinal microbiota in infants, adults, and elders (Rodrı´guez et al., 2015).

1.6.3. Association of host genetics and microbiota composition

Even though the composition of microbiota is predominantly affected by environmental factors, the Microbiome Genome-wide Association Studies (mMWAS) have demonstrated an association that exists between common traits (BMI or height) and many genetic variants in human host (Visscher et al., 2012; Weissbrod et al., 2018). They have also shown, using monozygotic (MZ) and dizygotic (DZ) twins that some bacterial taxa are heritable. All these suggests that the host genetics do in part influence the intestinal microbiota (Polderman et al., 2015; Goodrich et al., 2016; Wang et al., 2016; Turpin et al., 2016). Interestingly, a study by O'Connor et al, 2014, profiled 8 ancestral mice strains (129S1/SvImJ; C57BL/6J; A/J; NZO/HILtJ; NOD/ShiLtJ; PWK/PhJ; CAST/EiJ; WSB/EiJ) using 16 rRNA to compare the enteric microbial communities under the same diet as well under a different diet. Their studies revealed that some microbial communities were strain-specific and were even retained under different diets indicating that their presence was associated with the host genetics (O'Connor et al, 2014).

1.6.4. Influence of altered microbiota (Dysbiosis)

The alterations to microbial compositions, also termed as dysbiosis, are associated in many cases, with triggering local and systemic inflammation (Cardin et al, 2015; Marchesi et al., 2016). Within the intestine, dysbiosis results in severe disorders such as irritable bowel syndrome (IBS), inflammatory bowel disease (IBD), and coeliac, as well as other disorders

resulting from outside the intestine which include asthma, allergy, metabolic syndrome, obesity, and cardiovascular disease (Cardin et al., 2015). Although the composition of the microbiota which can be classified as healthy is not yet fully known – and appears to be disease-specific, many MWAS have shown that some species of bacteria are normally associated with healthy microbiota (Zaiss et al., 2015; Cardin et al., 2015) while some constitute unhealthy or bad microbiota (Blanton et al., 2016; Cardin et al., 2015). Some species of the bad microbiota have also been associated and implicated as potential biomarkers of disease (Surana and Kasper, 2017).

Given that the immune system has developed alongside the commensal microbiota, this co-existence has resulted in the development of a tolerogenic immune response that can tolerate the presence of the microbiota in a host (Reynolds et al., 2015). The host has also developed mechanisms which allows it to identify the presence of harmless, pathogenic and as well as beneficial microbes which enables an appropriate response to each type of microbe (Hooper et al., 2012; Reynolds et al., 2015). Tolerance to these microbes is achieved through activation of suppressive regulatory T cells which would inhibit Th1/Th17 effector responses against the microbes (Reynolds et al., 2015). The induction of the suppressive regulatory T cells is a common feature for both the microbiota as well as the intestinal helminth parasites to enable their colonisation within a host (Geuking et al., 2011; Yazdanbakhsh et al. 2001; Maizels and Smith, 2011). The presence of these microbes, both the microbiota and the helminths, have beneficial significance within the host in that they mediate amelioration of autoimmune diseases (Kostic et al., 2014; Wen et al., 2008; McSorley et al., 2012).

1.7. Association of Helminths and microbiota

Although the helminths may target and regulate the host immune response to ensure they survive, their presence also results in changes to the microbial composition and function (Reynolds et al., 2015). This was seen in studies that demonstrated that the chronic *H polygyrus* infection was able to induce an increase in abundance of bacterial species such as Enterobacteriaceae and Lactobacillaceae in the small intestine of mice (Reynolds et al., 2014; Walk et al., 2010; Rausch et al., 2013;). Similar studies have also shown chronic *Trichuris muris* infection to result in reduced bacterial diversity within the Bacteroidetes phylum and increased abundance in the *Lactobacillaceae* family members (Houlden et al., 2015; Holm et al., 2015). Schistosomiasis disease was also shown to induce a significant increase of bacterial

abundance from within the *Prevetella* genus in a cohort of children that were infected from Zimbabwe (Kay et al., 2015). Interestingly, treatment with anti-helminthic drugs did not have any effect on the microbial composition and this indicated that the parasites have long term effects on the changes in microbial composition (Kay et al., 2015). Furthermore, the presence of helminth infections also induces the release of excretory secretory products that influences an increase in production of antimicrobial peptides which alters the microbial compositions within a host (D'Elia et al., 2009; Su et al., 2014). Another important feature within the host is the induction of mucosal IgA from the lamina propria plasma cells, and it is responsible for the containment of the intestinal microbiota (Macpherson et al., 2012).

Conversely, the gut microbiota also helps the helminth infections allowing for their successful colonization within mammalian hosts (Hayes et al., 2010). This was shown using germ-free mice which resulted in less persistence of *H polygyrus* in relation to conventional mice, indicating the need for the commensal microbiota during the infection (Weinstein et al., 1969; Wescott, 1968). Furthermore, the use of antibiotic treatment in conventional mice even without reducing the microbial load, was enough to alter susceptibility of the mice to *H. polygyrus* (Reynolds et al., 2014). Some of the microbes have a beneficial relationship to the persistence of helminths and for this reason, the helminths themselves have developed mechanisms to selectively enhance for bacterial species that help promote their resistance within the host (Houlden et al., 2015; Holm et al., 2015). The beneficial microbes that are selected by the helminths can inhibit type 2 immune responses through TLR signalling pathways, thus allowing the survival of helminths in the host (Reynolds et al., 2012; Dea-Ayuela et al., 2008; Reynolds et al., 2014; Helmby and Grencis, 2003). The significance of the gut microbiota was also demonstrated during *Schistosoma mansoni* infection where administration of broad-spectrum antibiotics to reduce gut bacteria, resulted in reduced intestinal granulomatous inflammation even though the liver was not affected (Holzscheiter et al., 2014). The demonstrated that the commensal bacteria can act as bystander activators of the intestinal immune response during Schistosomiasis (Holzscheiter et al., 2014). All these highlight the significance of microbiota in contributing to health, therefore providing new attractive avenues to explore for generation of therapeutic strategies.

2. Aim and objectives of the study.

The aim of the study was to explore and identify the interrelationship between gut, the host genetic factor *Batf2* and the immune response during chronic Schistosomiasis. The first part of the project was focusing on understanding the interrelationship of a host genetic factor (*Batf2*) on both the microbiota and host immune response during chronic schistosomiasis using murine models. The second part of the project then focused further on the relationship between the microbiota and host's immune responses to chronic Schistosomiasis infection using murine models.

Part 1: The role of the Basic leucine zipper transcription factor ATF-like 2 (Batf2) in the regulation of immunopathology during chronic Schistosomiasis.

1. Assessment of Batf2 gene dynamics
2. Assessment of Batf2 gene deletion on susceptibility of mice during chronic Schistosomiasis
3. Assessment of intestinal microbiota in the absence of Batf2 on susceptibility of mice during chronic Schistosomiasis

Part 2: The role of the intestinal microbiota in the regulation of immunopathology during chronic Schistosomiasis.

1. Assessment of the susceptibility of genetically identical mice housed under two different specific-pathogen-free facilities.
2. Assessment of intestinal microbiota of genetically identical mice housed under two different specific-pathogen-free facilities.
3. Assessment of antibiotic treatment in resistant C57BL/6 mice during chronic Schistosomiasis.
4. Comparative analysis of the intestinal microbiota profiles of the genetically identical susceptible and resistant mice.

3. Materials and Methods

3.1. Ethics statement

Ethical clearance for use of experimental mouse models approved by the University of Cape Town Animal Ethics Committee was used to conduct all experiments outlined in the study under protocol numbers 018/029 and 016/027.

3.2. Mice

The mice that were used in the study were housed and maintained in specific pathogen-free facility using ventilated cages containing sterile wood shavings for bedding, in Biosafety level 2 (BSL2) facility of the University of Cape Town. Each cage was housing a maximum of 8 mice. The experimental work was conducted according to the recommendations from the University of Cape Town and South African national guidelines for use of procedures for handling of laboratory animals. All efforts were performed to reduce suffering on the animals. A total of 110 wildtype **C57BL/6** mice from a specific pathogen free 1 facility, 110 wildtype **C57BL/6** mice from a specific pathogen free 2 facility, and 220 of **129SvEV** (*Batf2*$^{+/+}$ and *Batf2*$^{-/-}$) mice purchased from the Jackson laboratory lab were used for the experiments. A sample size of 10 mice per group was utilized in each experiment with a percentage power of 95% and an effect size of 2.5 using a one tail t test. These were to potentially detect with confidence a difference between two independent means that will provide a significance level of $p < 0.05$ as calculated using a statistical tool called G. power 3.0.10 (Franz Faul, Universitat Kiel, Germany). Each experiment included both male and female mice aging between 7 and 10 weeks, and the animals were sex and age matched across each group of interest using an initial body weight of approximately 15 grams. Furthermore, the animals were subjected to the same food source containing a similar diet with a decontaminated water source.

3.3. Maintenance of *S. mansoni* life cycle

The *S. mansoni* parasites were maintained and expanded using both *Biomphalaria glabrata* snails and the **BALB/c** female mice which were monitored in a Bio-Safety level 2 facility, University of Cape Town.

3.4. Chronic *S. mansoni* infection

A total of 20 wildtype and 20 *Batf2* knockout mice were used for chronic mortality study. The mice were infected percutaneously with a low dose of 35 *S. mansoni* cercariae to establish a

chronic infection of Schistosomiasis which occurs from week 10 post infection. Mice were sex and age matched.

3.5. Study design

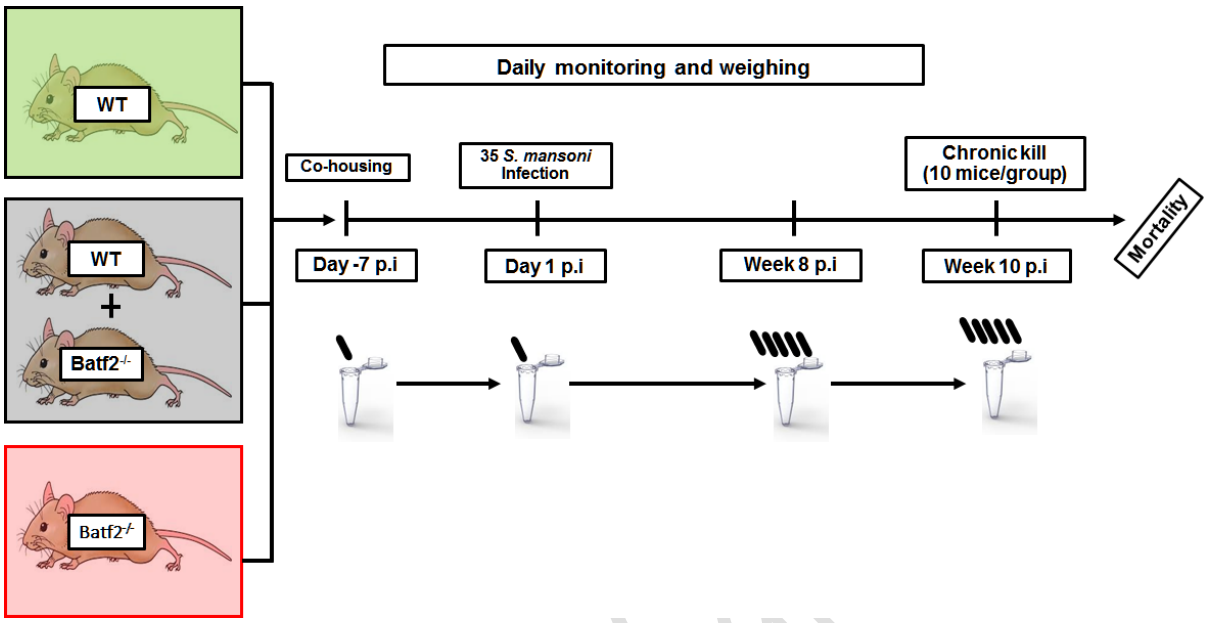

Figure 4: Establishment of faecal transfer between experimental (Batf2$^{-/-}$) and control WT groups, and induction of chronic Schistosomiasis infection using 35 live *S. mansoni* cercariae.

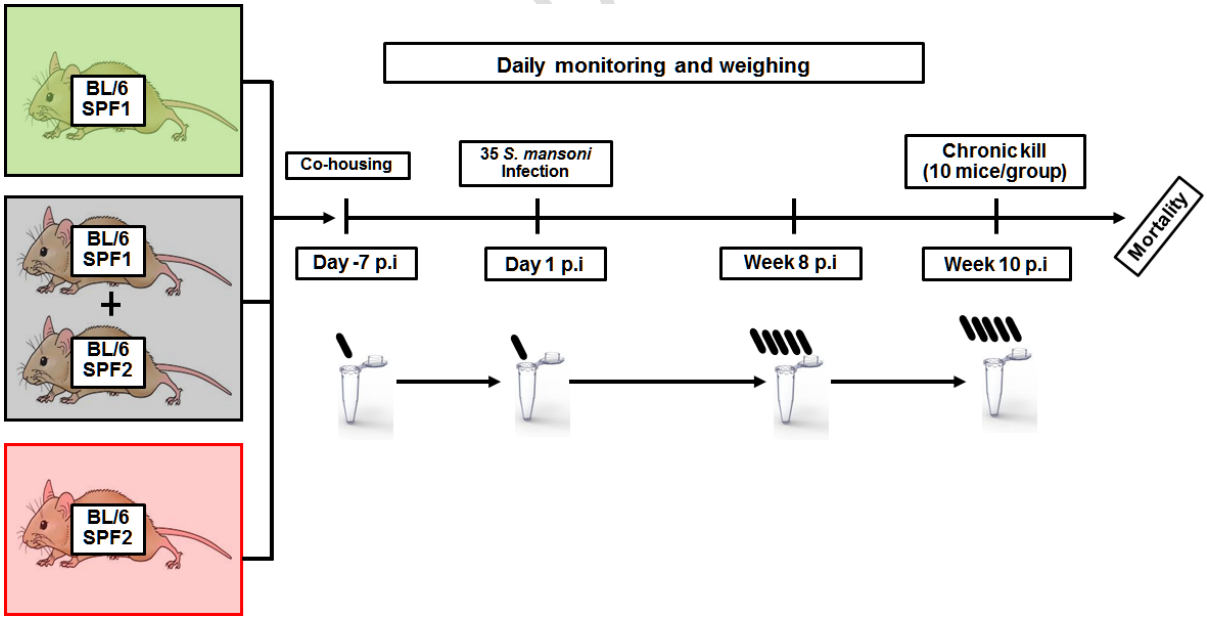

Figure 5: Establishment of faecal transfer between C57BL/6 mice from Specific Pathogen Free (SPF) 1 facility and those from SPF2 facility, and induction of chronic Schistosomiasis infection using 35 live *S. mansoni* cercariae.

The study was performed to include 4 groups as depicted in figure 4 and 5. Figure 4 shows an outline of (I) control group (Wildtype); (II) experimental group 1 (*Batf2*$^{-/-}$); (III) experimental group 2 (wildtype co-housed with *Batf2*$^{-/-}$); and experimental group 3 (*Batf2*$^{-/-}$ co-housed with wildtype). Figure 5 shows C57BL/6 from (I) Specific Pathogen Free 1 (SPF1) facility, (II) Specific Pathogen Free 2 (SPF2) facility, (III) SPF1 co-housed with SPF2, (III) SPF2 co-housed with SPF1. Faecal pellets were collected at 4 different time points (7 days prior infection, day 1, week 8, and week 10 post infection) to allow characterization of intestinal microbiota composition in each of the 4 groups mentioned above.

The primary experimental outcome assessed from the study was mortality of chronically infected mice. During the onset of the experiments the mice were monitored daily and weighed weekly until each mouse reached an experimental endpoint which was determined by loss of more than 20% body weight, and loss of strength as evidenced by inability to move or grip on metal bar cage.

The secondary experimental outcome assessed include behavioural and immunological changes where mice were euthanized during week 10 post infection and the following samples were collected for further analysis: Blood, liver, small intestine, mesenteric lymph node (MLN), and lung. Each of the experiments were independently conducted at least 2 times with a sample size of 10 mice per group in each experiment. The sample sizes were determined using G. power 3.0.10 statistical tool to detect significance level of $p < 0.05$.

3.6. Collection of samples and analysis

3.6.1. Blood collection from euthanized mice

Approximately 500 - 600µl of blood was drawn from each euthanized mouse using cardiac puncture with insulin syringe and collected using blood collection tubes (yellow capped tubes) containing anti-coagulant. The collected blood was centrifuged for 20 minutes at 8000 rpm to separate out serum from whole blood.

3.6.2. Egg count

From small intestine, liver and lung tissue

The worm burden from each mouse was calculated by quantifying the number of eggs present in each tissue affected by the *S. mansoni* parasites as follows; each tissue sample was first weighed and recorded prior to processing. The samples were then transferred into 15 mL falcon

tubes containing 5 mL of 5% potassium hydroxide (KOH) and incubated at 37°C incubator overnight. The samples were then centrifuged for 10 minutes at 2000 rpm and 3 mL of the supernatant was discarded for the small intestine and the lung to ensure a total volume of 2ml remained in each tube. The samples were then re-suspended by vortex. An aliquot of 50µl was used to calculate the number of *s. mansoni* eggs present in each sample using an inverted microscope. The total number of eggs in each sample was then calculated to determine egg burden.

3.6.3. Quantification of fibrosis levels in liver and small intestinal tissues

Hydroxyl-proline levels in small intestinal and liver tissues were quantified to determine the levels of fibrosis in the tissues. Each tissue sample was weighed and recorded prior to processing. The samples were then transferred into 15 mL falcon tubes containing 5 mL of 6M Hydrochloric acid (HCl) and were incubated overnight at 110°C incubator. The tubes were then topped up with distilled water up 10 mL and then mixed by vortex. From each sample 2 mL was filtered through a Whatman No.1 filter paper into a new 15 mL falcon tube and then a 1% of phenolphthalein in ethanol was added to the filtrate. A few drops of 10M sodium hydroxide (NaOH) were added into the filtrate until a colour change (from brown to pink) was observed, and then a few drops of 3M HCl were added to allow colour change back to light brown. The resulting titrate was topped up with distilled water up to 4 mL and 200µl of solution was transferred into a new 15 mL falcon tube. Hydroxyl-proline standards were prepared in a 2-fold dilution series using 9x15mL falcon tubes with a starting concentration of 200µg/ml. Four hundred microliters of isopropanol were added into all the tubes including the prepared standards and then mixed by vortex. Two hundred microliters of solution A were added, and the samples were then incubated at room temperature for 10 minutes. Furthermore, 2.5 mL of solution B was also added, and the samples were then added into a 60°C water-bath to incubate for 25 minutes. The samples were then immediately cooled on ice then an aliquot of 200µl from each sample was transferred into 96 well flat bottom plate (Nunc International, USA). The concentrations of hydroxyl-proline in each sample were determined by measuring the absorbance of the aliquoted samples on a wavelength of 558nm (excitation) and 570 nm (emission) using VERSAmax microplate reader.

3.6.4. Quantification of enzymes (ALT and AST) associated with tissue toxicity levels.

The serum samples obtained were diluted by 1:20 using sterile 0.9% Saline solution and then submitted to the National health Laboratory Services for further analysis on the levels of ALT and AST enzymes using commercially available Biochemical diagnostic kits BIO-LA-TEST (Erba Lachema s.r.o). Briefly, a 250µl of AST substrate (0,1 mol/l phosphate buffer at pH 7,4; 0,1 mol/l L-aspartate; 2 mmol/l 2-oxoglutarate) was added into Eppendorf tube and incubated for 3 minutes in 37 °C. Following the incubation, 50µl of serum sample was added while the control tube received 50µl of saline and were all incubated for 60 minutes in 37 °C. A 250µl of 2,4-DNPH was then added into sample & control tubes and were then allowed to stand for 20 minutes at room temperature. Lastly, 2.5ml of Sodium hydroxide was also added into the sample & control tubes and were then incubated at room temperature for 10 minutes. The absorbance of the samples was read at 510nm against the control tubes.

3.6.5. Histological analysis

The liver and small intestinal samples were fixed in neutral buffered formalin solution and then processed. About 5µm sections were stained with haematoxylin and eosin (H&E) or Chromotrope aniline blue (CAB) staining. The diameters of each granuloma that had a single egg were quantified using a computerized morphometry analysis program. The egg diameter was subtracted from the diameter of the whole granuloma. A total of 100 granulomas per group of mice were measured for analysis. Quantification of CAB from each tissue sample (Liver and small intestine) was determined using computerized morphometry analysis program to determine the intensity of each staining as a measure of tissue fibrosis.

3.6.6. Liver and small intestinal homogenate preparation for cytokine testing

The samples were thawed on ice and 500µl of extraction buffer (1X PBS buffer with 0.1% Tween and 0.02µm/ml of protease inhibitor) was added to each of the samples. The samples were then homogenized using 5mm stainless steel bead for 5 minutes with break intervals after each 30 seconds (10x 30 seconds) allowing the samples to be completely homogenized. Another 500µl of the extraction buffer was added and the samples centrifuged at 4800 rpm for 5 minutes in a 4°C. The supernatant was transferred into new labelled 2mL Eppendorf tubes and the protein content of each sample was quantified using BCA assay (Thermo Scientific, USA. Catalog number 23225) according to the manufacturer's instructions.

3.6.7. ELISA for cytokine measurement

Cytokine responses were measured in serum, liver, and small intestinal homogenates from non-infected and infected mice. Ninety-six well plates (Nalge Nunc International, USA) were coated with primary capture antibodies specific for each cytokine of interest. The capture antibodies diluted in 1X PBS buffer were used.

The plates were then incubated overnight in 4°C fridge, and then washed with wash buffer (20g KCl, 800g NaCl, 20g $KH_2HPO_4.2H2O$, 50ml Tween-20, dissolved in 5 litres, then diluted 1:20 in ddH2O) 3 times. About 200µl of blocking solution containing 2% of milk powder was added and then incubated for 2 hours in 37°C to block the coating antibodies. The plates were washed 5 times with wash buffer and then 50µl of samples were added together with recombinant standards for each cytokine tested into the plates. In the case of TGF-β, 48µl of samples plus 2µl of 1M HCl pH 3 was added and left to incubate for 1 hour in 4°C. The reaction was stopped by adding 2µl of 1M of NaOH. All the plates were incubated overnight in 4°C. The recombinant proteins were used as standards.

Following overnight incubation, the plates were again washed 5 times with wash buffer. Secondary biotinylated antibodies were then added to the appropriate plates for each of the test cytokines and the plates incubated for 2 hours in 37°C. The plates were then washed 5 times using wash buffer and then strep-avidin substrate conjugated with either alkaline phosphatase (AP) was added in 1/1000 dilution. The plates were then incubated in 37°C for 1 hour and then washed again 5 times using wash buffer. The plates were then developed by adding 1mg/ml of 4 Nitro-phenyl phosphate disodium salt hexahydrate (PNP) (Merck, Germany) diluted in AP substrate buffer into each well of the plates. The plates were incubated for 10 minutes in 37°C to allow for colour development in positive samples, and the optical density (OD) was quantified on a VERSAmax microplate reader (Molecular devices, USA) to determine the cytokine concentrations in each sample.

3.6.8. MLN single cell preparation for Flow cytometry analysis

Mesenteric Lymph Nodes were collected in 2 mL Eppendorf tubes containing 1mL of Iscove's Modified Dulbecco's Medium (IMDM) (Gibco, USA) that was supplemented with 10% heat inactivated Fetal Bovine Serum (iFBS) (Roche Diagnostics, Germany) and 0.5% Penicillin-Streptomycin (Pen-strep) (Gibco, USA). Each sample was teased through a 70µm sieve (Thermo Scientific, USA) on a petri-dish. The solution was collected and sieved further through 40µm sieve into a new labelled 50ml tube, and then topped up to 5ml total solution.

The samples were centrifuged for 10 minutes at 1200 rpm and the resultant supernatant was discarded. Five millilitres of medium (IMDM supplemented with 0.5% Pen-strep and 10% iFBS) was used to re-suspend the samples. The cells were then counted using 2% trypan blue using 1 in 20 dilution.

3.6.9. Liver, lung, and small intestinal single cell preparation for Flow cytometry analysis

Liver and small intestinal samples were initially collected in 15ml tubes containing ice-cold 5mL medium IMDM supplemented with 0.5% Pen-strep and 10% iFBS. The samples were placed on a petri-dish and chopped into small pieces then placed into 15ml tube containing 5mL digestion buffer (IMDM supplemented with 5% iFBS, plus 50 U/ml Collagenase I or II (Sigma, USA), plus 13µg/ml DNase (Thermo Scientific, USA). The samples were then placed inside a 37°C incubator with a shaker for 30 minutes. Following the incubation, the samples were sieved through a 100µm sieve on a petri-dish and sieved again through a 70µm sieve into a new labelled 50ml tube. The samples were again centrifuged at 1200 rpm for 10 in a 4°C and the supernatant was discarded. Three millilitres of 1X PBS + 3% foetal calf serum (FCS) was used to re-suspend the samples and 1.7ml of isotonic percoll (9ml percoll + 1ml of 10X PBS) was added, and then mixed thoroughly by inverting the tubes gently. The tubes were centrifuged at 500g in 4°C without brakes for 10 minutes. The supernatants were carefully removed from the tubes and 5ml of red blood cell (RBC) lysis buffer was used to re-suspend the samples, then incubated for 10 minutes at room temperature. Five millilitres of medium (IMDM supplemented with 0.5% Pen-strep and 10% iFBS) was added to the solutions and then centrifuged for 10 minutes at 1200 rpm in 4°C. The supernatants were carefully removed, and the samples were re-suspended in 1mL of medium (IMDM supplemented with 0.5% Pen-strep and 10% iFBS). The cells were quantified using 1 in 2 dilution with 2% of trypan blue.

3.6.10. Flow cytometry

From the single cell suspensions obtained, a total of 2 million cells in 200µl medium (IMDM supplemented with 0.5% Pen-strep and10% iFBS) was added into a V bottom 96 well plate (Nalge Nunc International, USA) and then centrifuged at 15 000 rpm for 5 minutes. The cells were then re-suspended in a staining antibody cocktail containing FACS buffer (0.02 % NaN_3 and 0.1% BSA in 1x PBS buffer), 2% heat inactivated rat serum (iRS), 1% FcγRIII plus surface antibody markers of interest. The samples were incubated for 30 minutes in 4°C fridge. Following incubation, 200µl of FACS buffer was added to wash the cells and then centrifuged at 15 000 rpm for 5 minutes. The supernatants were then discarded, and the samples were re-

suspended in 100µl of FACS buffer for acquisition on LSR Fortessa (BD Immuno-cytometry system, USA).

3.7. Anti-CD8 treatment/administration to Batf2$^{-/-}$ mice during chronic *S. mansoni* infection.

The WT and Batf2$^{-/-}$ mice were percutaneously infected with a dose of 35 S. *mansoni* cercariae to induce chronic Schistosomiasis. At the beginning of 7 weeks post infection, the Batf2$^{-/-}$ mice were treated with 200ug of α-CD8 antibodies 4x every 3rd day to neutralize the CD8+ T cells in the knockout mice. The study made used of an already well characterized, unequivocally specific and robustly established set of antibodies (Rolot et al., 2018) which were consistent with reported proceedings of the literature (Jung et al., 2018; Czuprynski and Brown, 1990; Adams et al., 1993; Cano et al., 2000). The mice were monitored until they reached the experimental endpoint. The α-CD8 treated Batf2$^{-/-}$ mice were compared to the untreated Batf2$^{-/-}$ mice during the chronic Schistosomiasis.

3.8. Bacterial community profiling

3.8.1. Serum bacterial profiling

The bacterial profile from serum samples were submitted to Biomedical Diagnostics (BioDoc, Germany) for serological analysis using Immunofluorescence Assay (IFA). Briefly, 20µl of each serum sample were fixed to multiwell microscope slide and fixed by heating for 20 minutes in 60 °C thermo-stated plate. Following the fixation, 20µl of diluted antiserum solution was applied to the window of each slide. The slides were first rinsed with IF-Buffer-Tween (0.1% Tween 20-, and 10-mM phosphate buffered saline (PBS) at pH 7.2) and then washed 2 times for 7 minutes using IF-Buffer (10 mM phosphate buffered saline (PBS) at pH 7.2). Sterile water was then used to rinse and remove excess moisture from the slides. The slides were applied with 20µl of secondary labelled antibody and were incubated for 30 minutes in the dark at room temperature. The slides were again rinsed with IF-Buffer-Tween, and then washed 2 times with IF-Buffer for 7 minutes. Once the slides were washed, 10µl of phosphate buffered glycerol were added into each window of the slides and a cover slip was applied. These slides were examined using an epifluorescence microscope.

3.8.2. Antibiotic treatment

SPF1 C57BL/6 mice were orally administered with an antibiotic cocktail containing 0.8mg of Amoxicillin 1.7mg of enrofloxacin, 2mg neomycin, and 2mg ampicillin dissolved in sterile

water which were previously reported to be effective at reducing broad spectrum of bacteria (Marx, et al., 2014; Bayer et al., 2019; Slate et al., 2014; Andes and Craig, 1998; Kennedy et al., 2018). The SPF1 C57BL/6 mice were given the cocktail for 14 days then followed by co-housing with the SPF2 C57BL/6 mice. Following the co-housing, the SPF1 C57BL/6 mice were further treated with the antibiotic cocktail for 7 days making a total of 21 days pf treatment for the SPF1 C57BL/6 to ensure reduction in bacterial growth as much as possible (Figure 6). Following the 21 days of antibiotic treatment, the mice were percutaneously infected with a dose of 35 live *S. mansoni* cercariae to establish a chronic infection and monitored until mice reached their experimental endpoint (Figure 6).

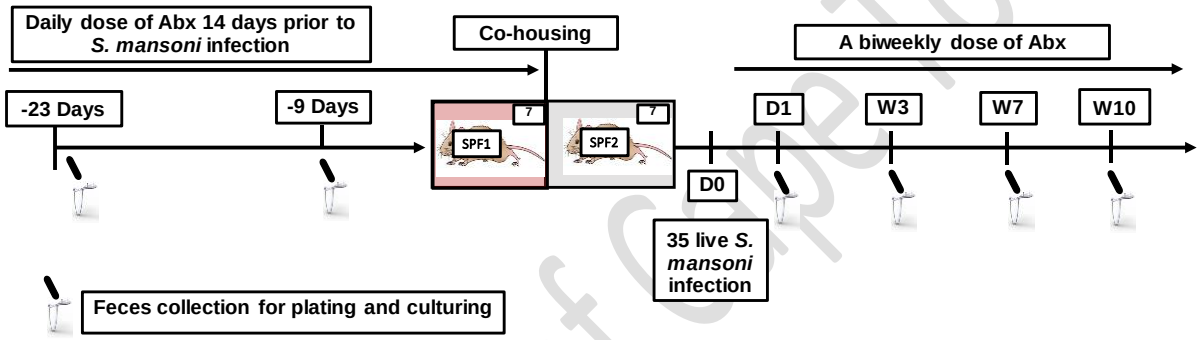

Figure 6: Figure illustrating the administration of antibiotic cocktail to SPF1 C57BL/6 mice before and following co-housing with SPF2 C57BL/6 mice.

3.8.3. Stool sample collection and DNA extraction

Faecal samples were collected freshly from mice 8 weeks after percutaneous infection with *S. mansoni* as these animals defecate and the faeces directly collected in tubes were immediately frozen at -20ºC until use. Bacteria DNA was extracted from the samples using commercially available kit, the Powersoil isolation kit (Mobio Laboratories). Briefly, each bacterial pellet weighing between 50 to 100mg was added into a **ZR BashingBead™** Lysis Tube (0.1 mm & 0.5 mm) containing 750µl BashingBead™ Buffer. The tubes were processed for 20 minutes using a bead beater. The tubes were then centrifuged for 1 minute at 10 000xg. From the resultant supernatant, 400µl was transferred to **Zymo-Spin™III-F Filter** in a Collection Tube and was then centrifuged at 8 000 xg for 1 minute. Following the centrifuge, 1200µl of Genomic Lysis Buffer was added to the filtrated in the collection tubes. From the mixture, 800µl was filtered through **Zymo-Spin™ IICR Column** in a collection Tube at 10 000 xg for

1 minute. This step was repeated twice while discarding the flow through. A 200µl of **DNA Pre-Wash Buffer** was filtered through **Zymo-Spin™ IICR Column** in a collection Tube at 10 000 xg for 1 minute. Following the wash step, 900µl **g-DNA Wash Buffer** was also filtered through **Zymo-Spin™ IICR Column** in a collection Tube at 10 000 xg for 1 minute. The **Zymo-Spin™ IICR Column** was transferred to a clean 1.5ml Eppendorf tube and the DNA was eluded from the column by filtering DNA Elution Buffer directly through the column matrix at 10 000 xg for 1 minute to elute the DNA. Final DNA concentration was quantified by the Picogreen dsDNA HS kit (Invitrogen, UK).

3.8.4. 16SrRNA gene sequencing

DNA sequencing targeting the V6 region was performed using extracted DNA. Briefly, the V6 hypervariable region which belongs to the 16S rRNA gene was multiplied using two step PCR procedure: the initial step involved barcoding of the samples while the following step involved adding Illumina paired-end sequencing adapters (Caporaso et al., 2011). The amplicons that were generated from the PCR were then purified using the Qiagen 96 well purification kit (Qiagen, CA). The Quanti-It dsDNA BR assay (Invitrogen, UK) was used to quantify the concentrations of the amplicons and 50ng from each was pooled together into one tube. The DNA which was pooled was then ran on A 1.5% agarose gel was used to run and visualize the pooled DNA. Using the gel purification kit (Qiagen, CA), a band of 330 bp was cut out carefully from the gel and purified. The final DNA concentration was then quantified, and sequencing of the libraries was done from both ends on the Illumina HiSeq platform.

3.8.5. Quantification of faecal bacteria

Faecal bacterial communities in antibiotic treated mice as well as control groups, were quantified using tryptic soy ager (TSA) plates as well as tryptic soy broth (TSB) media to assess the effectiveness of the antibiotic cocktail used in the study. The faecal bacterial communities in experimental groups were analysed to measure their differences in the test groups. A faecal pellet from each mouse was collected under sterile conditions into sterile 1.5ml Eppendorf tube. The weights of each pellet collected were measured to ensure each pellet is resuspended with appropriate volume of 1x PBS to obtain a concentration of 50mg/ml. The samples were mixed well using a P1000 pipette and 10ul of the suspension was transferred into a new Eppendorf tube containing 990ul sterile 1x PBS to make a 1/100 dilution from the suspension (figure 7). The plating was then done by adding 50ul of the 1/100 solution into a TSA plate and spread evenly across the plate under sterile conditions (figure 8). The plates were then

incubated for 16 hours in 37°C incubator. From each concentrate (50mg/ml suspension) of the initial tubes, 2x50ul were transferred into 2x15ml falcon tubes containing 2ml TSB media (figure 7). One falcon tube from each sample was allowed access to atmospheric oxygen by not closing the lid properly, while the other tube was deprived of oxygen by closing the lid properly. The samples were then incubated for 16 hours in a 37°C incubator with the oxygen fed tubes left on a shaker. Following the incubation, the OD of the TSB samples were measured at 640nm wavelength using a VERSAmax microplate reader (Molecular devices, USA).

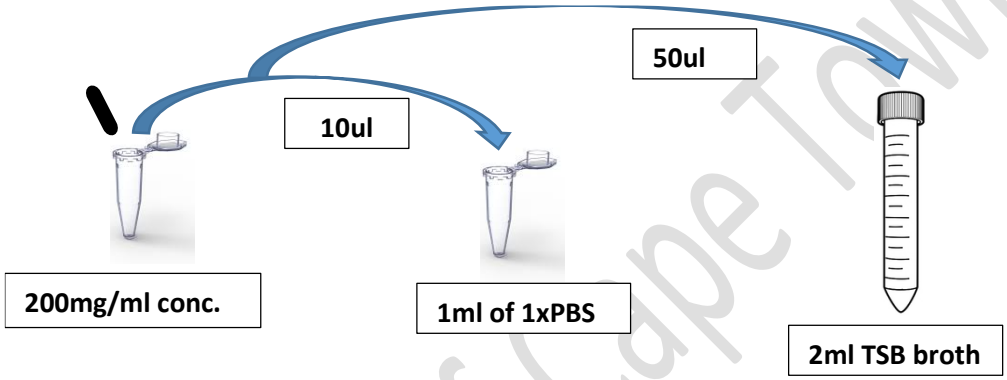

Figure 7: Preparation of faecal dilutions for plating and culturing in TSB media.

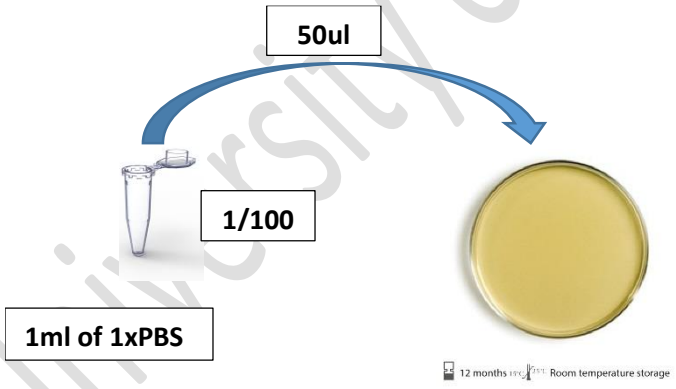

Figure 8: Plating of faecal bacteria on TSA plate.

3.9. RNA extraction

RNA extraction was done using RNA elute Column protocol (Qaigen kit). Briefly, 1ml of sample was supplemented with 200µl of chloroform and mixed vigorously by shaking up and down. The sample were then incubated at room temperature for 3 minutes. Again, the samples were vigorously mixed and then centrifuged at 10 000 rpm for 15 minutes in a 4°C microfuge.

A colourless upper aqueous layer was displaced into a new 2mL tube. Then 1mL of 70% ethanol was then added and mixed by pipetting up and down. Seven hundred microliters of the sample were transferred into a RNeasy spin column that was placed in 2mL collection tube. The samples were centrifuged at 10 000 rpm for 15 seconds and 700µl of RW1 buffer was added to the spin column placed in a clean 2mL collection tube. The samples were then centrifuged for 15 seconds at 10 000 rpm and 500µl of RPE buffer was added to the spin column. The samples were further centrifuged for 2 minutes at 10 000 rpm and the spin columns were transferred to clean 2mL tube. From the spin column, 30µl of nuclease free water was added and the samples were centrifuged at full speed for 1 minute. RNA was quantified using a nanodrop ND1000 (Thermo Scientific).

3.10. cDNA synthesis

Following the RNA extraction, cDNA synthesis was performed by reverse transcribing the RNA samples using Transcriptor First Strand cDNA Synthesis Kit (Roche). Random hexamer primer and anchored oligo dT primers were used to reverse transcribe the RNA samples according to the manufacturer's instructions. The mixture of template-primer was denatured through heating the tubes for 10 minutes at 65°C in a thermal block cycler (BioRad PTC-100), and then followed by first strand synthesis using the following conditions: 25°C for 10 minutes, 50°C for 60 minutes, 80°C for 5 minutes, and the PCR reaction was then be stopped by placing the tubes on ice for 5 minutes.

3.11. Quantitative Polymerase chain reaction

Real-time qPCR was performed using Light Cycler® 480 SYBR Green I Master mix in Light Cycler® 480 II (Roche). GAPDH was used as a housekeeping gene to normalise the expression of batf2. The primer sequences used were as follows, 5′-CTCCTCCTGTTCGACAGTCAGC-3′ (sense), and 5′-CCCAATACGACCAAATCCGTT-3′ (antisense) for GAPDH and 5′-AGACCCCAAGGAGCAACA-3′ (sense), and 5′-CTTTTTCCAGAGACTCGTGCT-3′ (antisense) for BATF2.

3.12. Statistical analysis

The sample size for each experiment performed in the study was a minimum of 6 mice per group, and this was determined based on the observation from previous experiments from our group which have shown a high variation between individuals within each group which made it difficult to pick differences unless a higher number was used per group. The selected sample

size gives an expected variability/variation of measured values of 30 with a statistical power of 0.8. The significance threshold was determined to be 0.05. The GraphPad Prism v 6.0 was used to analyse most data, and the statistical tests used included student t-distribution (one-tailed) for bar graphs, while the survival curves were analyzed using Log-rank (Mantel-Cox). Means were shown as ± SEM. *, ** and *** indicating $P < 0.05$, $P < 0.01$ and $P < 0.001$, respectively. The microbiota data were analysed using Wilcoxon rank and Kruskal-Wallis test and p values were adjusted using Benjamini-Hochberg false discovery rate (FDR) for multiple comparisons.

4. Part 1 of results:

The role of the Basic leucine zipper transcription factor ATF-like 2 (Batf2) in the regulation of immunopathology during chronic Schistosomiasis.

4.1. Introduction

The aim of this study was to explore the influence of host and microbial factors in the susceptibility of mice to helminth infections. For this a two-model system was designed (figure 9) which also allowed the exploration of the interrelationship between a host's factor (Batf2), gut commensal microbiota, as well as the immune response in the context of controlling chronic Schistosomiasis disease in murine models.

A

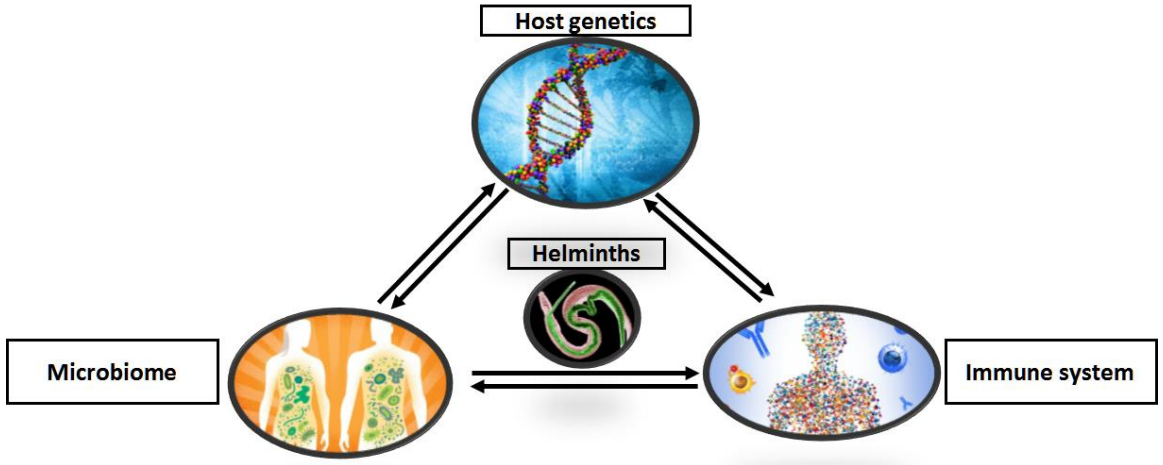

B

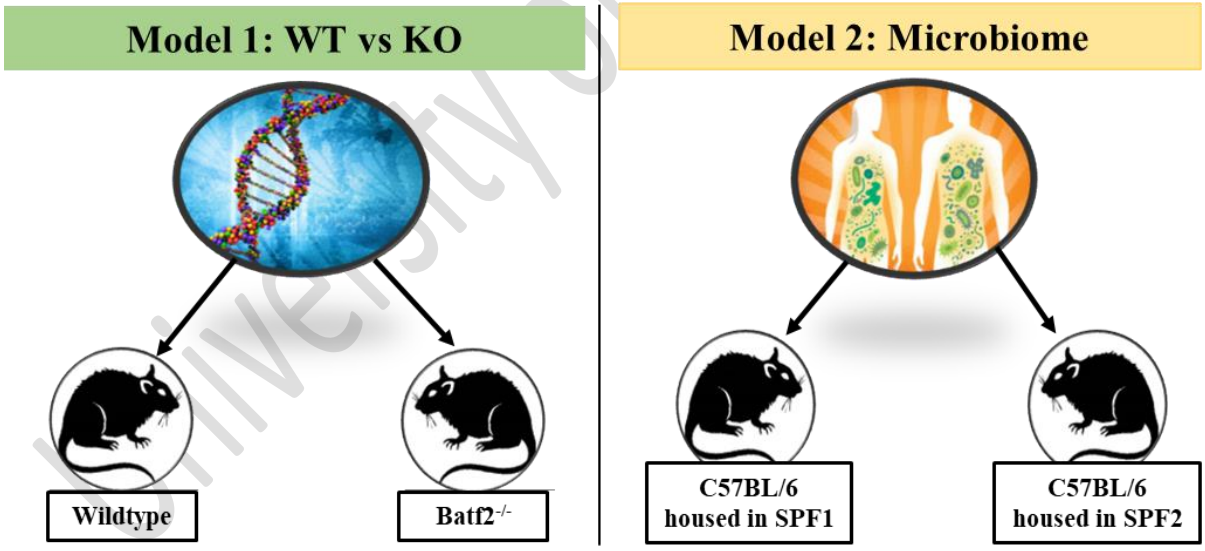

Figure 9: Tripartite model system to explore the interrelationship between host's genetic factor (Batf2), commensal microbiota, and immune responses to control helminth infection.

The figure 9A illustrates a graphical overview of the tripartite interrelationship between the host's genetic factor Batf2, commensal microbiota, and Immune responses against helminth infection. While figure 9B illustrates a murine model-system used to study and explore the interrelationships between host's genetic factor Batf2, commensal microbiota, and the Immune responses, with model 1 showing mice that were different in their genetic component batf2, which was previously shown to play a key role in driving immune system that is crucial during schistosomiasis disease (Mpotje, 2017). The model 2 on the other hand included mice of the same genetic

background but with differential microbial composition. This model was used to explore the effect of microbiota during chronic schistosomiasis.

4.2. Batf2 deficient mice have improved pathological profiles and prolonged survival during chronic *S. mansoni* infection.

4.2.1. Batf2 expression dynamics in tissues during murine schistosomiasis.

The role of Batf2 during Schistosomiasis was demonstrated using Batf2 deficient mice which at homeostasis did not have any major physiological impairments except for minimal changes in immune cells' distributions in the small intestine in relation to the control **WT** mice (Guler et al 2018; Mpotje, 2017). The mice had comparable organ (liver, lung, spleen, heart) weights as well as their associated cellular counts with no observable effect on the tissue damage as measured by ALT and AST enzymes (Guler et al., 2018). Although, the immune profiles of the liver and the lung were not affected by the removal of Batf2, in the small intestine there were elevated levels of immune cells as well as cytokines indicating that the removal of Batf2 was associated with altered intestinal immune response (Guler et al 2018; Mpotje, 2017). The current study further explored the intestinal tissue for more changes associated with the transcription factor as well as the observed changes in immune profile. Given that the intestinal tissue harbours a great number of commensal bacteria which also plays a significant role of priming the immune system (Wu et al., 2012; Turnbaugh et al., 2006), faecal pellets were analysed using 16S rRNA sequencing. Removal of the Batf2 did not affect the species richness (alpha diversity) in the mice (figure 10A), however, there was a different clustering (figure 10B) and abundance (figure 10C) of the bacteria indicating differences in microbial composition in **Batf2**$^{-/-}$ mice in relation to the **WT** mice. Despite the observed alterations of intestinal immune profile and microbiota, the overall fitness of the mice was not affected during homeostasis (Guler et al 2018; Mpotje, 2017). However, the effects of these alterations were potentiated during acute Schistosomiasis as evidenced by increased intestinal immunopathology as well as reduced survival in the absence of Batf2 (Guler et al 2018). Furthermore, the mice retained expression of Batf2 in the intestine hinting that the transcription factor potentially plays a vital regulatory role in the tissue during homeostasis and upon acute Schistosomiasis (Guler et. al, 2018).

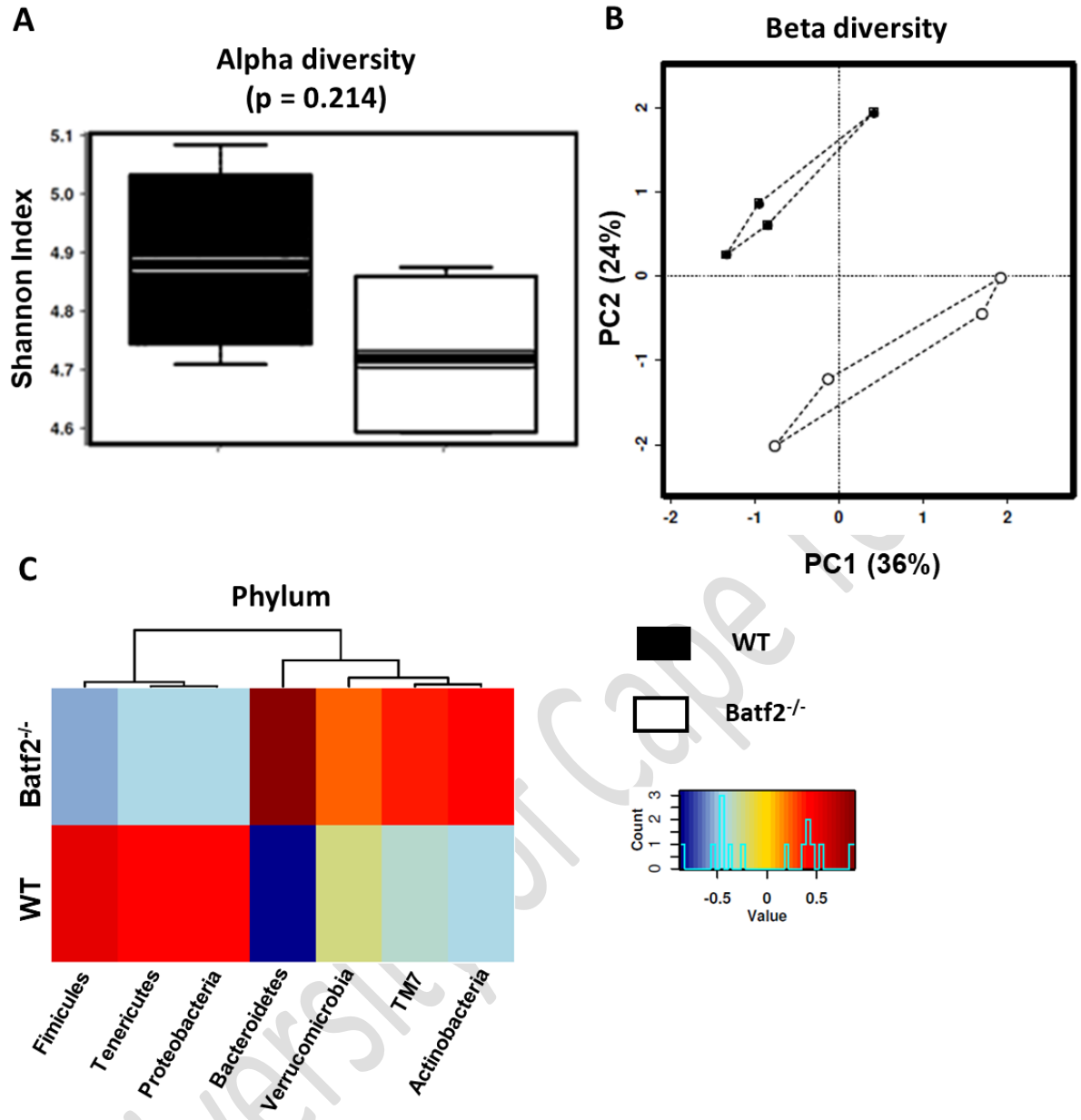

Figure 10: Removal of Batf2 alters the composition of intestinal microbiota of 129Sv mice.

Faecal pellets were collected from Wild-type (129Sv) mice that were 8 weeks old with no complications. (A) Boxplot of alpha diversity measurement using Shannon index estimator for the faecal microbial communities from **WT** and **Batf2**$^{-/-}$ mice. (B) Principal component analysis (PCA) and beta diversity of microbial community compositions in **WT** and **Batf2**$^{-/-}$ mice. (C) Heatmap of relative abundance of microbial communities at a phylum level in *S. mansoni* infected **WT** and **Batf2**$^{-/-}$ mice. **WT**, n = 8; **Batf2**$^{-/-}$, n = 8 analysed as 4 samples per group. The comparisons of the graphs were performed by student t test. *p value< 0.05 and **p value < 0.01.

The previous study reported a maintained expression of Batf2 in the small intestinal tissue while in the liver, the expression was significantly increased during acute schistosomiasis (Guler et al., 2018). Despite the reported increase in expression of Batf2, removal of this

transcription factor did not affect the tissue immunopathology during acute Schistosomiasis (Guler et. al, 2018). This, therefore, demonstrated a tissue specific role for the Batf2 which was most critical to help control the intestinal immunopathology during acute Schistosomiasis. Interestingly, the expression of Batf2 in the liver was still significantly increased during a chronic phase of the infection in relation to naïve mice (figure 11). It was, however, unclear how the increased expression was contributing to the liver immunopathology during chronic Schistosomiasis.

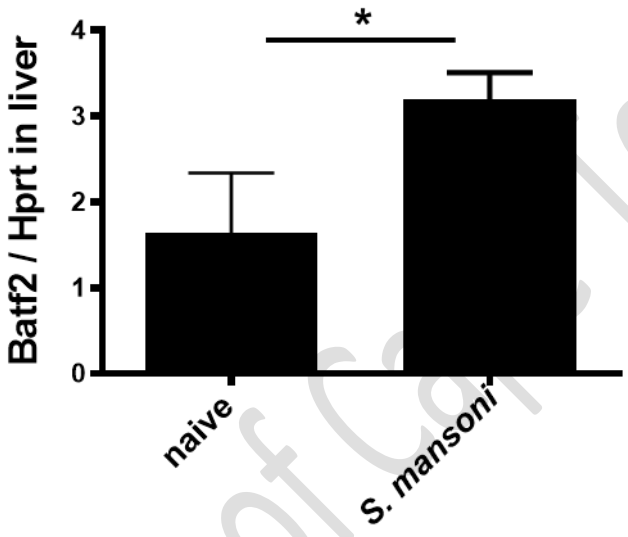

Figure 11: Increased expression of Batf2 mRNA in the liver during chronic *S. mansoni* infection when compared to naïve mice.

Wild-type (129Sv) mice were percutaneously infected with a low dose of 35 *S. mansoni* cercaria and sacrificed at week 0, and 10 post infection. The levels of Batf2 mRNA were measured in the liver of naïve, and chronic *S. mansoni* infected mice to compare the expression levels of Batf2 at week 0, and 10 (chronic phase) post *S. mansoni* infection. Data represents two experiments conducted independently (n = 7-10). The comparisons of the bar graphs were performed by student t test. *p value < 0.05 and **p value < 0.01.

4.2.2. Batf2 gene deletion prolongs mice survival during chronic *S. mansoni* infection.

Given that the Batf2 mRNA expression in one of the most highly affected organs (liver) was significantly increased during chronic *S. mansoni* infection in relation to naïve mice, it was hypothesised that the transcription factor was potentially contributing a crucial role for the survival of *S. mansoni* infected mice. To test this, **wild-type** (**WT**) and **Batf2**$^{-/-}$ mice were percutaneously infected with a low dose of 35 *S. mansoni* cercariae to introduce a chronic infection in the mice. Interestingly, removal of Batf2 resulted in improved survival of the mice in relation to the control (**WT**) mice (figure 12A), and the differences in susceptibility observed

were not caused by the worm burden as evidenced by similar *S. mansoni* egg counts in liver tissues of both **Batf2**$^{-/-}$ and **WT** mice (figure 12B). This highlighted a potentially significant detrimental role that the transcription factor may be playing during chronic Schistosomiasis in infected hosts, and therefore, supports the idea of exploring further the Batf2 for its therapeutic potential during infections such as *S. mansoni* infection.

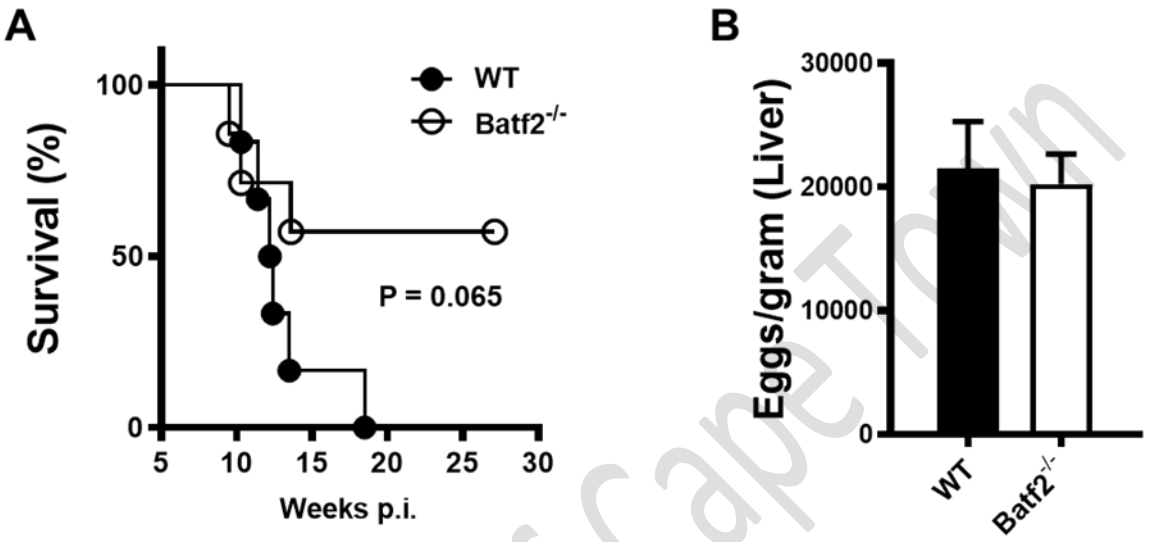

Figure 12: Removal of Batf2 prolongs survival of the mice during chronic *S. mansoni* infection.

The survival of **Batf2**$^{-/-}$ mice was compared to that of **WT** mice during chronic *S. mansoni* infection (A). Quantification of *S. mansoni* eggs comparing the worm burden between **WT** and **Batf2**$^{-/-}$ mice during the infection (B). Data represents three experiments conducted independently (n = 7 - 12). Comparisons of the survival curves were performed by Logrank test. The comparisons of the bar graphs were performed by student t test. *p value < 0.05 and **p value < 0.01.

4.2.3. Batf2 gene deletion ameliorates tissue immunopathology in mice during chronic *S. mansoni* infection.

The following objective was to find out the effect of removing Batf2 on the pathogenesis of mice during chronic *S. mansoni* infection which contributed to prolonged survival of the mice. The tissue organs that are associated with *S. mansoni* infection which include liver, lung, spleen, and the small intestine were analysed to identify the role of this transcription factor on the pathogenesis of the infected mice.

4.2.3.1. Removal of Batf2 results in reduced liver granulomatous immunopathology during chronic S. mansoni infection.

Given that the primary organs that are normally affected by *S. mansoni* infection include the liver and small intestine, further analysis was done to assess the immuno-pathological features that were associated with these organs during the infection in relation to the role of Batf2. The histopathological analysis of formalin-fixed liver tissue stained with H&E (figure 13A) together with granuloma measurements (figure 13B) showed a significantly reduced granulomatous inflammatory response in the absence of Batf2 during chronic *S. mansoni* infection. Further analysis showed an increase in CAB staining (figure 13C) as well as in hydroxyproline levels in **Batf2**$^{-/-}$ mice in relation to the **WT** mice (figure 13D) which together indicated increased hepatic fibrosis that has a primary role of repairing incurred tissue damage during the infection (Kamdem, 2018). Altogether, these data indicate that the removal of Batf2 results in improved regulation of liver immunopathology during chronic Schistosomiasis disease.

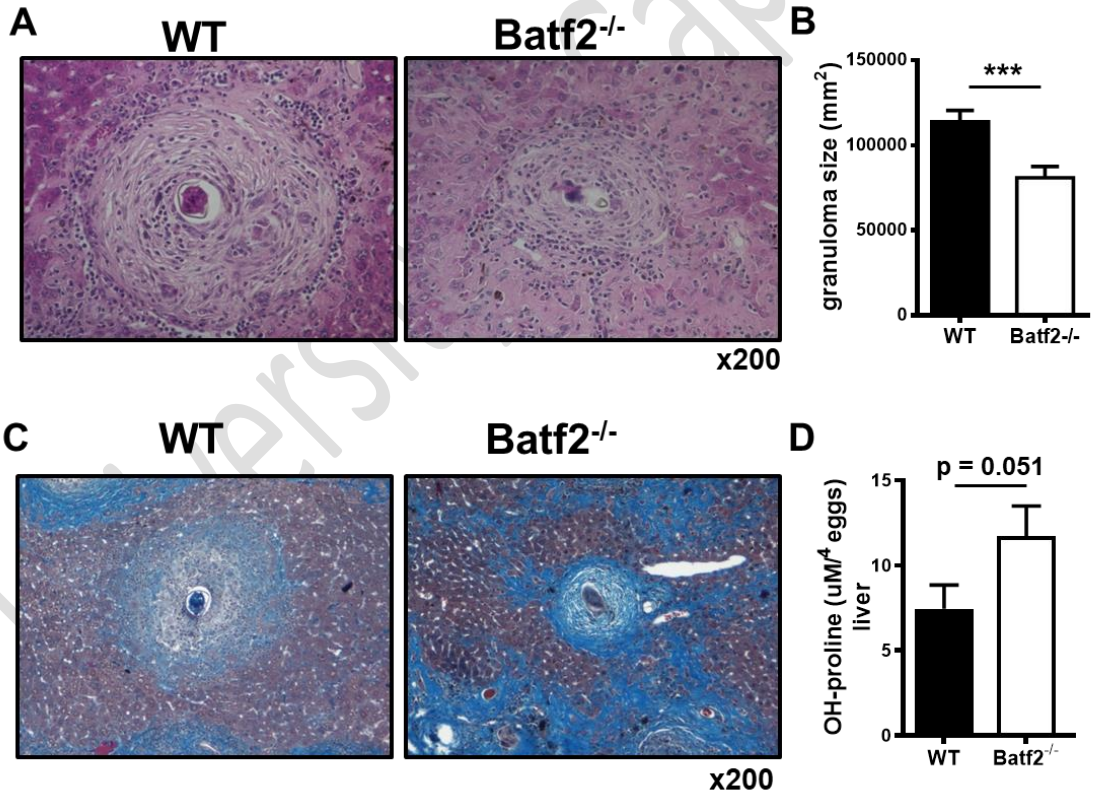

Figure 13: Removal of Batf2 results in reduced liver granulomatous immunopathology during chronic *S. mansoni* infection.

Batf2$^{-/-}$ and **WT** mice were infected percutaneously with a low dose of 35 *S. mansoni* cercariae and analysed at week 10 post infection. The liver sections fixed in formalin were stained with H&E for morphological analysis of the egg-surrounding granuloma (200x) (A). Granuloma measurements quantified using microscopic analysis from H&E-stained sections (B). Liver sections fixed in formalin were stained with CAB staining for morphological

analysis of fibrosis development in the liver of infected mice (200x) (C). Fibrosis measurements quantified using hydroxyproline assay on liver tissues (D). Data represents two experiments conducted independently (n = 7-10). The comparisons of the bar graphs were performed by student t test. *p value < 0.05 and ** p value < 0.01.

4.2.3.2. Removal of Batf2 results in reduced small intestinal tissue granulomatous immunopathology during chronic S. mansoni infection.

Following analysis of the liver pathology, the small intestinal tissue was also analysed as the second majorly affected tissue that contributed to increased susceptibility of the **Batf2**$^{-/-}$ mice during acute schistosomiasis as previously reported (Guler *et al*., 2018; Mpotje, 2017). The histopathological analysis of formalin-fixed small intestinal tissue stained with H&E (figure 14A) together with tissue cellular counts (figure 14B) showed a significantly reduced granulomatous immunopathology in the absence of Batf2 during chronic *S. mansoni* infection. Further analysis on the tissue showed an increase in CAB staining (figure 14C) as well as in hydroxyproline levels (figure 14D) which together indicated increased small intestinal fibrosis in the absence of Batf2. The observed increase in fibrosis was potentially a mechanism mediated by the infected host to repair the incurred damage in the small intestinal tissue during Schistosomiasis disease. Furthermore, the observed differences in small intestinal pathology were not a result of worm burden as evidenced by similar egg counts between **Batf2**$^{-/-}$ and **WT** mice (figure 14E). Therefore, the absence of Batf2 also results in reduced granulomatous immunopathology in the small intestinal tissue during chronic *S. mansoni* infection like what is observed in the liver pathology.

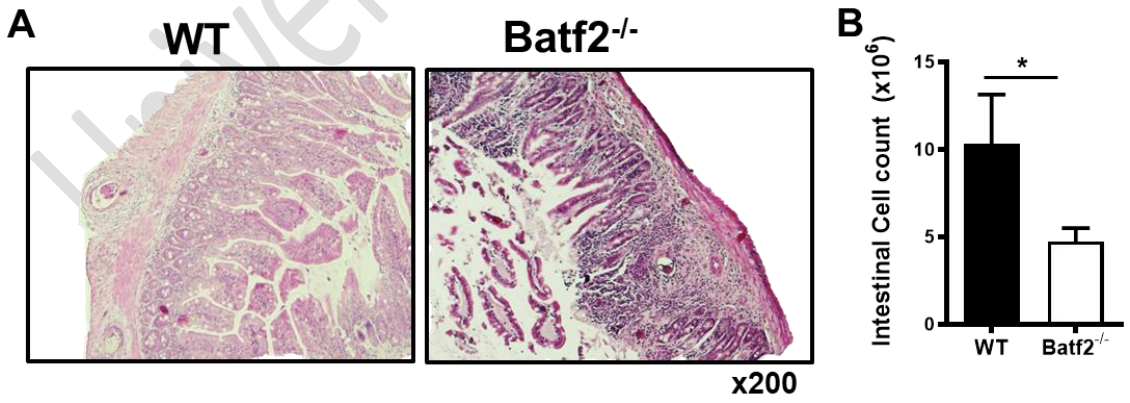

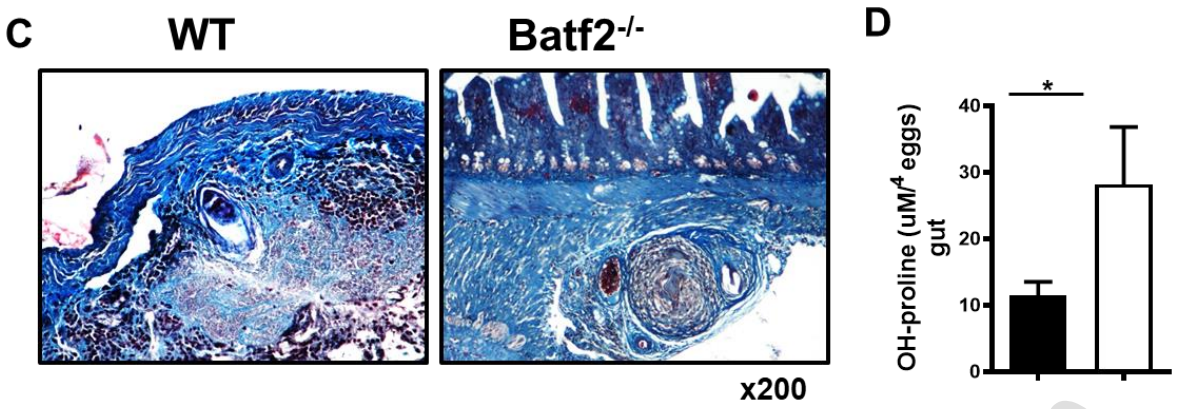

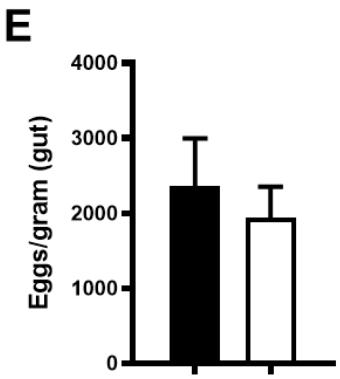

Figure 14: Removal of Batf2 results in reduced small intestinal tissue granulomatous immunopathology during chronic *S. mansoni* infection. Formalin-fixed small intestinal sections stained with H&E for morphological analysis of the cellular recruitment around the trapped *S. mansoni* eggs (200x) (A). Quantification of small intestinal cell counts (B). Formalin fixed small intestinal sections stained with CAB staining for morphological analysis of fibrosis development in the small intestinal of infected mice (200x) (C). Fibrosis measurements quantified using hydroxyproline assay on liver tissues (D). Quantification of *S. mansoni* egg counts (E). Data represents two experiments conducted independently (n = 7-10). The comparisons of the bar graphs were performed by student t test. *p value < 0.05 and **p value < 0.01.

4.2.3.3. Removal of Batf2 results in reduced immunopathology of spleen and lung during chronic S. mansoni infection.

The removal of Batf2 did not influence the weight indices of liver, lung, and heart (figure 15A - C). However, this absence of Batf2 resulted in reduced spleen index (figure 15D) in relation to **WT** mice. This indicated a reduced schistosomiasis-induced splenomegaly in the **Batf2**$^{-/-}$ mice during chronic *S. mansoni* infection. Similar to what was observed in acute schistosomiasis as previous reported (Mpotje, 2017), the small intestinal length was still increased in **Batf2**$^{-/-}$ mice in relation to **WT** mice during chronic *S. mansoni* infection (figure 15E). Further analysis, revealed that the enzymes (ALT and AST) that are associated with tissue cytotoxicity between the **WT** and **Batf2**$^{-/-}$ mice were not affected (figures 15F, G). However, there was a moderate redution in the levels of AST in the **Batf2**$^{-/-}$ mice in relation to the **WT** mice during the infection (figure 15G). Even though, the lung weight measurements were not different between **WT** and **Batf2**$^{-/-}$ mice, the tissue cellular count was modetely reduced in **Batf2**$^{-/-}$ mice indicating a potential reduction in cellular infiltration to the organ and thus may have caused a reduction in inflammatory response in Batf2$^{-/-}$ mice (figure 15H).

Altogether, it is evident that the absence of Batf2 results in reduced immunopathology of the spleen and lung that is also associated with reduced tissue toxicity during chronic *S. mansoni* infection.

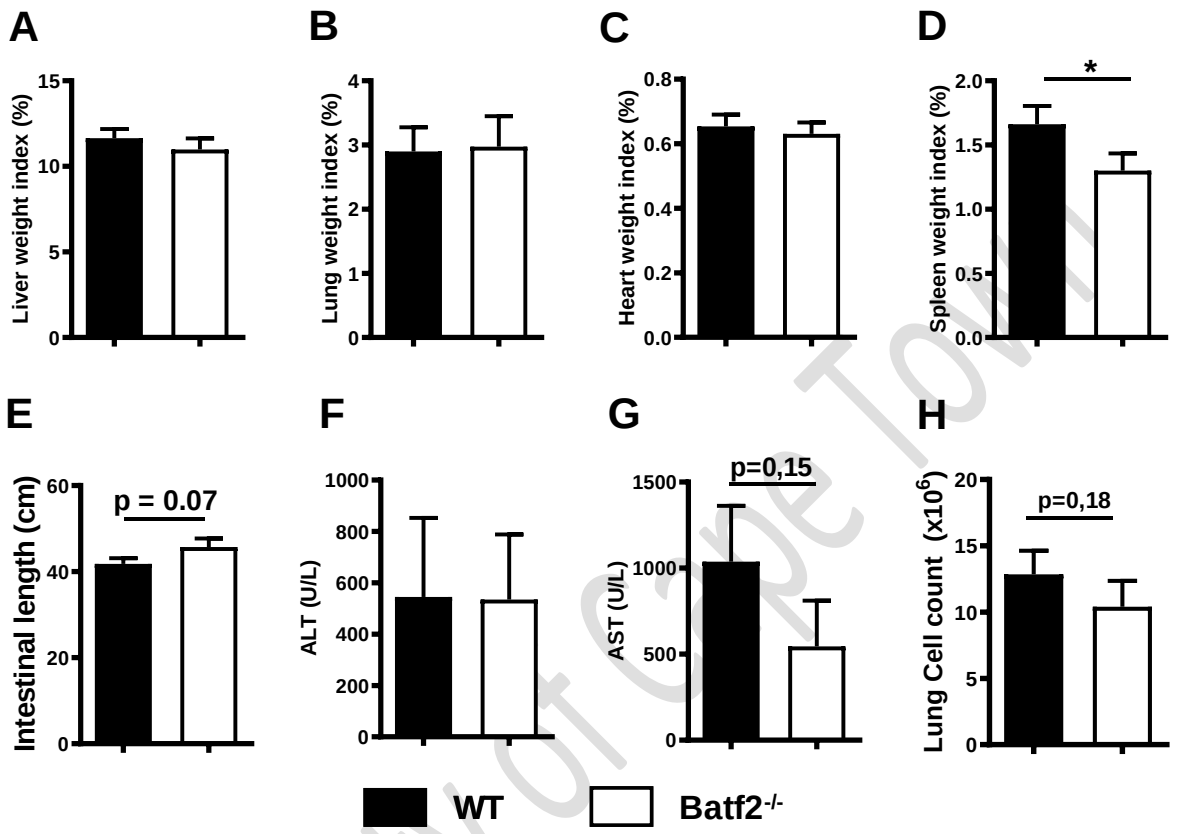

Figure 15: Removal of Batf2 results in reduced immunopathology of the spleen and lung during chronic *S. mansoni* infection.

Batf2$^{-/-}$ and **WT** mice were infected percutaneously with a dose of 35 *S. mansoni* cercariae and analysed at week 10 post infection. Liver (A), lung (B), heart (C), and spleen (D) weight were measured during chronic *S. mansoni* infection. Small intestinal lengths in centimetres were measured during the infection. Serum levels of enzymes associated with tissue toxicity, ALT (F) and AST (G), were also measured. Quantification of lung cellular count (H). Data represents two experiments conducted independently (n = 7-10). The comparisons of the bar graphs were performed by student t test. *p value < 0.05 and **p value < 0.01.

The current data show that the removal of Batf2 promotes protection against chronic *S. mansoni* infection that was associated with significantly reduced tissue immunopathology. Although the immunopathology in both the liver and small intestinal tissues were regulated, there was however, increased fibrosis, which was believed to be a mechanism that the infected **Batf2**$^{-/-}$ mice used to repair the organs against damage inflicted during the *S. mansoni* infection. We

speculated that the presence of Batf2 might be detrimental to the infected mice by potentiating granulomatous immunopathology during chronic Schistosomiasis.

4.2.4. Altered immune responses in tissues of Batf2$^{-/-}$ mice during chronic Schistosomiasis.

4.2.4.1. Liver immune responses in Batf2$^{-/-}$ mice during chronic S. mansoni infection.

The immune profile that was associated with the reduced liver granulomatous immunopathology along with increased fibrosis during chronic *S. mansoni* infection was explored. The absence of Batf2 resulted in significantly reduced lymphocyte recruitment i.e. CD19+ B and CD4+ T lymphocytes (figure 16A). Other myeloid cells were also of diminished representation in the liver tissue i.e., eosinophils, neutrophils, and dendritic cells (figure 16B) which all participate to the hepatic granulomatous inflammation that develops around the trapped *S. mansoni* eggs. Although both **WT** and **Batf2$^{-/-}$** mice were dominated by a Th2 immune response (figure 16C, D), there was a significant decrease in overall polarization of CD4+ T cells into Th1 (T-bet), and Th2 (Gata3) subtypes in **Batf2$^{-/-}$ mice.** Regulatory (Foxp3) CD4+ T cells were also moderately decreased in **Batf2$^{-/-}$** mice in relation to the **WT** mice (figure 16C). In the case of CD8+ T cells, polarization into Th1 (T-bet) and Th2 (Gata3) was moderately reduced while the regulatory (Foxp3) subtypes were not affected in the **Batf2$^{-/-}$** mice in relation to **WT** mice during the infection (figure 16D). Further analysis showed a reduction in IL-4 and IL-5 producing CD4+ and CD8+ T cells in **Batf2$^{-/-}$** mice in relation to **WT** mice (figure 16E, F). Although, the IFN-γ and IL-13 producing CD4+ T cells in these mice were not affected in relation to the **WT** mice (figure 16E), the CD8+ T cells producing these cytokines (IFN-γ and IL-13) were significantly increased in the **Batf2$^{-/-}$** mice in relation to the **WT** mice (figure 16F). More analysis of the overall tissue specific cytokines in the liver using ELISA revealed that there was a significant increase of IFN-γ and IL-10 cytokines in **Batf2$^{-/-}$** mice in relation to **WT** mice (figure 16G, H). The TNF-α cytokine production was also significantly reduced in **Batf2$^{-/-}$** mice in relation to **WT** mice during the infection (figure 16G). Although, there was a significant increase in inflammatory mediators including IL-5 and IL-17 cytokines (figure 16G, H) during the infection, the recruitment of type 2 immune populations that contribute to hepatic granulomatous immunopathology were reduced in **Batf2$^{-/-}$** mice in relation to **WT** mice during chronic *S. mansoni* infection.

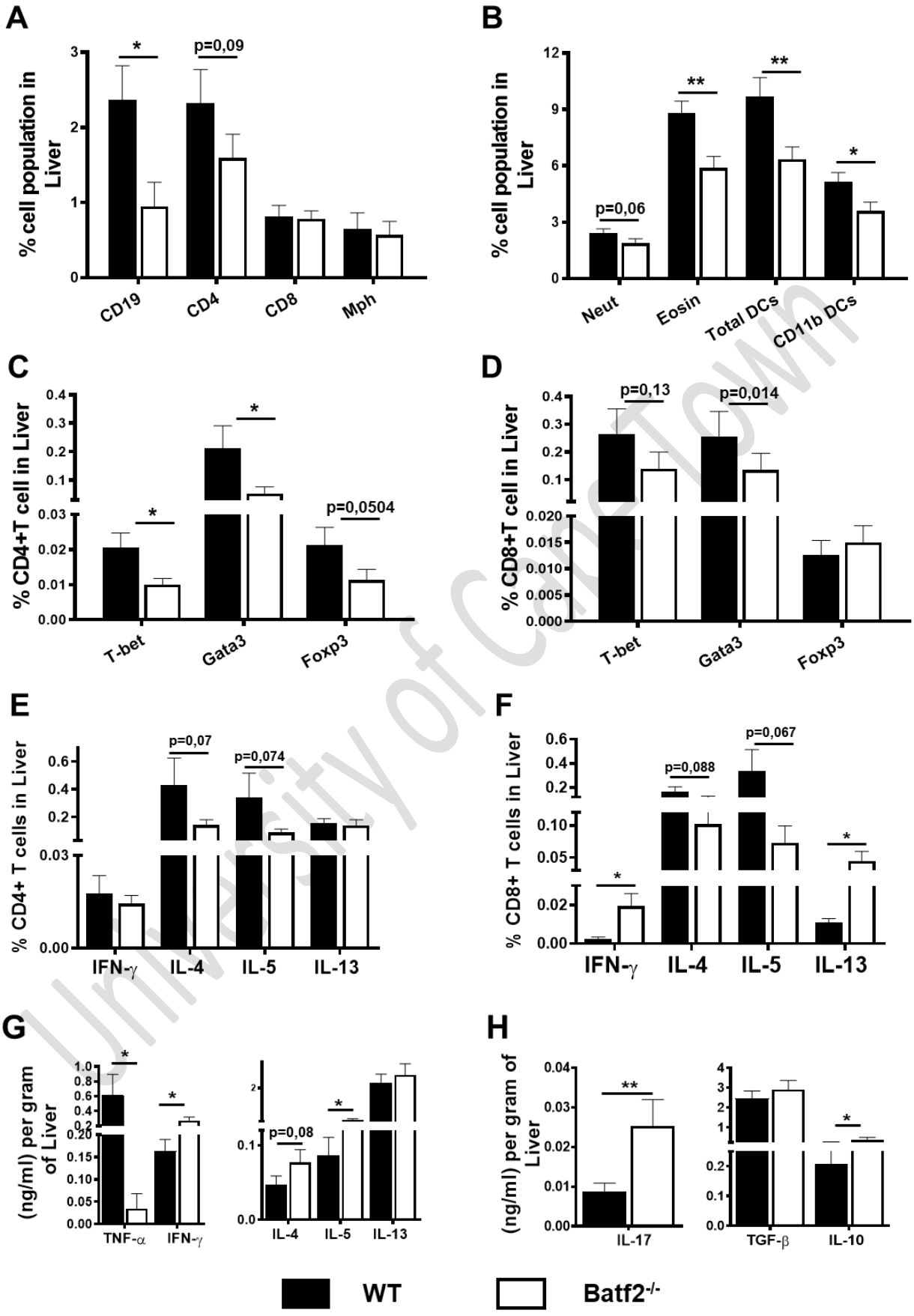

Figure 16: Removal of Batf2 results in reduced recruitment of type 2 immune populations to the liver during chronic *S. mansoni* infection.

Batf2$^{-/-}$ and **WT** mice were percutaneously infected with a dose of 35 *S. mansoni* cercariae and the immune responses were analysed in the liver tissue during week 10 post infection. Quantification of immune cellular populations analysed using flow cytometry (A, B). Quantification of CD4+ (C) and CD8+ (D) T lymphocyte polarization during the infection analysed using flow cytometry. Quantification of cytokine producing CD4+ (E) and CD8+ (F) T lymphocytes re-stimulated with PMA/Ionomycin and analysed on flow cytometry. Liver cytokine concentrations per gram of tissue measured using ELISA (G, H). Data represents two experiments conducted independently (n = 7-10). The comparison of bar graphs was made using student t test. *p value < 0.05 and **p value < 0.01.

4.2.4.2. Intestinal immune response in Batf2$^{-/-}$ *mice during chronic S. mansoni infection.*

Next, the immune profile that was associated with the observed immunopathology of the small intestinal tissue during chronic *S. mansoni* infection was explored. In the mesenteric lymph nodes (MLN) of **Batf2**$^{-/-}$ mice, the CD4+ T cells were significantly decreased while the CD8+ T cells were moderately increased in relation to **WT** mice during chronic *S. mansoni* infection (figure 17A). In terms of the myeloid populations recruited in the small intestinal tissue, there was a moderate reduction in macrophages, and eosinophils in **Batf2**$^{-/-}$ mice in relation to **WT** mice during the infection (figure 17B). This data shows that the cell populations known to contribute to Schistosomiasis-induced inflammatory immune response (CD4+ T cells, macrophages, eosinophils) were decreased in the gut of **Batf2**$^{-/-}$ mice. Conversely, the cells that have been reported to contribute to Schistosomiasis-induced immune regulation (CD8+ T cells) were increased in the small intestinal tissue of **Batf2**$^{-/-}$ mice in relation to **WT** mice during chronic *S. mansoni* infection (Pedras-Vasconcelos, 1996). Further analysis of the lymphocyte populations from the MLN revealed no significant differences in polarization for both CD4+ and CD8+ T cells in **Batf2**$^{-/-}$ mice in relation to **WT** mice (figure 17C, D). In terms of the effector function of these lymphocytes from MLN, the absence of Batf2 resulted in significantly reduced IL-4 and IL-5 producing CD4+ as well as CD8+ T cells (figure 17E, F). There was also a moderate reduction in the production of IL-13 by CD4+ T cells in **Batf2**$^{-/-}$ mice in relation to **WT** mice (figure 17E). These reduced immune effector populations suggested a reduced Th2 inflammatory immune response in the absence of Batf2 during chronic *S. mansoni* infection. On the other hand, there was also a moderate increase of IFN-γ producing CD8+ T cells in **Batf2**$^{-/-}$ mice in relation to the **WT** mice (figure 17F). Furthermore, the overall tissue specific cytokines including IFN-γ, TNF-α, IL-4, IL-5, IL-13 and IL-17 in the small intestinal tissue measured using ELISA (figure 17G, H), showed that the removal of

Batf2 results in significant reduction of IL-17 and moderate reduction of TGF-beta which might both contribute to the observed reduction in small intestinal inflammation during chronic schistosomiasis. Altogether, the data revealed that the absence of Batf2 contributes to reduced inflammatory immune response in the small intestinal tissue during chronic Schistosomiasis disease.

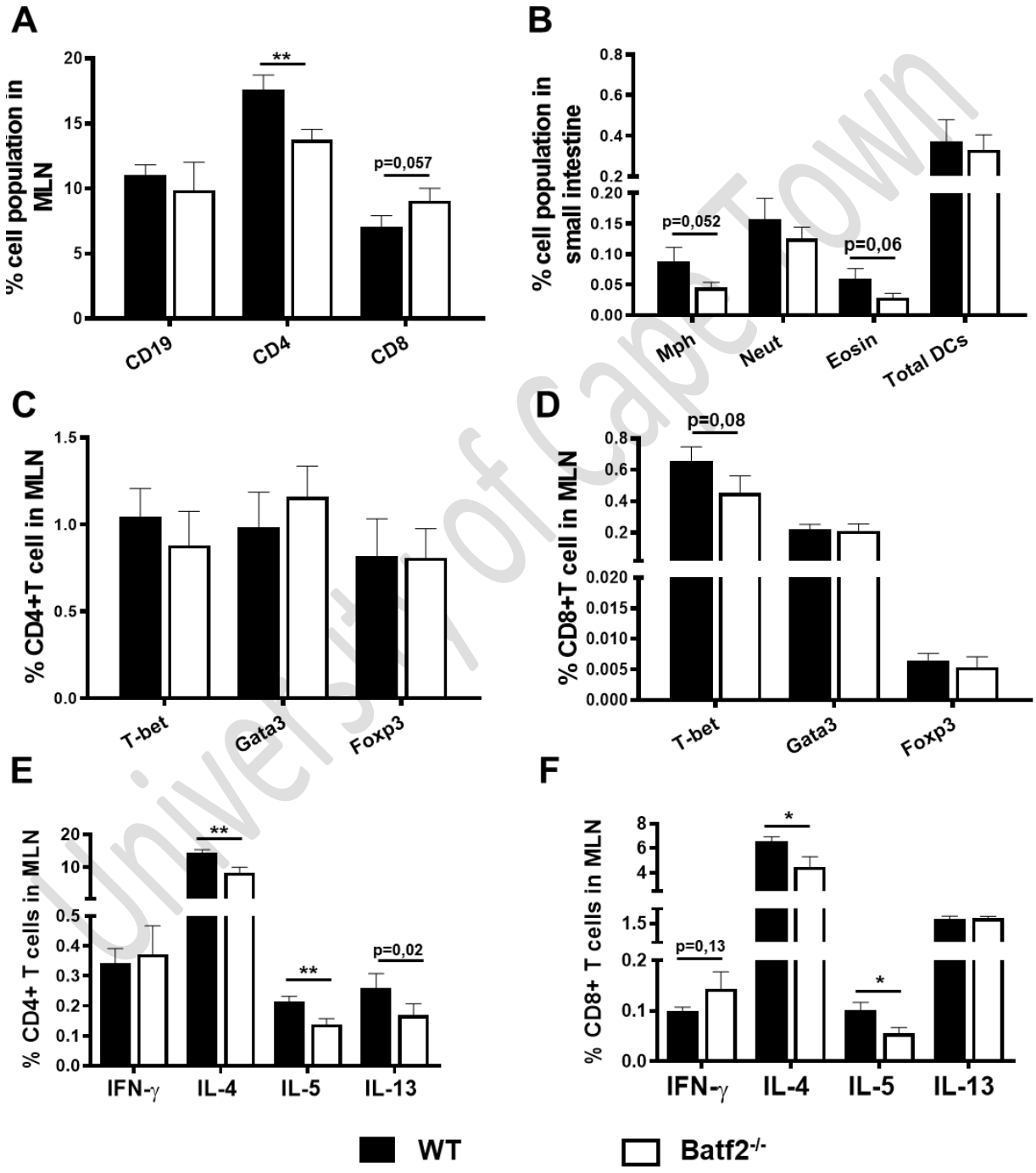

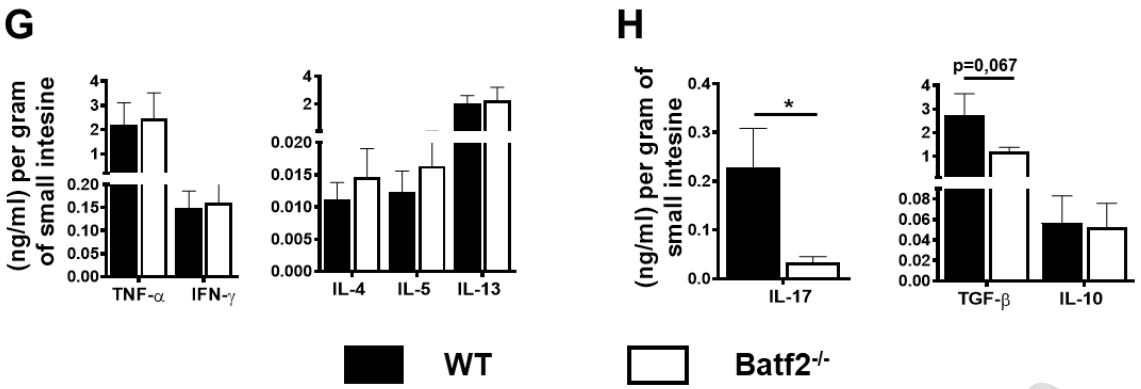

Figure 17: Removal of Batf2 results in reduced small intestinal inflammatory immune response during chronic *S. mansoni* infection.

Batf2$^{-/-}$ and **WT** mice were percutaneously infected with a dose of 35 *S. mansoni* cercariae and the immune responses were analysed in the small intestinal tissue and mesenteric lymph nodes (MLN) during week 10 post infection. Quantification of MLN lymphocytes (A) and myeloid cellular populations in the small intestine (B) analysed using flow cytometry. Quantification of MLN CD4+ (C) and CD8+ (D) T lymphocyte polarization during the infection analysed using flow cytometry. Quantification of cytokine producing CD4+ (E) and CD8+ (F) T lymphocytes from MLN re-stimulated with PMA/Ionomycin and analysed on flow cytometry. Small intestinal cytokine concentrations per gram of tissue measured using ELISA (G, H). Data represents two experiments conducted independently (n = 7-10). The comparisons of the bar graphs were performed using student t test. *p value < 0.05 and **p value < 0.01.

4.2.4.3. Lung immune response in Batf2$^{-/-}$ mice during chronic S. mansoni infection.

The absence of Batf2 results in reduced lung tissue cellular count which suggested a potentially reduced inflammation (figure 15). Although the immune profile of the lung revealed a moderate increase in the recruitment of CD8+ T cells as well as eosinophils (figure 18A), what was prominently affected in the tissue, which may have contributed to reduced tissue inflammation, were the significantly reduced recruitment of mature neutrophils in **Batf2**$^{-/-}$ mice in relation to the **WT** mice (figure 18B). Furthermore, the absence of Batf2 moderately increased polarization of the CD4+ T cells into Th2 subsets (figure 18C) while the CD8+ T cells were significantly more polarized into regulatory subset (figure 18D) in relation to the control **WT** mice. Even though the cytokine-producing CD4+ T cells were not significantly different (figure 18E), there was, however, a moderate increase in IL-4 producing CD8+ T cells (figure 18F) in the absence of Batf2. Collectively the data show a reduced lung neutrophilic inflammatory immune response that is linked with increased regulatory CD8+ T cells in the absence of Batf2 during chronic *S. mansoni* infection.

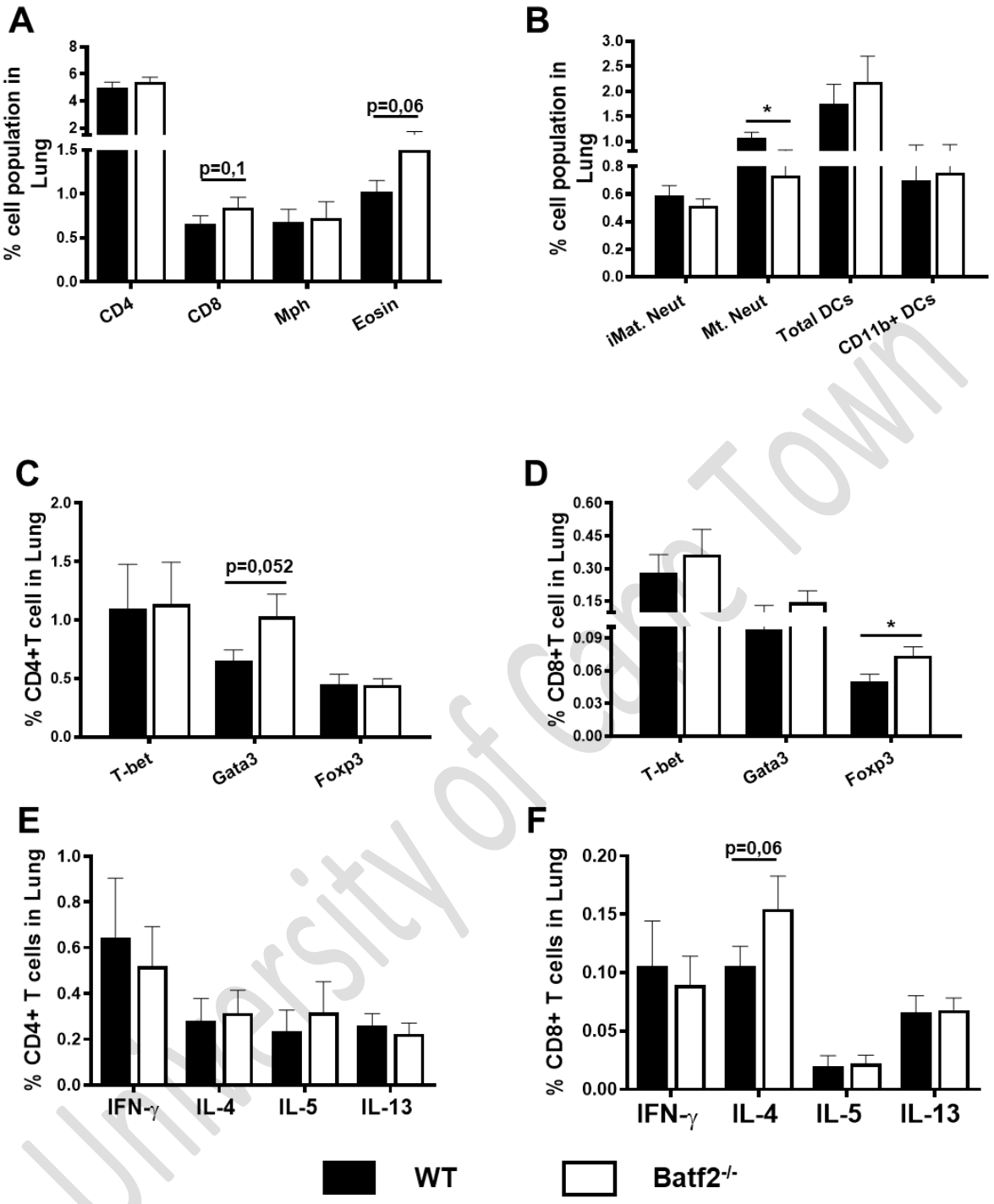

Figure 18: The absence of Batf2 results in reduced lung neutrophilic inflammation during chronic *S. mansoni* infection.

Batf2$^{-/-}$ and **WT** mice were percutaneously infected with a dose of 35 *S. mansoni* cercariae and the immune responses in the lung tissue were analysed during week 10 post infection. Quantification of immune cellular populations in percentages analysed using flow cytometry (A, B). Percentage quantification of CD4+ (C) and CD8+ (D) T cell polarization measured using flow cytometry. Percentage quantification of cytokine producing CD4+ (E) and CD8+ (F) T lymphocytes re-stimulated with PMA/Ionomycin and analysed on flow cytometry.

Data represents two experiments conducted independently (n = 7-10). The comparisons of bar graphs were performed by student t test. *p value < 0.05 and **p value < 0.01.

Of interest considering the reduced liver immunopathology, the recruitment of immune populations especially the CD19+ B cells and regulatory foxp3+ T cells were either reduced or not affected by the absence of Batf2, however, the effector CD8+ T cells (IFN-γ and IL-13 producing CD8+ T cells) were significantly increased during the infection. This highlighted the potential of the CD8 T lymphocytes as key immune cell populations that may have contributed to the observed liver immunopathology in **Batf2**$^{-/-}$ mice during chronic *S. mansoni* infection.

4.2.5. Injection of CD8 antibodies abrogates the prolonged survival and reduced tissue immunopathology of Batf2$^{-/-}$ mice during chronic *S. mansoni* infection.

To address the significance of the CD8+ populations as key immune cell populations which contributed to liver granulomatous immunopathology in **Batf2**$^{-/-}$ mice during chronic *S. mansoni* infection, the mice were administered 200µg of α-CD8 antibodies orally to neutralize the population of CD8-expressing cells in **Batf2**$^{-/-}$ mice as previously demonstrated (Jung et al., 2018; Czuprynski and Brown, 1990; Adams et al., 1993). The **α-CD8 treated Batf2**$^{-/-}$ mice resulted in a significantly exacerbated liver granulomatous immunopathology in relation to the control untreated **Batf2**$^{-/-}$ mice during chronic schistosomiasis (figure 19A, B). There was also a moderate reduction in hepatic fibrosis in the liver tissue of **α-CD8 treated Batf2**$^{-/-}$ mice in relation to the control **Batf2**$^{-/-}$ mice (figure 19C, D). The data, therefore, show the CD8-expressing immune populations play a significant role of regulating liver granulomatous immunopathology during chronic Schistosomiasis. Interestingly, failure of the CD8-expressing cells to regulate the immunopathology led to reduced survival of the **α-CD8 treated Batf2**$^{-/-}$ mice in relation to the **Batf2**$^{-/-}$ mice that did not receive α-CD8 during chronic *S. mansoni* infection (figure 19E), and this was not caused by differential worm burden (figure 19F). The study demonstrates a poorly understood vital role of CD8-expressing populations as one of the predominant cells that are required to regulate liver granulomatous immunopathology during chronic *S. mansoni* infection.

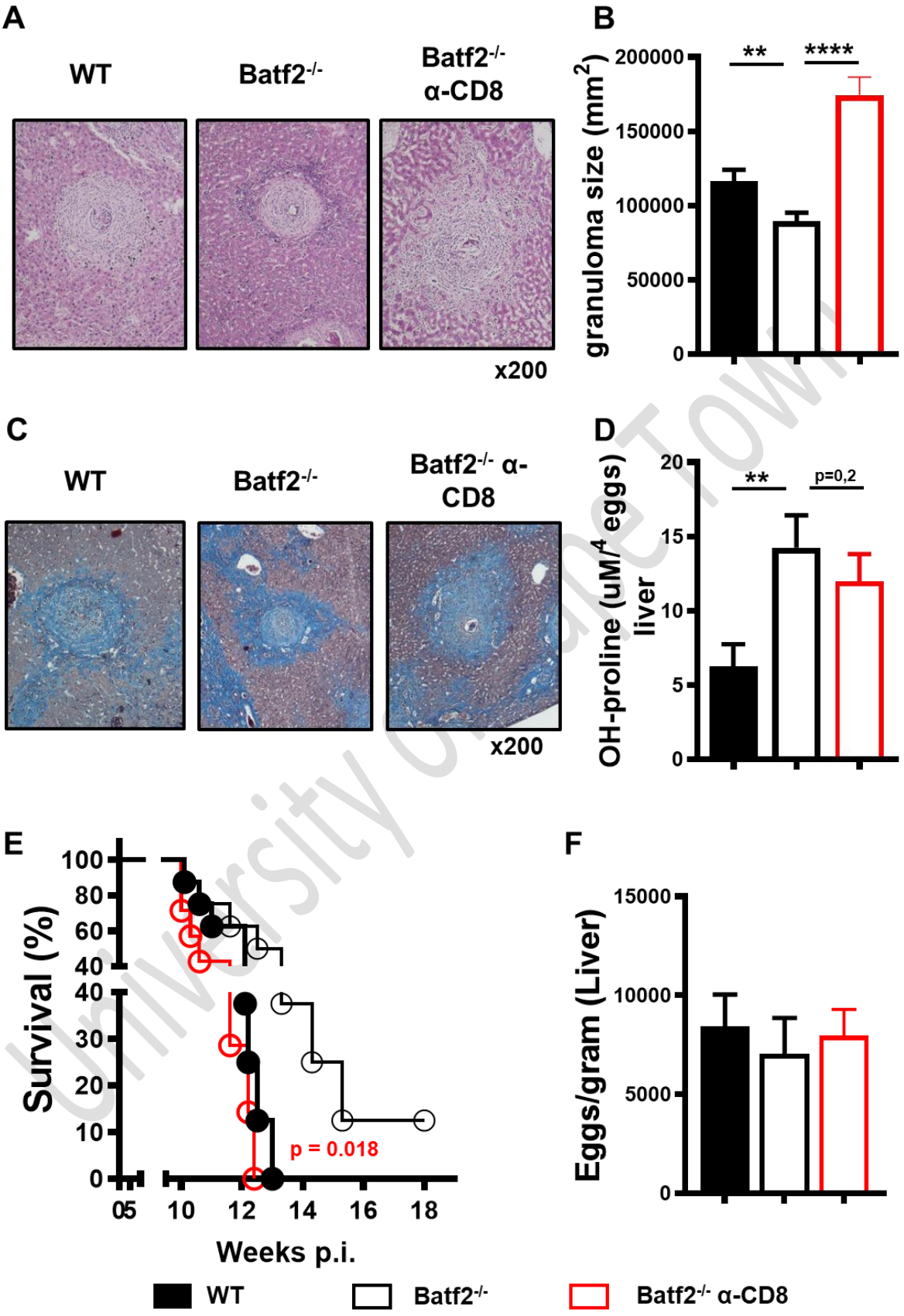

Figure 19: Administration of α-CD8 antibodies abrogates the prolonged survival and reduced tissue immunopathology of Batf2$^{-/-}$ mice during chronic *S. mansoni* infection.

Batf2$^{-/-}$ and **WT** mice were infected percutaneously with a dose of 35 *S. mansoni* cercariae and were monitored up to 18 weeks post infection. Liver sections fixed in formalin were stained with H&E for morphological analysis of the egg-surrounding granuloma (200x) (A). Granuloma measurements quantified using microscopic analysis from H&E-stained sections (B). Liver sections fixed in formalin were stained with CAB staining for morphological analysis of fibrosis development in the liver of infected mice (200x) (C). Fibrosis measurements quantified using hydroxyproline assay on liver tissues (D). The survival of α-CD8 treated Batf2$^{-/-}$ mice was compared to that of **Batf2$^{-/-}$** and **WT** mice during chronic *S. mansoni* infection (E). Quantification of *S. mansoni* eggs comparing the worm burden between **WT**, **Batf2$^{-/-}$** and **α-CD8 treated Batf2$^{-/-}$** mice during the infection (F). Comparison of survival curves were performed by Logrank test. The comparison of bar graphs was made using student t test. *p value < 0.05 and **p value < 0.01. (n = 7-12).

4.3. Role of the intestinal microbiota of Batf2$^{-/-}$ mice during chronic *S. mansoni* infection.

The commensal microbiota has been reported to be involved in a variety of physiological processes which include priming of the immune system to help maintain homeostasis and to protect from pathogens that invade the host (Wu, 2012; Turnbaugh, 2006). As demonstrated in figure 10, the removal of Batf2 results in altered intestinal microbiota, however, it was still unclear whether these changes do contribute to the observed pathogenesis of the mice during chronic Schistosomiasis. Considering the data presented so far, it was also possible that the observed changes in the immune system, especially the increased inflammatory mediators (IL-17, IL4, IL5 and IFN-γ cytokines) in the liver were a result of the commensal microbiota during chronic *S. mansoni* infection. To address the role of the commensal microbiota of **Batf2$^{-/-}$** mice during chronic Schistosomiasis, a co-housing model system was employed where the susceptible **WT** and the resistant **Batf2$^{-/-}$** mice were placed in the same cage to allow the transfer of the commensal microbiota between the groups of mice prior and during the infection. This was a good model to follow given that mice are coprophagic and therefore, this allowed a continuous exchange of intestinal microbiota between the groups of mice throughout the infection (Stappenbeck and Virgin, 2016). Furthermore, some of the microbiota components such as enveloped virus, and anaerobic bacteria which may contribute to the phenotype, do not normally survive faecal transplantation procedure, and therefore, the co-housing model allows for successful transfer of these microbes (Stappenbeck and Virgin, 2016)

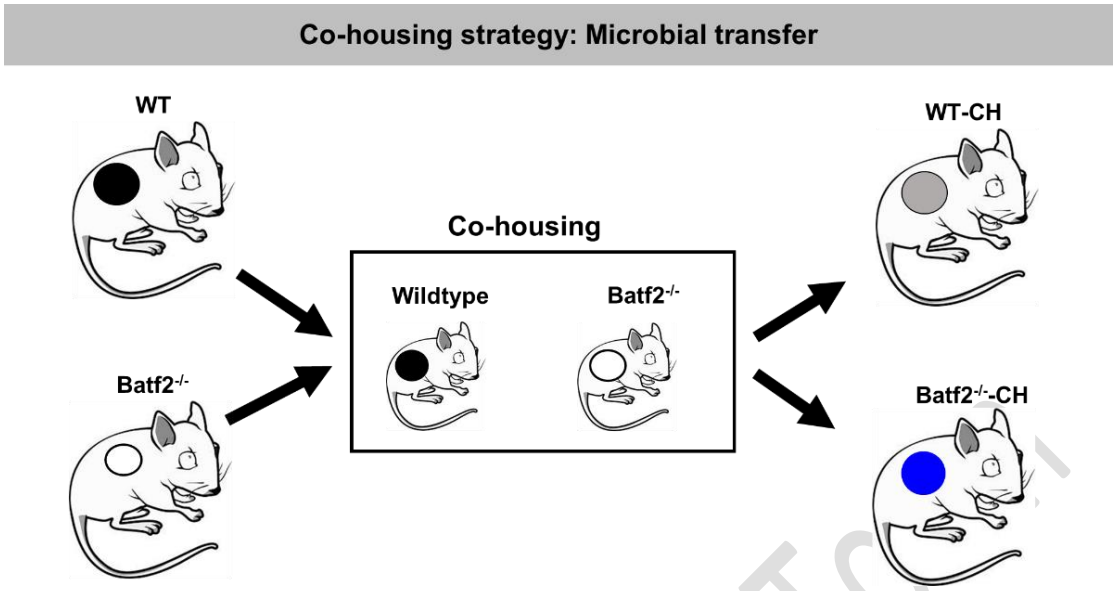

Figure 20: Diagram illustrating the co-housing strategy used to allow the transfer of microbiota between WT and Batf2$^{-/-}$ mice during chronic *S. mansoni* infection.

The WT and Batf2$^{-/-}$ mice were co-housed together 7 days prior to *S. mansoni* infection to allow gut microbial reprogramming within the mice. Using this model, four groups were generated i.e. (i) WT, (ii) Batf2$^{-/-}$, (iii) WT Co-housed (WT-CH), (iv) Batf2$^{-/-}$ Co-housed (Batf2$^{-/-}$ CH).

4.3.1. Intestinal microbiota transfer from Batf2$^{-/-}$ mice to wild type mice alters inflammatory immune responses in wild type mice during chronic *S. mansoni* infection.

4.3.1.1. Alterations of hepatic immune responses in wild type mice recipient of Batf2$^{-/-}$ intestinal microbiota during chronic schistosomiasis.

The study included four groups (**WT, WT-CH, Batf2$^{-/-}$ and Batf2$^{-/-}$-CH**) as depicted in figure 20. The mice were percutaneously infected with a low dose of 35 *S. mansoni* cercariae to induce a chronic infection in the mice. The immune profile associated with liver immunopathology following the microbial transfer was analysed. There was a significantly reduced recruitment of myeloid cells including total DCs, CD11b+ DCs, eosinophils and neutrophils in relation to the susceptible **WT** mice (figure 21A – D). Although, the recruitment of CD4+ T cells were not affected in the **WT-CH** mice in relation to the susceptible **WT** mice (figure 21E), their polarization into Th1 (T-bet) and Th2 (Gata3) subsets was significantly reduced during the infection (figure 21F - H). The recruitment of the CD8+ T cells together with their polarization into Th1 (T-bet) and Th2 (Gata3) subsets were not affected (figure 21I - K), however, their polarization into regulatory (Foxp3) subsets were significantly increased in the **WT-CH** mice in relation to the susceptible **WT** mice (figure 21L). In terms of the effector function of the T

lymphocytes, the IL-4, IL-5, and IL-13 producing CD4+ T cells were not affected in the **WT-CH** mice in relation to the susceptible **WT** mice (figure 21M - O), however, the IFN-γ producing CD4+ T lymphocytes which were similar in **WT** mice in relation to **Batf2**$^{-/-}$ mice, were significantly increased in **WT-CH** and **Batf2**$^{-/-}$**-CH** mice indicating that this was an effect resulting from the alterations of intestinal microbiota of the mice during the infection (figure 21P). Unlike with the IFN-γ producing CD4 T lymphocytes, the IFN-γ producing CD8+ T lymphocytes in **WT-CH** mice were significantly increased in relation to the susceptible **WT** mice while that of the **Batf2**$^{-/-}$ mice were reduced (figure 21Q). Conversely, the production of IL-4 producing CD8+ T lymphocytes were significantly decreased in the **WT-CH** mice in relation to the susceptible **WT** mice, and those of the **Batf2**$^{-/-}$ **-CH** mice were significantly decreased in relation to **Batf2**$^{-/-}$ mice during the infection (figure 21R). The IL-5 producing CD8+ T lymphocytes were not affected by the transfer of intestinal microbiota in **WT-CH** mice (figure 21S), however the IL-13 producing CD8+ T lymphocytes were significantly increased in **WT-CH** mice in relation to those of susceptible **WT** mice (figure 21T). The data highlights a potential role of the microbiota of **Batf2**$^{-/-}$ mice in contributing to increased IFN-γ and IL-13 producing CD8 T lymphocytes and reduced CD8+ IL-4+ T lymphocytes during the chronic *S. mansoni* infection. Altogether, the intestinal microbiota of Batf2$^{-/-}$ mice induce alterations to Schistosomiasis-induced immune responses.

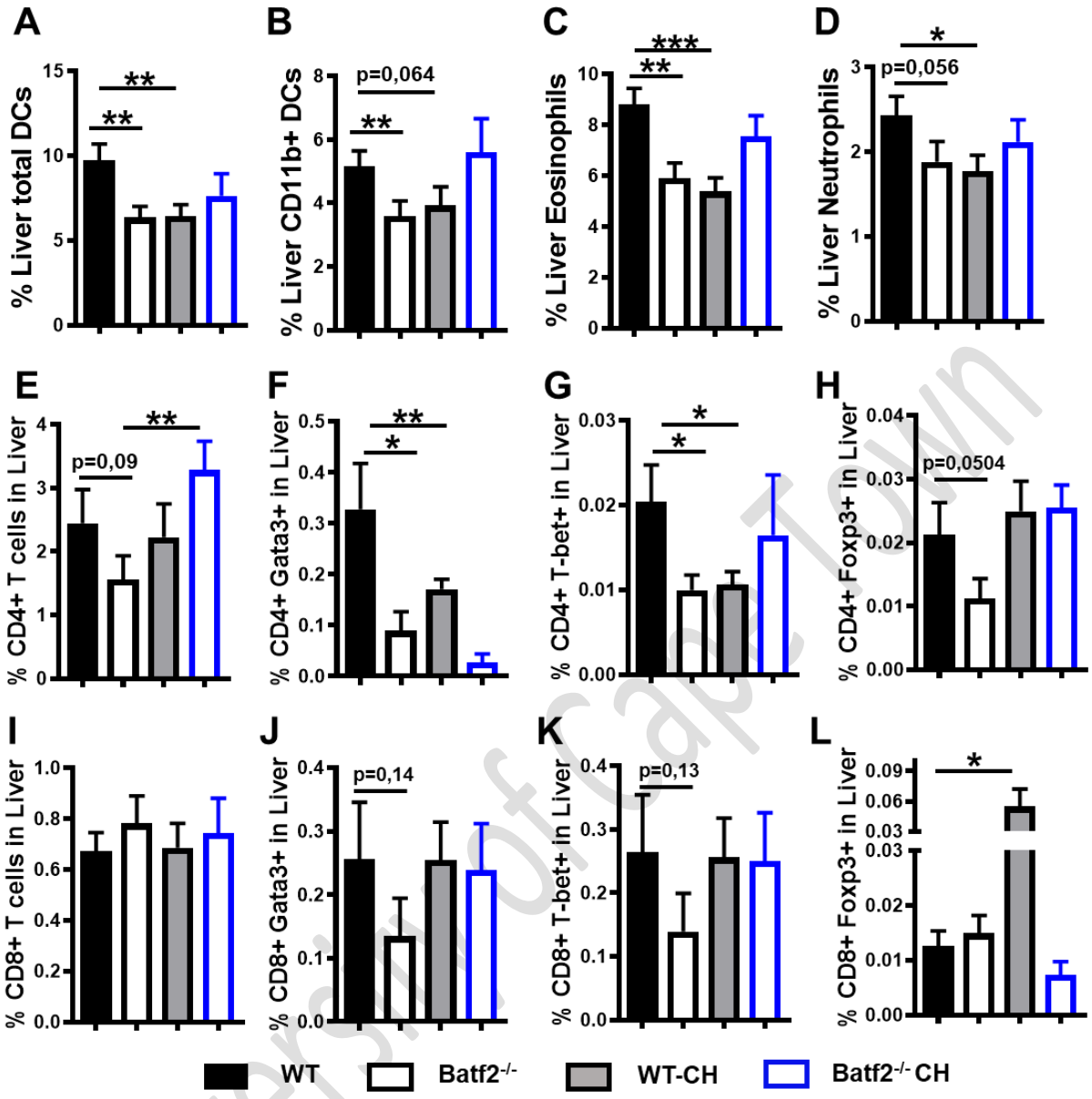

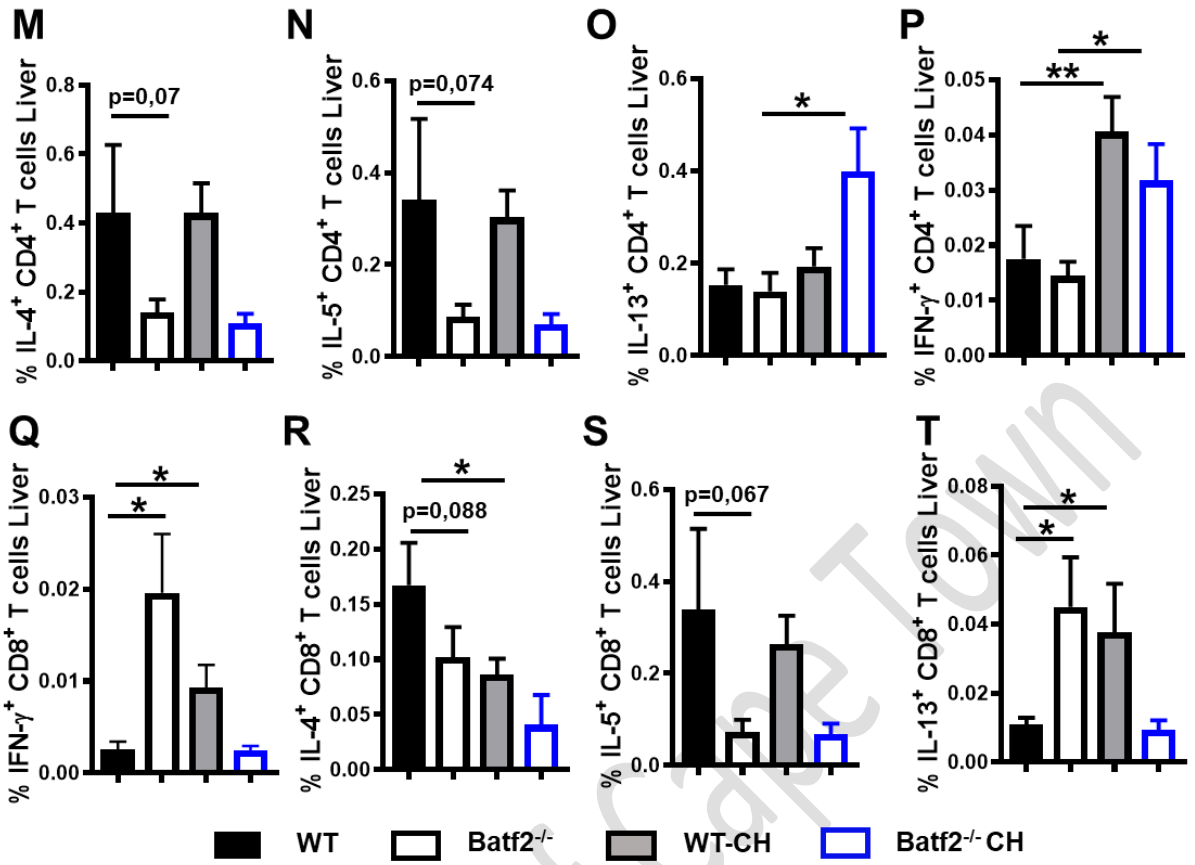

Figure 21: Co-housing results in alterations of hepatic immune responses in wild type mice recipient of Batf2$^{-/-}$ intestinal microbiota during chronic Schistosomiasis.

Batf2$^{-/-}$, **WT**, **Batf2$^{-/-}$-CH**, and **WT-CH** mice were percutaneously infected with a dose of 35 *S. mansoni* cercariae and the immune responses were analysed in the liver tissue during week 10 post infection. Quantification of myeloid populations including total DCs, CD11b Dc, eosinophils, and neutrophils analysed using flow cytometry (A – D). Quantification of CD4+ T cells and polarization of the cell types in the liver analysed using flow cytometry (E – H). Quantification of CD8+ T cells and polarization of the cell types in the liver analysed using flow cytometry (I – L). Quantification of cytokine producing CD4+ T lymphocytes re-stimulated with PMA/Ionomycin and analysed on flow cytometry (M - P). Quantification of cytokine producing CD8+ T lymphocytes re-stimulated with PMA/Ionomycin and analysed on flow cytometry (Q - T). Data represents two experiments conducted independently (n = 7-10). The comparison of bar graphs was made using student t test. *p value < 0.05 and **p value < 0.01.

Furthermore, the tissue specific cytokines of the liver tissue were also analysed using ELISA. The concentrations of the tissue cytokines, IL-10 and IFN-γ, were increased in the **WT-CH** mice in relation to those of susceptible **WT** mice, although the differences in IL-10 cytokine concentrations were not significant (figure 22A, B). Interestingly, the inflammatory cytokines, IL-5 and IL-17, which were also increased in the resistant **Batf2$^{-/-}$** mice, were also increased following the microbial transfer in the **WT-CH** mice in relation to the susceptible **WT** mice

(figure 22C, D). However, the concentrations of IL-4, IL13, and TNF-α in **WT-CH** mice were not affected in relation to those of the **WT** mice during the chronic infection indicating that the microbiota had no significant influence on the production of these cytokines during the infection (figure 22E - G). Altogether, the data from tissue specific cytokine profile shows that the microbiota from **Batf2**$^{-/-}$ mice results in altered immune mediators such as IL-10, IL-5, IFN-γ, and IL-17 cytokines.

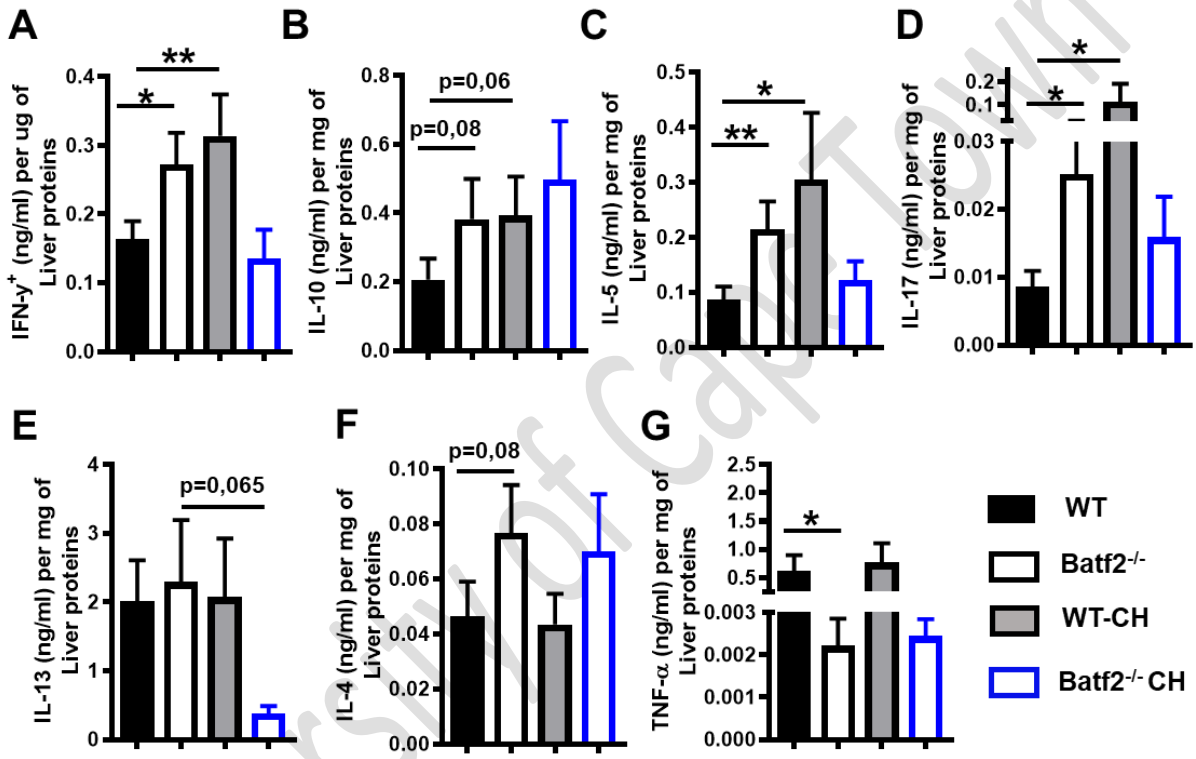

Figure 22: Co-housing results in alterations of hepatic cytokine responses in wild type mice recipient of Batf2$^{-/-}$ intestinal microbiota during chronic Schistosomiasis.

Quantification of liver cytokine concentrations per gram of tissue measured using ELISA (A - G). Data represents two experiments conducted independently (n = 7-10). The comparisons of bar graphs were performed by student t test. *p value < 0.05 and **p value < 0.01.

4.3.1.2. Alterations of intestinal immune responses in wild type mice recipient of Batf2$^{-/-}$ gut microbiota during chronic schistosomiasis.

In terms of the small intestine, the intestinal microbiota of **Batf2**$^{-/-}$ mice resulted in significantly reduced recruitment of CD4+ T cells in **WT-CH** mice in relation to the susceptible **WT** mice during the chronic *S. mansoni* infection (figure 23A). However, the recruitment of the CD8+ T cells in the **WT-CH** mice were not affected in relation to **WT** mice (figure 23B). In the case

of myeloid cell populations including the macrophages and eosinophils, there were no notable differences in the recruitment of these cell populations as result of intestinal microbiota of **Batf2**$^{-/-}$ mice with the eosinophils being increased even further (figure 23C, D). Further analysis showed a significant reduction in Th2 CD4+ and CD8+ T cells (figure 23E – L) as evidenced by the reduction in IL-4, IL-5, IL-13 producing CD4+ T cells (figure 23E - G) as well as the IL-4 and IL-5 producing CD8 T cells in the mesenteric lymph nodes of the **WT-CH** mice in relation to the susceptible **WT** mice during chronic *S. mansoni* infection (figure 23I, J). This therefore showed that the microbiota of **Batf2**$^{-/-}$ mice have a significant role of regulating the small intestinal Th2 granulomatous inflammation during the chronic infection. Additionally, the IFN-γ producing CD8+ T lymphocytes in the **WT-CH** mice were moderately increased in relation to the susceptible **WT** mice (figure 23L). Analysis of the small intestinal tissue-specific cytokine revealed a significantly reduced production of IL-17 and TGF-β cytokines in **WT-CH** mice in relation to the susceptible **WT** mice during the infection indicating the significant impact of the intestinal microbiota of **Batf2**$^{-/-}$ mice on these cytokines in the intestine (figure 23M, N). The overall data from the small intestinal tissue show that the microbiota of **Batf2**$^{-/-}$ mice potentially have a vital role in regulating granulomatous inflammatory immune responses in the tissue during chronic *S. mansoni* infection.

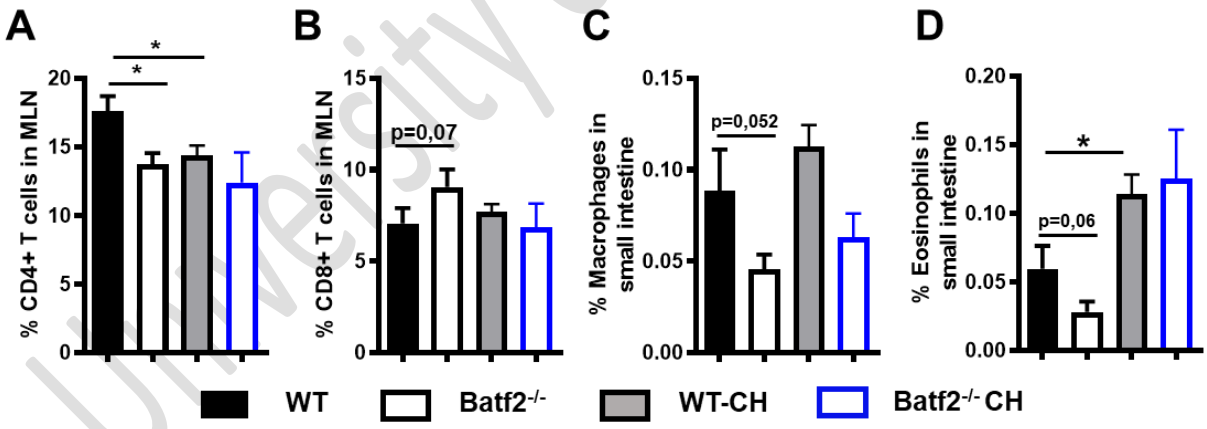

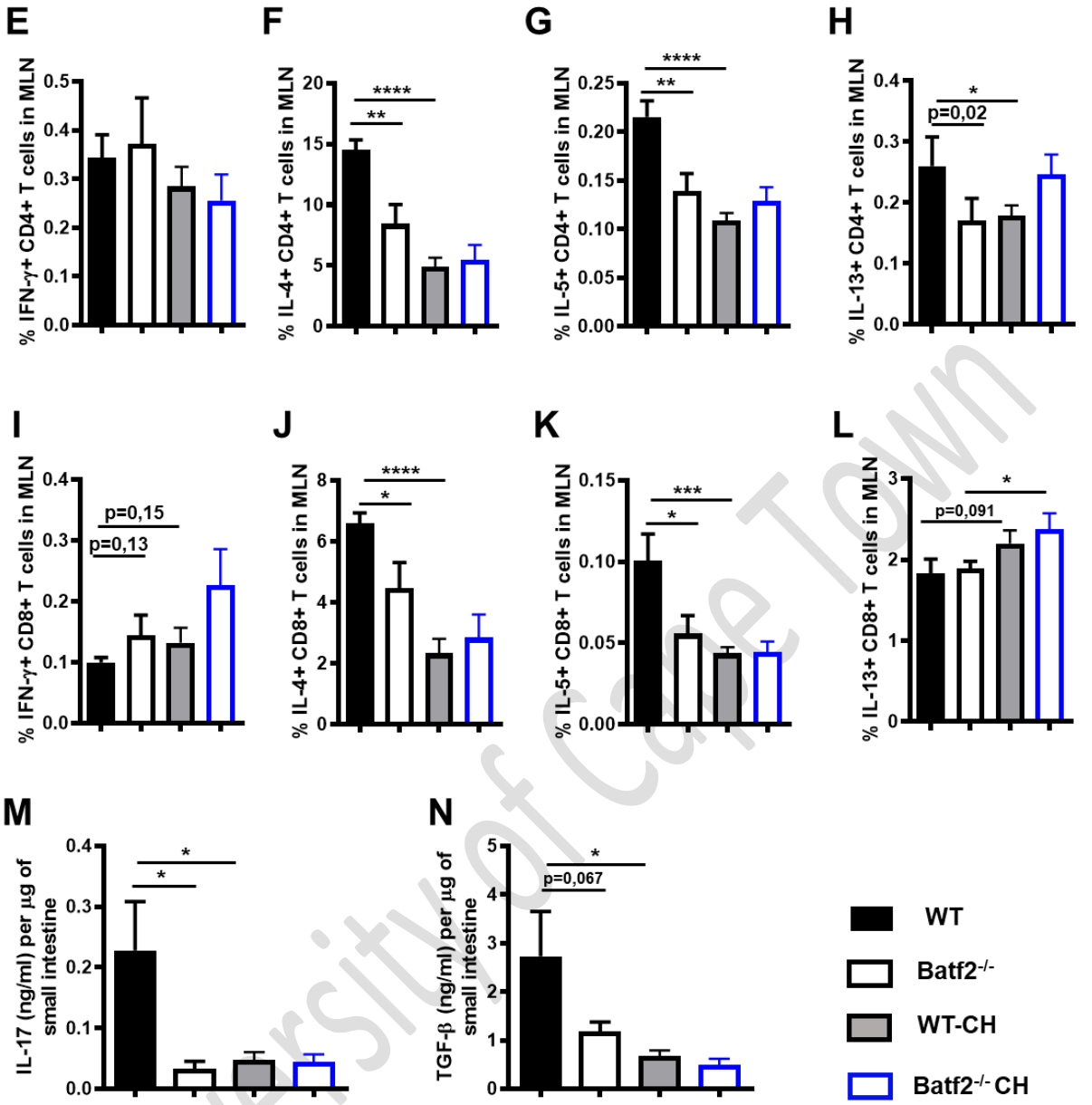

Figure 23: Co-housing results in alterations of intestinal immune responses in wild type mice recipient of Batf2$^{-/-}$ intestinal microbiota during chronic Schistosomiasis.

Quantification of MLN CD4+ (A) and CD8+ (B) T lymphocytes as well as macrophages (C) and eosinophil (D) populations in the small intestine analysed using flow cytometry. Quantification of cytokine producing CD4+ (E - H) and CD8+ (I - L) T lymphocytes from MLN re-stimulated with PMA/Ionomycin and analysed on flow cytometry. Small intestinal cytokine concentrations per gram of tissue measured using ELISA (M, N). Data represents two experiments conducted independently (n = 7-10). The comparisons of bar graphs were performed by student t test. *p value < 0.05 and **p value < 0.01.

4.3.1.3. Alterations of lung immune responses in wild type mice recipient of Batf2$^{-/-}$ intestinal microbiota during chronic schistosomiasis.

In the case of the immune profile in the lung, the intestinal microbiota of **Batf2**$^{-/-}$ mice resulted in significant reduction on the recruitment of mature neutrophils in the **WT-CH** mice in relation to the susceptible **WT** mice during the infection (figure 24A). These immune populations were also prominently reduced in the **Batf2**$^{-/-}$ mice in relation to the **WT** mice indicating a potential role of the commensal microbiota of the **Batf2**$^{-/-}$ mice in regulating the cells during the infection. On the other hand, the microbiota of **Batf2**$^{-/-}$ mice resulted in significantly increased recruitment of eosinophils in **WT-CH** mice in relation to the susceptible **WT** mice (figure 24B). Although, the recruitment of the CD4+ T cells was not affected (figure 24C), their polarization into Th2 subsets were significantly increased in the **WT-CH** mice in relation to the susceptible **WT** mice (figure 24E). Together, these cell populations (Eosinophils and CD4+ gata3+ T cells) were indicative of increased type 2 inflammatory immune response in the **WT-CH** mice in relation to the susceptible **WT** mice during the chronic *S. mansoni* infection. Regarding the CD8+ T cells, their recruitment to the lung tissue was moderately reduced in the **WT-CH** mice in relation to the susceptible **WT** mice during the infection (figure 24G). Despite this reduction, the IL-5 producing CD8+ T cells were significantly increased in the **WT-CH** mice in relation to the susceptible **WT** mice during the infection. The observed increase in IL-5 producing CD8+ T cells were potentially contributing to the increased recruitment of the eosinophils in the **WT-CH** mice reported in figure 24B. With the data presented so far, it is evident that the intestinal microbiota of **Batf2**$^{-/-}$ mice induce alterations to immune responses in the tissue organs that are normally affected by the infection indicating their potential significance for the control of the disease-induced immunopathology.

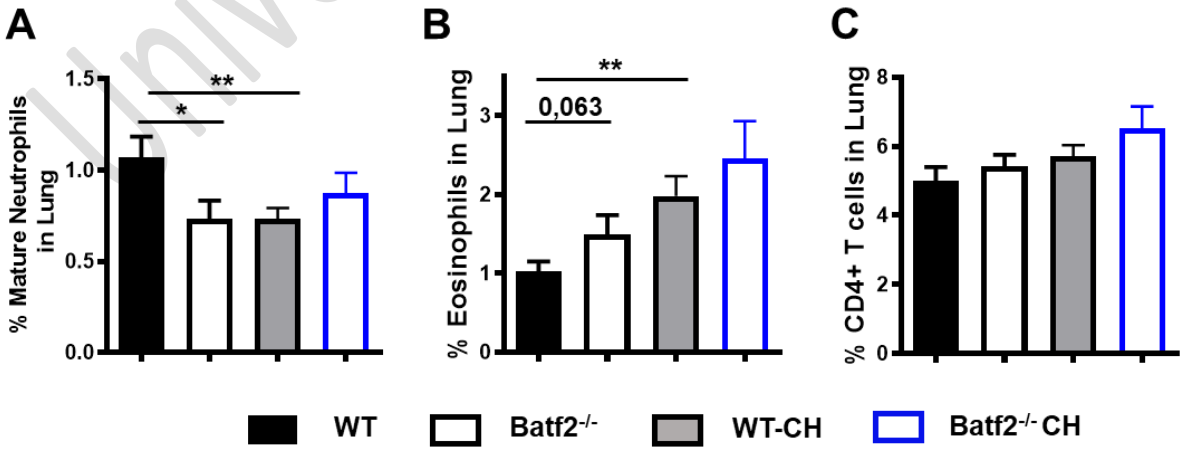

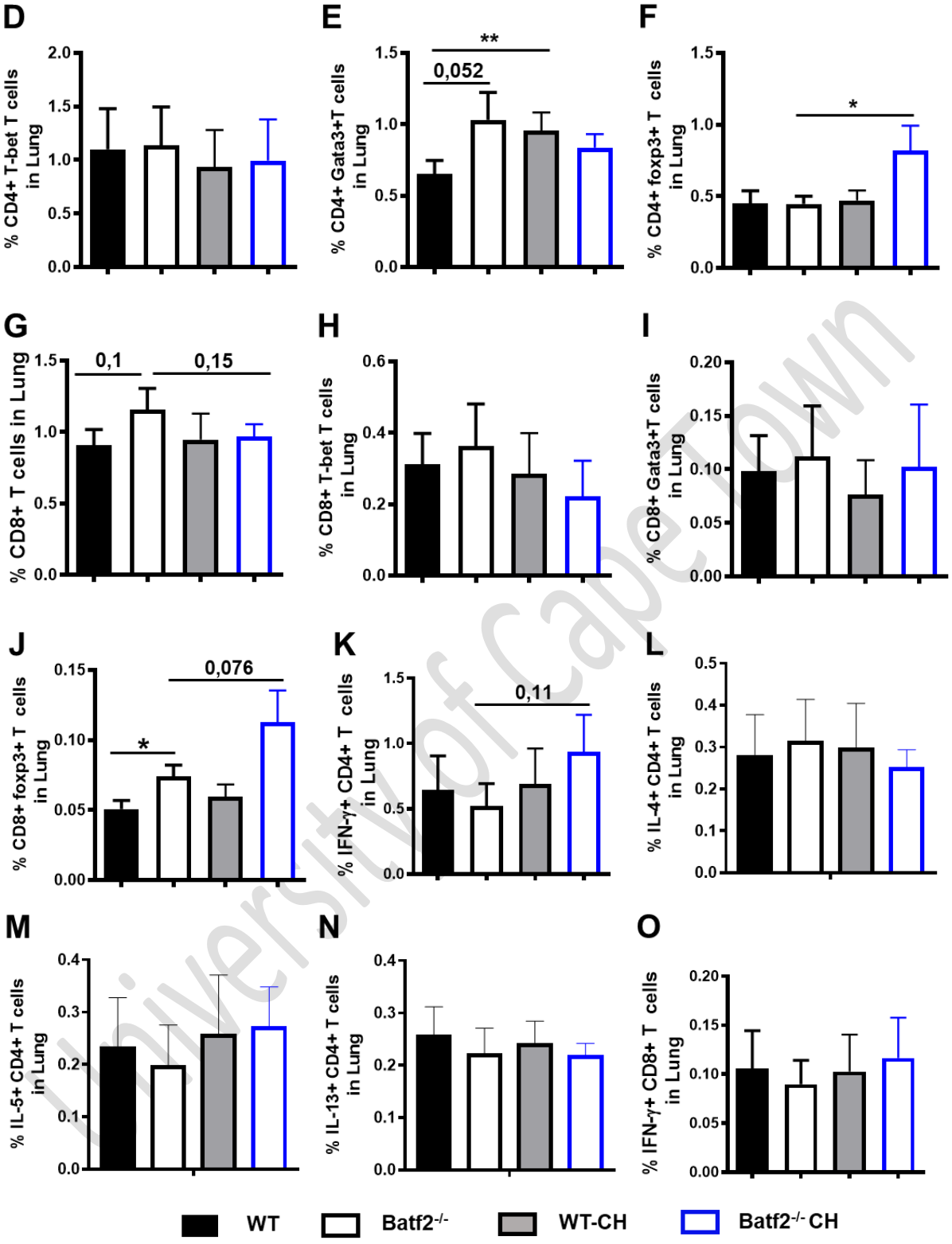

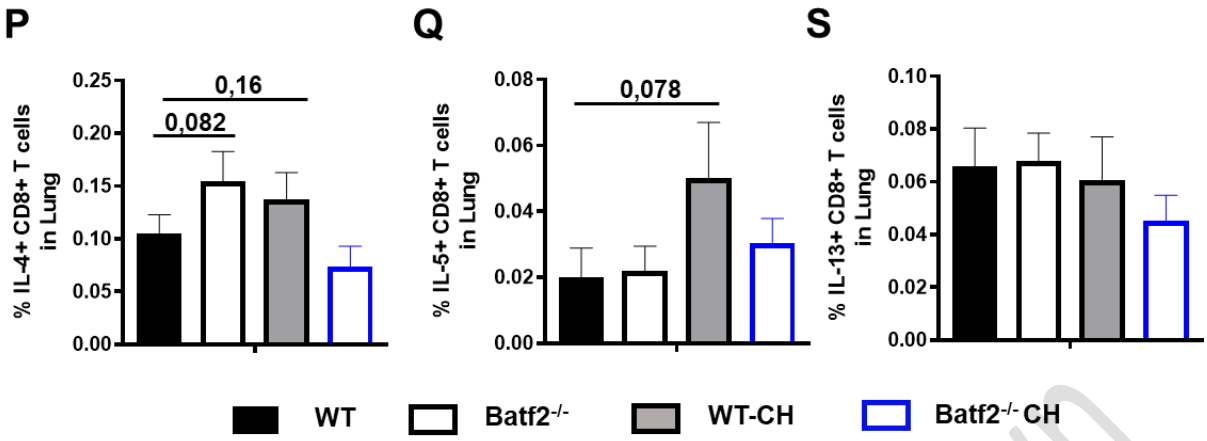

Figure 24: Co-housing results in alterations of lung immune responses in wild type mice recipient of Batf2$^{-/-}$ intestinal microbiota during chronic Schistosomiasis.

Batf2$^{-/-}$, **WT**, **Batf2$^{-/-}$-CH**, and **WT-CH** mice were percutaneously infected with a dose of 35 *S. mansoni* cercariae and the immune responses in the lung tissue were analysed during week 10 post infection. Quantification of percentage myeloid cells mature neutrophils (A) and eosinophils (B) analysed on flow cytometry. Percentage CD4+ T cells (C) and their polarization into Th1 (T-bet+), Th2 (Gata3+), as well as into regulatory (Foxp3+) subsets (D - F). Percentage CD8+ T cells (G) and their polarization into Th1 (T-bet+), Th2 (Gata3+), as well as into regulatory (Foxp3+) subsets (H - J). Quantification of cytokine producing CD4+ T cells re-stimulated with PMA/Ionomycin and analysed on flow cytometry (K - N). Quantification of cytokine producing CD8+ T cells re-stimulated with PMA/Ionomycin and analysed on flow cytometry (O - S). Data represents two experiments conducted independently (n = 7-10). The comparisons of bar graphs were performed by student t test. *p value < 0.05 and **p value < 0.01.

4.3.2. Transfer of the intestinal microbiota from Batf2$^{-/-}$ mice ameliorates the tissue immunopathology in wild type mice during chronic *S. mansoni* infection.

4.3.2.1. Co-housing of wild type mice with Batf2$^{-/-}$ mice results in significantly reduced liver granulomatous immunopathology in wild type mice during chronic S. mansoni infection.

The following objective was to explore whether the immune alterations induced by the microbiota of **Batf2$^{-/-}$** mice would result in any changes to the tissue immunopathology of the infected **WT-CH** mice. In terms of the liver, the altered immune responses in the tissue together with the intestinal microbiota from **Batf2$^{-/-}$** mice resulted in significantly reduced hepatic granulomatous immunopathology in the **WT-CH** mice in relation to the susceptible **WT** mice during the chronic *S. mansoni* infection (figure 25A, B). Furthermore, this was also associated with moderately increased hepatic fibrosis in the **WT-CH** mice (figure 25C, D). This, therefore, showed that the intestinal microbiota from **Batf2$^{-/-}$** mice contributed to the observed reduction in liver immunopathology in both the **Batf2$^{-/-}$** and the **WT-CH** mice during chronic

S. mansoni infection. Conversely, the pathogenesis of **Batf2**$^{-/-}$ and **Batf2**$^{-/-}$**-CH** mice were not affected, which indicated that the intestinal microbiota from the susceptible **WT** mice had no effect on the pathogenesis of the mice during the infection.

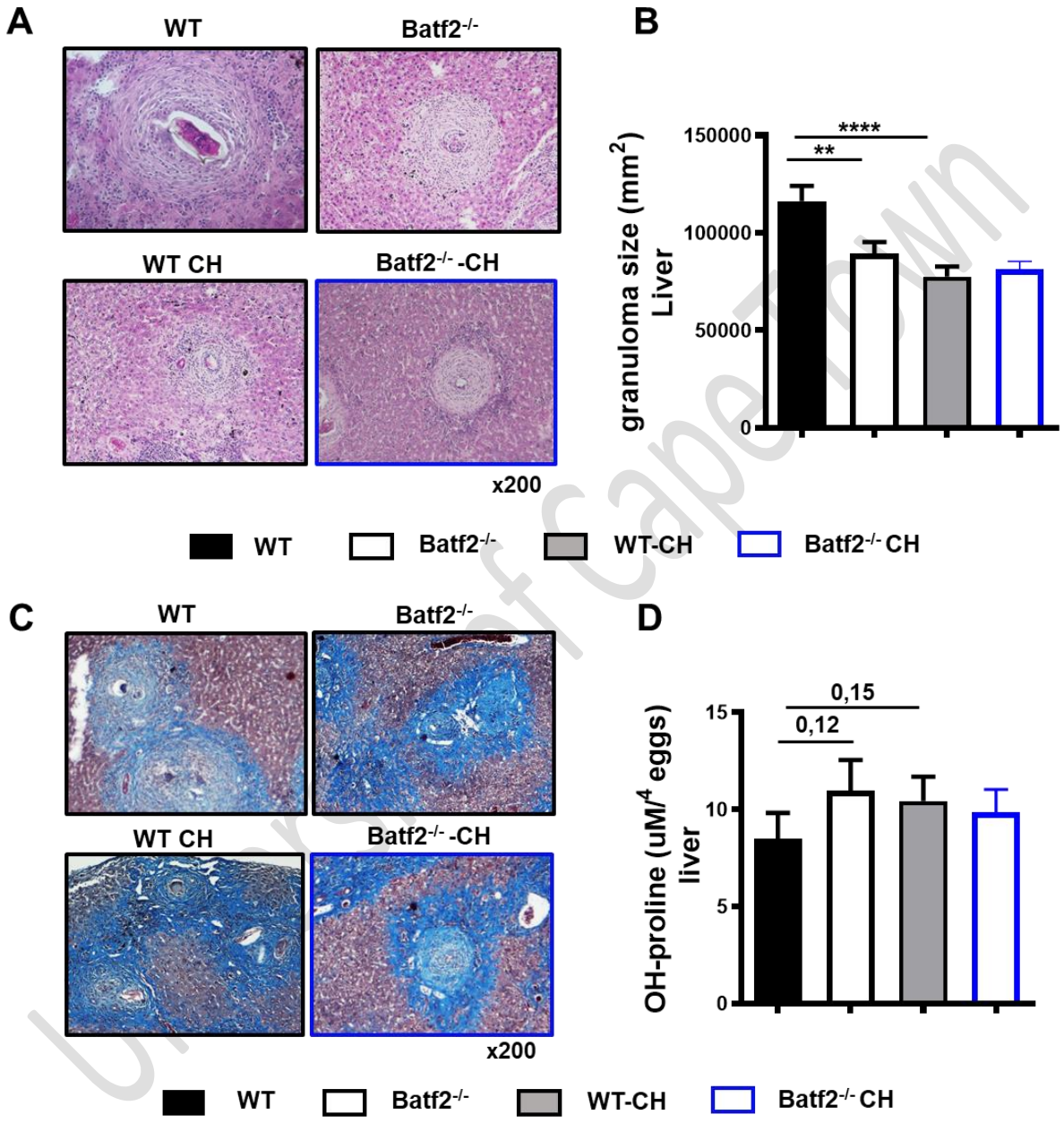

Figure 25: Co-housing of wild type mice with Batf2$^{-/-}$ **mice results in significantly reduced liver granulomatous immunopathology in wild type mice during chronic *S. mansoni* infection.**

Liver sections fixed in formalin were stained with H&E for morphological analysis of the egg-surrounding granuloma (200x) (A). Granuloma measurements quantified using microscopic analysis from H&E-stained sections (B). Liver sections fixed in formalin were stained with CAB staining for morphological analysis of fibrosis development in the liver of infected mice (200x) (C). Fibrosis measurements quantified using

hydroxyproline assay on liver tissues (D). Comparisons of survival curves were performed by Logrank test. The comparisons of bar graphs were performed by student t test. *p value < 0.05 and **p value < 0.01. (n = 7-12).

4.3.2.2. Cohousing of wild type mice with Batf2$^{-/-}$ mice results in increased small intestinal fibrosis in wild type mice during chronic S. mansoni infection.

Further analysis on the small intestinal tissue of the **WT-CH** mice showed no significant differences in the tissue immunopathology in relation to the susceptible **WT** mice during the chronic *S. mansoni* infection (figure 26A, B). This indicated that the immune alterations caused by the microbiota of **Batf2$^{-/-}$** mice had no major influence on the granulomatous immunopathology observed in the small intestinal tissue of the **WT-CH** mice. Despite this, the development of fibrosis was significantly increased in the **WT-CH** mice in relation to the susceptible **WT** mice showing that the microbiota of **Batf2$^{-/-}$** mice do contribute to mechanisms of tissue repair during the infection (figure 26C, D). Altogether, the data show that the microbiota from **Batf2$^{-/-}$**mice contributed a significant role of potentiating the release of fibrosis in the small intestinal tissue of mice during chronic *S. mansoni* infection.

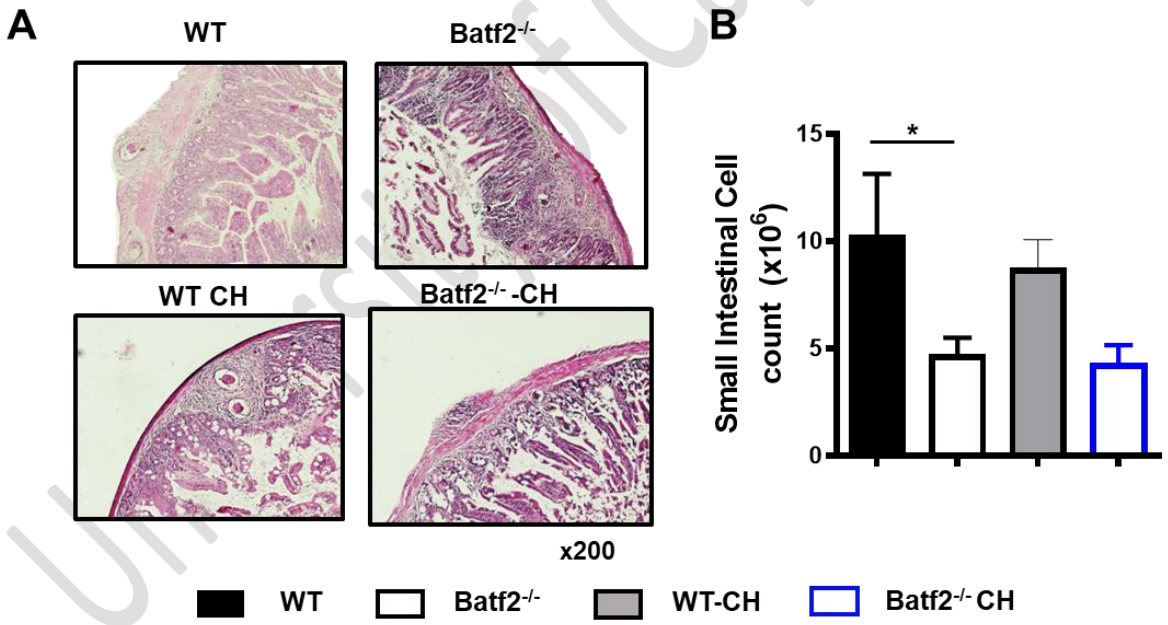

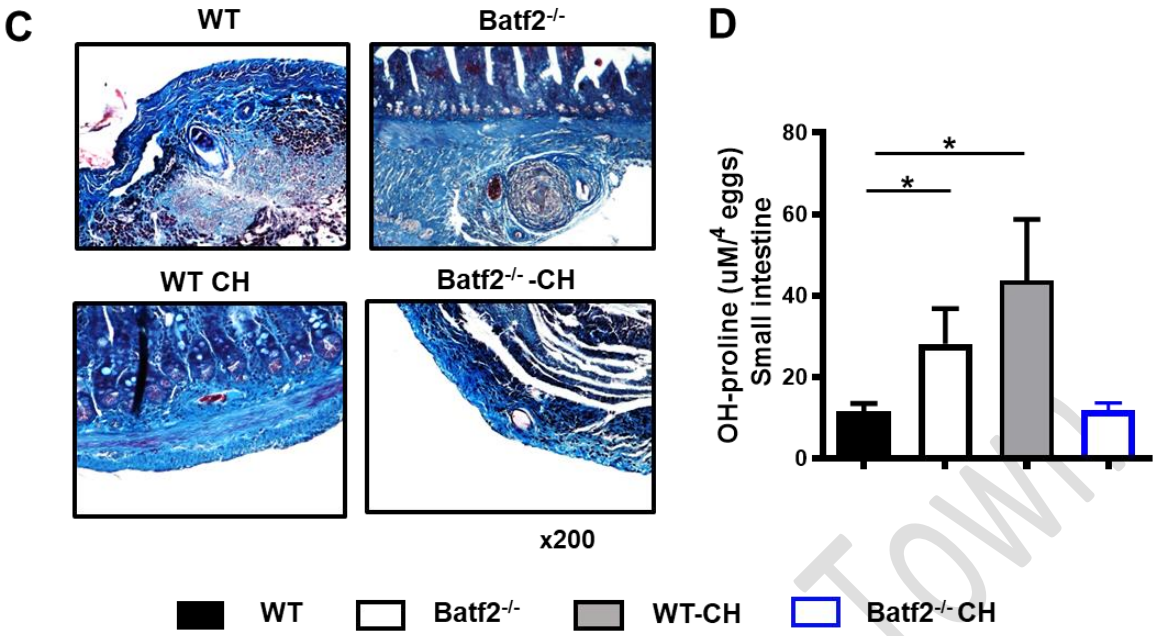

Figure 26: The intestinal microbiota of Batf2$^{-/-}$ mice results in increased small intestinal fibrosis during chronic *S. mansoni* infection.

Formalin-fixed in small intestinal sections stained with H&E for morphological analysis of the cellular recruitment around the trapped *S. mansoni* eggs (200x) (A). Quantification of small intestinal cell counts (B). Formalin fixed small intestinal sections stained with CAB staining for morphological analysis of fibrosis development in the small intestinal of infected mice (200x) (C). Fibrosis measurements quantified using hydroxyproline assay on liver tissues (D). Quantification of *S. mansoni* egg counts (F). Data represents two experiments conducted independently (n = 7-10). The comparisons of bar graphs were performed by student t test. *p value < 0.05 and **p value < 0.01.

4.3.2.3. Co-housing of wild type mice with Batf2$^{-/-}$ mice results in reduced immunopathology of the spleen and lungs in wild type mice during chronic S. mansoni infection.

Lastly, there were no significant differences in liver, lung, and heart indices, as well as the small intestinal lengths between the groups of mice **(WT, WT-CH**, **Batf2$^{-/-}$** and **Batf2$^{-/-}$-CH)** during the infection (figure 27A - E). However, the **WT-CH** mice had significantly reduced splenomegaly in relation to the susceptible **WT** mice during the infection (figure 27E). Although the lung weight was not affected (figure 27B), the tissue cellular count was, however, significantly reduced in the **WT-CH** mice in relation to the susceptible **WT** mice indicating an overall reduction in lung inflammation during the infection (figure 27F). The data, therefore, demonstrate that the immune alterations caused by the microbiota of **Batf2$^{-/-}$** mice were contributing to Schistosomiasis-induced immunopathology.

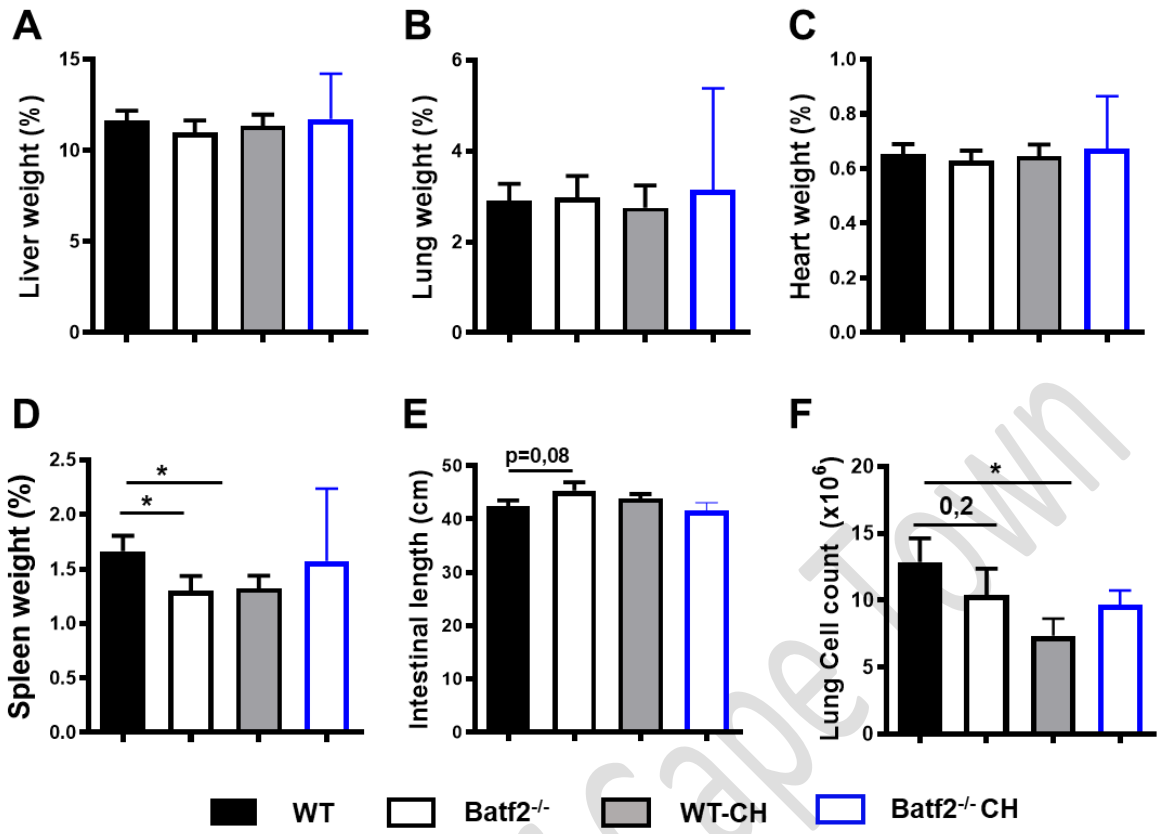

Figure 27: The intestinal microbiota of Batf2$^{-/-}$ mice results in reduced immunopathology of the spleen and lung in mice during chronic *S. mansoni* infection.

WT, WT-CH, Batf2$^{-/-}$-CH and **Batf2$^{-/-}$** mice were infected with a dose of 35 *S. mansoni* cercariae and analysed at week 10 post infection. Liver (A), lung (B), heart (C), and spleen (D) weight indices were measured during chronic *S. mansoni* infection. Quantification of intestinal length in centimetres (E). Quantification of lung tissue cellular count (F). Data represents two experiments conducted independently (n = 7-10). The comparisons of bar graphs were performed by student t test. *p value < 0.05 and **p value < 0.01.

4.3.3. Transfer of the gut microbiota from Batf2$^{-/-}$ mice prolongs the survival of wild type mice during chronic *S. mansoni* infection.

Given all the changes the intestinal microbiota of **Batf2$^{-/-}$** mice induced on tissue-immune responses which lead to the control of the disease-induced immunopathology during chronic Schistosomiasis, it was still to be determined if all these changes would affect the susceptibility of the mice to the infection. To confirm this, the mice were percutaneously infected with a low of 35 *S. mansoni* cercariae to induce chronic infection and were monitored throughout until each mouse succumbed to the infection. Interestingly, the susceptibility of the **WT-CH** mice was significantly reduced in relation to the **WT** mice (figure 28A). This was a result of the **Batf2$^{-/-}$** mice-intestinal microbiota and not due to differences in infection intensity (figure 28B, C). However, the microbiota from the susceptible **WT-CH** mice did not affect or reduce the

survival of **Batf2$^{-/-}$-CH** mice in relation to the **Batf2$^{-/-}$** mice, and this further indicated that the microbiota of **WT** mice had no major influence on the pathogenesis and susceptibility of the mice during chronic Schistosomiasis and this was indicative of a unidirectional transfer of the causal intestinal microbiota during the infection (figure 28A). What has been demonstrated at this point is that the removal of Batf2 induces changes in the commensal microbiota which contributes to the increased resistance of the mice during chronic *S. mansoni* infection. Altogether, the data highlights the interrelationship that exist between the host factor (Batf2), and the commensal microbiota on the susceptibility of mice during chronic *S. mansoni* infection.

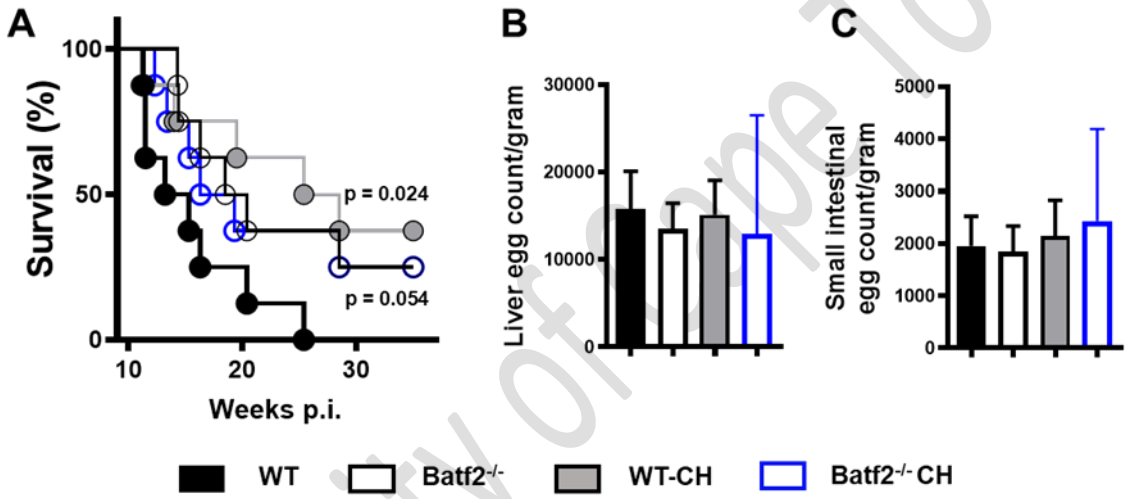

Figure 28: The microbiota from Batf2$^{-/-}$ mice contribute to increased resistance of mice during chronic *S. mansoni* infection.

The survival **of WT, WT-CH, Batf2$^{-/-}$-CH** and **Batf2$^{-/-}$** mice during chronic *S. mansoni* infection were compared(A). Quantification of *S. mansoni* eggs comparing the worm burden in the small intestinal tissue (B) as well the liver (C) during the infection. Data represents two experiments conducted independently (n = 7-12). Comparison of survival curves was made using Logrank test. The comparisons of bar graphs were performed by student t test. *p value < 0.05 and **p value < 0.01.

5. Part 2 of the results:

The role of the intestinal microbiota in the regulation of immunopathology during chronic Schistosomiasis.

5.1. Exacerbated immunopathogenesis of C57BL/6 mice housed under SPF facility during chronic Schistosomiasis.

Another interesting observation was made during a preliminary experiment that was performed prior to the current study, where **C57BL/6** mice from Specific Pathogen Free 2 (SPF2) facility of the University of Cape Town, were used to explore and understand the influence of Praziquantel on Schistosomiasis-induced immunopathology (Nono et al., 2020). The mice were percutaneously infected with a low dose of 35 *S. mansoni* cercariae and were to be monitored as per AEC approved protocol 016/027 for more than 10 weeks before administering praziquantel to the infected mice. The mice responded well to the infection for the first 7 weeks with no observable signs of distress and displayed a stable weight gain as is normally expected with Schistosomiasis infected mice (Figure 29A). Unexpectedly, the infected mice rapidly became lethargic and severely started losing weight from week 7 post infection onwards. The mice prematurely succumbed to the infection at a rapid rate of 6 mice dying within 3 days during week 7 to week 8 post infection. Surprisingly, the premature mortality of these mice was not a result of a technical error where a higher pathogenic dose of infecting *S. mansoni* cercariae was administered as evidenced by even a lower parasite infiltration in the liver tissue (figure 29B). Despite the low dose of infection, the mice still resulted in increased liver granulomatous immunopathology that was characteristic of the Schistosomiasis disease (figure 29C) indicating that the reported mortality was mediated in response to the infection. These observations, therefore, warranted a more in-depth investigation to understand further the cause of early mortality.

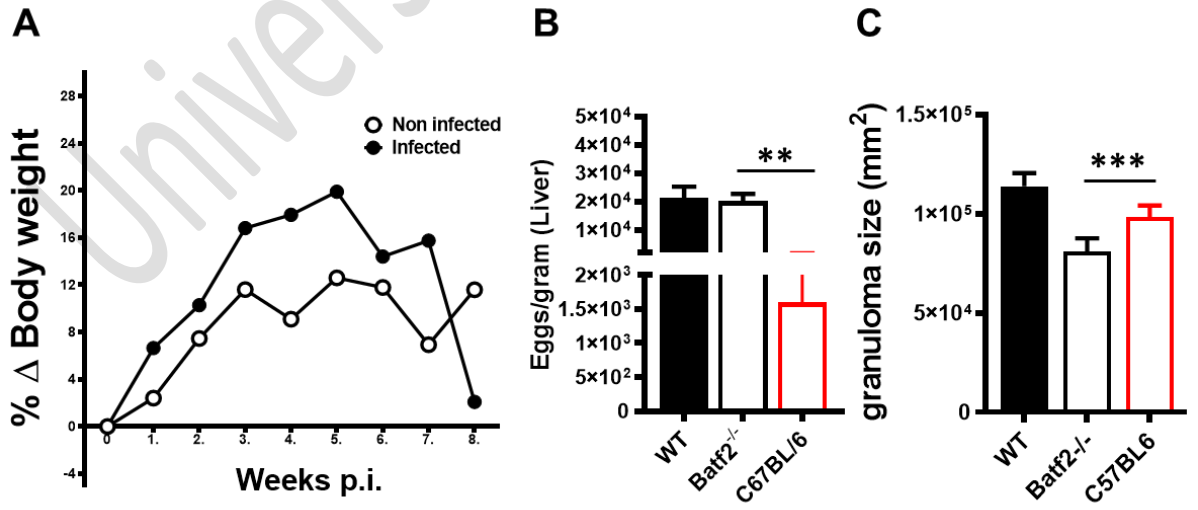

Figure 29: Confirmation of low-dose infection by assessment of body weight and liver immunopathology of C57BL/6 mice.

Liver egg burden from the Batf2 experiment taken from figure 12 that were infected with a low dose of 35 *S. mansoni* cercariae (Black and white filled bars) were compared to liver egg burden of C57BL/6 mice from a low dose infection of 35 *S. mansoni* cercariae per infection (Red bar). The bar graphs were compared using student t test. *p value < 0.05 and **p value < 0.01.

It was hypothesised that the increased susceptibility of these **SPF2 C57BL/6** mice (**C57BL/6 from SPF2**) was potentially driven by their intestinal microbiota composition. To test this, the **SPF2 C57BL/6** mice were compared to **C57BL/6** mice that were originating from another facility at the institute called the Specific Pathogen Free 1 (SPF1) facility. The comparison was made because of a previous demonstration that mice which originate from different environmental backgrounds result in commensal microbiota that are distinct from each other (Velazquez, 2019). The current study, therefore, aimed to extensively assess whether the observed susceptibility of the **SPF2 C57BL/6** mice was different from that of the **SPF1 C57BL/6** mice and potentially report on the influence of microbiota to the susceptibility of these mice during chronic Schistosomiasis.

5.2. Comparative survival of genetically identical mice housed in two different specific-pathogen-free facilities during chronic *S. mansoni* infection.

5.2.1. Differential susceptibility of genetically identical mice housed under two different specific-pathogen-free facilities.

The first objective was to test out if there were differences in susceptibility between the **SPF1** and **SPF2 C57BL/6** mice during chronic *S. mansoni* infection, and for this the mice were percutaneously infected with a low dose of 35 *S. mansoni* cercariae. We noted that the **SPF1 C57BL/6** mice were more resistant to the chronic infection in relation to the **SPF2 C57BL/6** mice showing that there were differences which contributed to the susceptibility of **C57Bl/6** mice during chronic *S. mansoni* infection (Figure 30A). The differences in susceptibility were not caused by the trapped egg burden as there were similar liver egg counts between the mice (figure 30B).

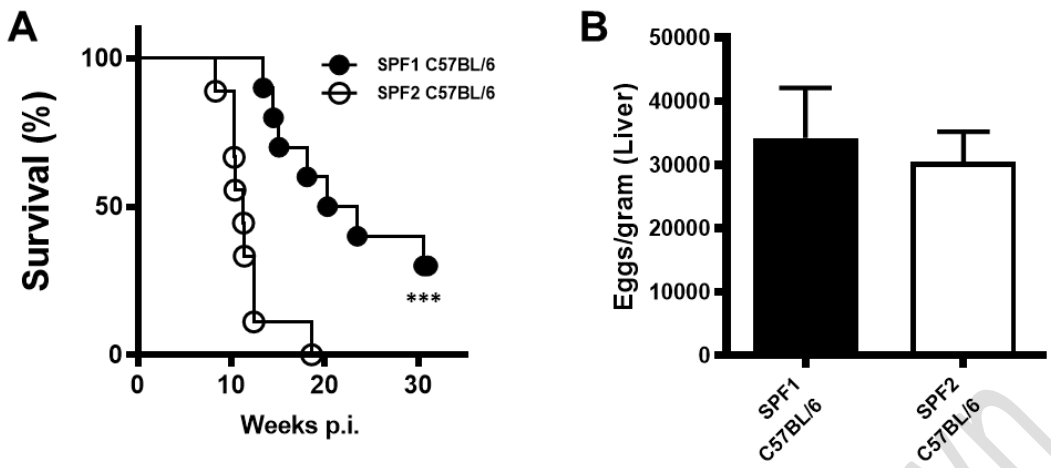

Figure 30: Differential susceptibility of genetically identical mice housed under two different specific-pathogen-free facilities.

The survival of **SPF1 C57BL/6** mice was compared to that of **SPF2 C57BL/6** mice during chronic *S. mansoni* infection (A). Quantification of *S. mansoni* eggs comparing the worm burden between **SPF1** and **SPF2 C57BL/6** mice during the infection (B). Data represents two experiments conducted independently (n = 7-12). Comparison of survival curves were performed by Logrank test. The comparisons of bar graphs were performed by student t test. *p value < 0.05 and **p value < 0.01.

5.2.2. Increased granulomatous immunopathology around trapped eggs in tissues of susceptible mice (SPF2 C57BL/6) during chronic *S. mansoni* infection.

5.2.2.1. Increased liver granulomatous response and reduced formation of fibrotic walls around trapped eggs in the liver of susceptible mice during chronic S. mansoni infection.

The immunopathological features that were associated with the differences in susceptibility of the **SPF1** and **SPF2 C57BL/6** mice to chronic *S. mansoni* infection were explored. In terms of the liver pathology there was a significantly increased granulomatous immunopathology around the trapped *S. mansoni* eggs in the susceptible **SPF2 C57BL/6** mice in relation to the resistant **SPF1 C57BL/6** mice during the chronic infection (figure 31A, B). The observed increase in liver granulomatous immunopathology was associated with moderately reduced levels of hydroxyproline in the tissue (figure 31C, D). Altogether, the susceptibility of **SPF2 C57BL/6** mice was linked with significantly increased granulomatous immunopathology and reduced fibrosis in the liver tissue in relation to the resistant **SPF1 C57BL/6** mice during the chronic *S. mansoni* infection.

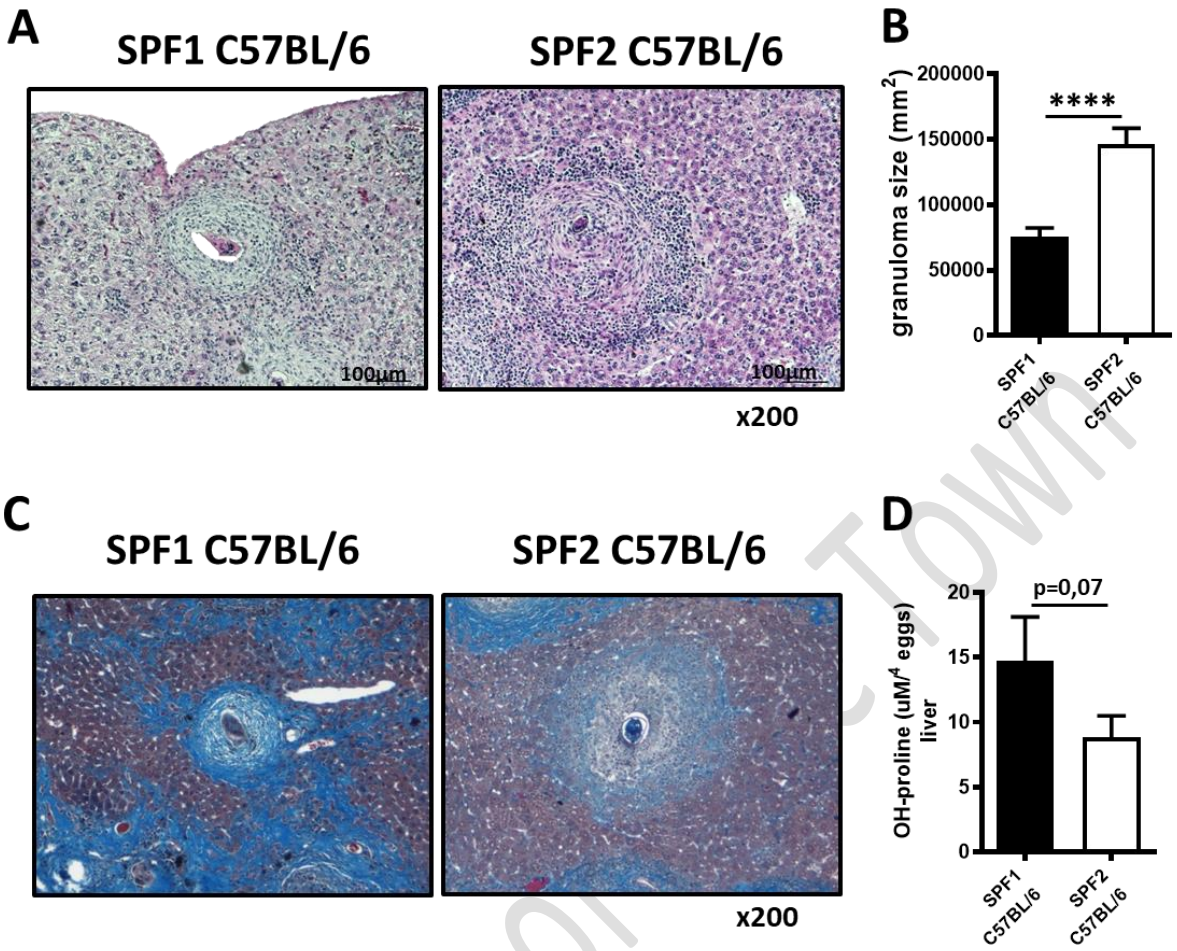

Figure 31: Increased liver granulomatous response and reduced formation of fibrotic walls around trapped eggs in the liver of susceptible mice (SPF2 C57BL/6) during chronic *S. mansoni* infection.

SPF1 and **SPF2 C57BL/6** mice were infected percutaneously with a dose of 35 *S. mansoni* cercariae and analysed at week 10 post infection. Liver sections fixed in formalin were stained with H&E for morphological analysis of the egg-surrounding granuloma (200x) (A). Granuloma measurements quantified using microscopic analysis from H&E-stained sections (B). Liver sections fixed in formalin were stained with CAB staining for morphological analysis of fibrosis development in the liver of infected mice(200x) (C). Fibrosis measurements quantified using hydroxyproline assay on liver tissues (D). Data represents two experiments conducted independently (n = 7-10). The comparisons of bar graphs were performed by student t test. *p value < 0.05 and **p value < 0.01.

5.2.2.2. Increased granulomatous responses around trapped eggs in the intestine of susceptible mice during chronic S. mansoni infection.

Further analysis on immunopathology of the small intestinal tissue from the mice during the chronic *S. mansoni* infection revealed that the resistant **SPF1 C57BL/6** mice had significantly reduced recruitment of cells surrounding the *S. mansoni* eggs (figure 32A) as well as intestinal cellular count (figure 32B) in relation to the susceptible **SPF2 C57BL/6** mice. This indicated

a significantly reduced small intestinal inflammatory immunopathology of the resistant **SPF1 C57BL/6** mice in relation to the susceptible **SPF2 C57BL/6** mice during the infection. However, there were no differences in the formation of fibrosis as evidenced by similar CAB staining (figure 32C) as well as hydroxyproline levels (figure 32D) in the small intestinal tissue of both **SPF1** and **SPF2 C57BL/6** mice. The effects observed in the small intestinal tissue were not a result of differences in the worm burden in the tissue (figure 32E).

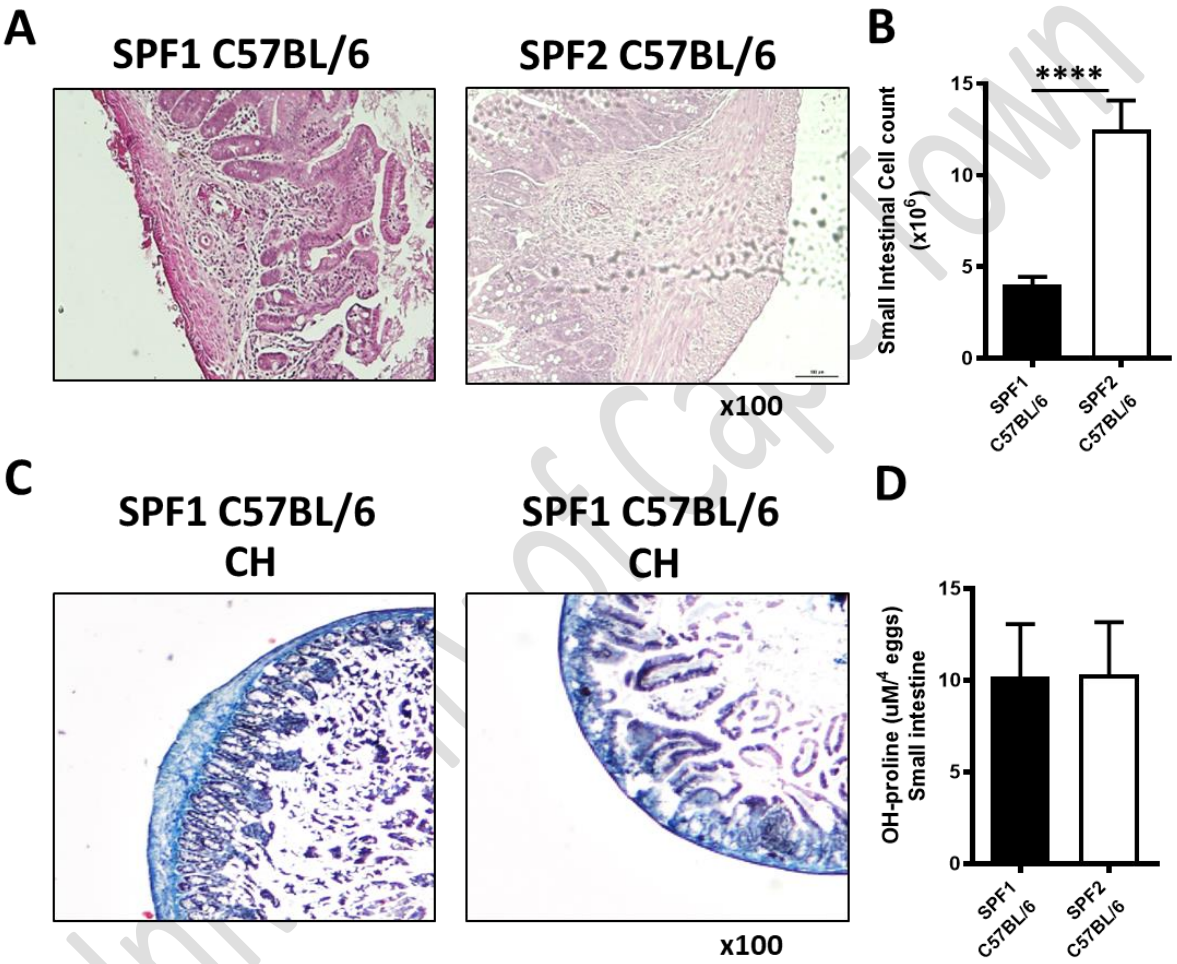

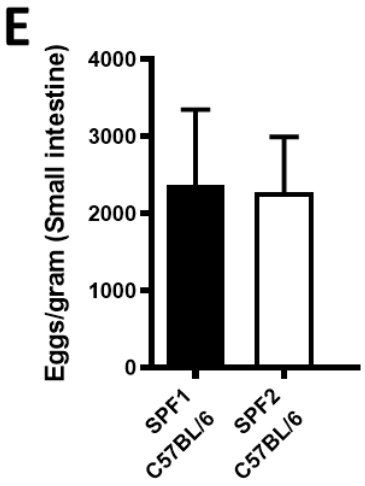

Figure 32: Increased granulomatous responses around trapped eggs in the intestine of susceptible mice chronic *S. mansoni* infection.

Small intestinal sections were formalin-fixed and stained with H&E for morphological analysis of the cellular recruitment around the trapped *S. mansoni* eggs (100x) (A). Quantification of small intestinal cell counts (B). Formalin fixed small intestinal sections stained with CAB staining for morphological analysis of fibrosis development in the small intestinal of infected mice (200x) (C). Fibrosis measurements quantified using hydroxyproline assay on liver tissues (D). Quantification of *S. mansoni* egg counts (E). Data represents two experiments conducted independently (n = 7-10). The comparisons of bar graphs were performed by student t test. *p value < 0.05 and **p value < 0.01.

5.2.2.3. Reduced lung weight index in susceptible mice during chronic S. mansoni infection.

Further analysis revealed that there were no major differences observed in organ weight indexes such as the liver, heart, and spleen (figure 33A - C). Interestingly, the lung weight indexes of **SPF2 C57BL/6** mice were significantly reduced in relation to that of **SPF1 C57BL/6** mice during the infection (figure 33D). However, despite this reduction, the lung cellular count was significantly increased in the susceptible **SPF2 C57BL/6** mice in relation to the resistant **SPF1 C57BL/6** mice (figure 33E). Considering all this, it can be concluded that the differences in susceptibility of the C57BL/6 mice from different SPF facilities are in part attributed to the lung immunopathology together with the liver and the small intestinal immunopathology during chronic Schistosomiasis.

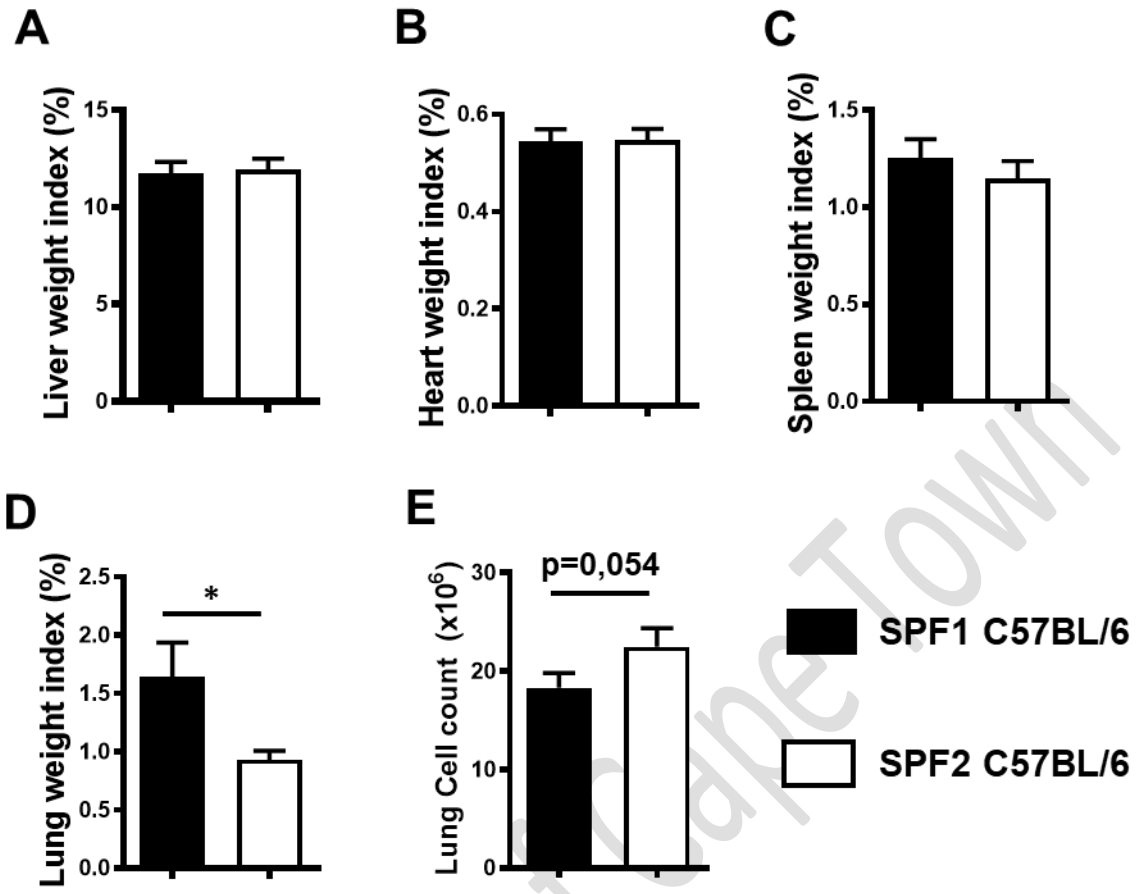

Figure 33: Reduced lung index in susceptible mice during chronic *S. mansoni* infection.

SPF1 C57BL/6 and **SPF2 C57BL/6** mice were infected percutaneously with a dose of 35 *S. mansoni* cercariae and analysed at week 10 post infection. Liver (A), heart (B), spleen (C), and lung (D) weights were measured during chronic *S. mansoni* infection. Quantification of lung cellular count (E). Data represents two experiments conducted independently (n = 7-10). The comparisons of bar graphs were performed by student t test. *p value < 0.05 and **p value < 0.01.

5.2.3. Tissue immune alterations in response to chronic *S mansoni* infection of genetically identical mice housed under two different specific-pathogen-free facilities.

5.2.3.1. Liver immune responses.

The immune profiles that were associated with the immunopathology of the liver of both the **SPF1** and **SPF2 C57BL/6** mice were analysed (figure 34). Looking at the recruited T lymphocytes, there susceptible **SPF2 C57BL/6** mice had significantly increased levels of CD8+ T cells in relation to those of the resistant **SPF1 C57BL/6** mice during the chronic *S. mansoni* infection, and the populations of CD4+ T cells were not affected or different (figure 34A). In the case of myeloid populations, the susceptible **SPF2 C57BL/6** mice had significantly increased recruitment of eosinophils, while the recruitment of other myeloid cells

such as the neutrophils, total dendritic cells (DCs) as well as CD11b+ DCs, were significantly reduced in relation to those of the resistant **SPF1 C57BL/6** mice (figure 34B). The data show that there was a dysregulated recruitment of protective immune populations forming the granuloma structure around the trapped *S. mansoni* eggs in the susceptible **SPF2 C57BL/6** mice in relation to the resistant **SPF1 C57BL/6** mice during the infection. Additionally, even though the recruitment of the CD4+ T cells was not affected, their polarization into Th2 (gata3) subsets was significantly increased in the susceptible **SPF2 C57BL/6** mice in relation to the resistant **SPF1 C57BL/6** mice (figure 34C). Polarization of these cells into other subtypes such as Th1 (T-bet) and regulatory (foxp3) subsets were not affected (figure 34C). The CD8+ T cells on the other hand had significantly increased polarization of both Th1 (T-bet) and Th2 (gata3) subsets while the regulatory CD8+ T cells were not affected in the susceptible **SPF2 C57BL/6** mice in relation to those of the resistant **SPF1 C57BL/6** mice (figure 34D). The effector functions of the CD4+ T cells were similar for both the susceptible **SPF2 C57BL/6** and the resistant **SPF1 C57BL/6** mice with the production of IFN-γ and IL-13 being moderately reduced (figure 34E). The CD8+ T cells producing IFN-γ were significantly reduced, while the IL-5 producing CD8+ T cell were only moderately reduced in the susceptible **SPF2 C57BL/6** mice (figure 34F). The IL-13 producing CD8+ T cells were increased in the susceptible **SPF2 C57BL/6** mice in relation to the resistant **SPF1 C57BL/6** mice during the infection (figure 34F).

In terms of the tissue specific cytokines, the susceptible **SPF2 C57BL/6** mice had moderately increased inflammatory cytokines such as TNF-α, IL-13, IL-17, and significantly increased TGF-β and IL-10 in the tissue in relation to those of the resistant **SPF1 C57BL/6** mice (figure 34G, H). Despite this, the tissue immune alterations resulted in increased liver immunopathology observed in the susceptible **SPF2 C57BL/6** mice in relation to the resistant **SPF1 C57BL/6** during chronic *S. mansoni* infection.

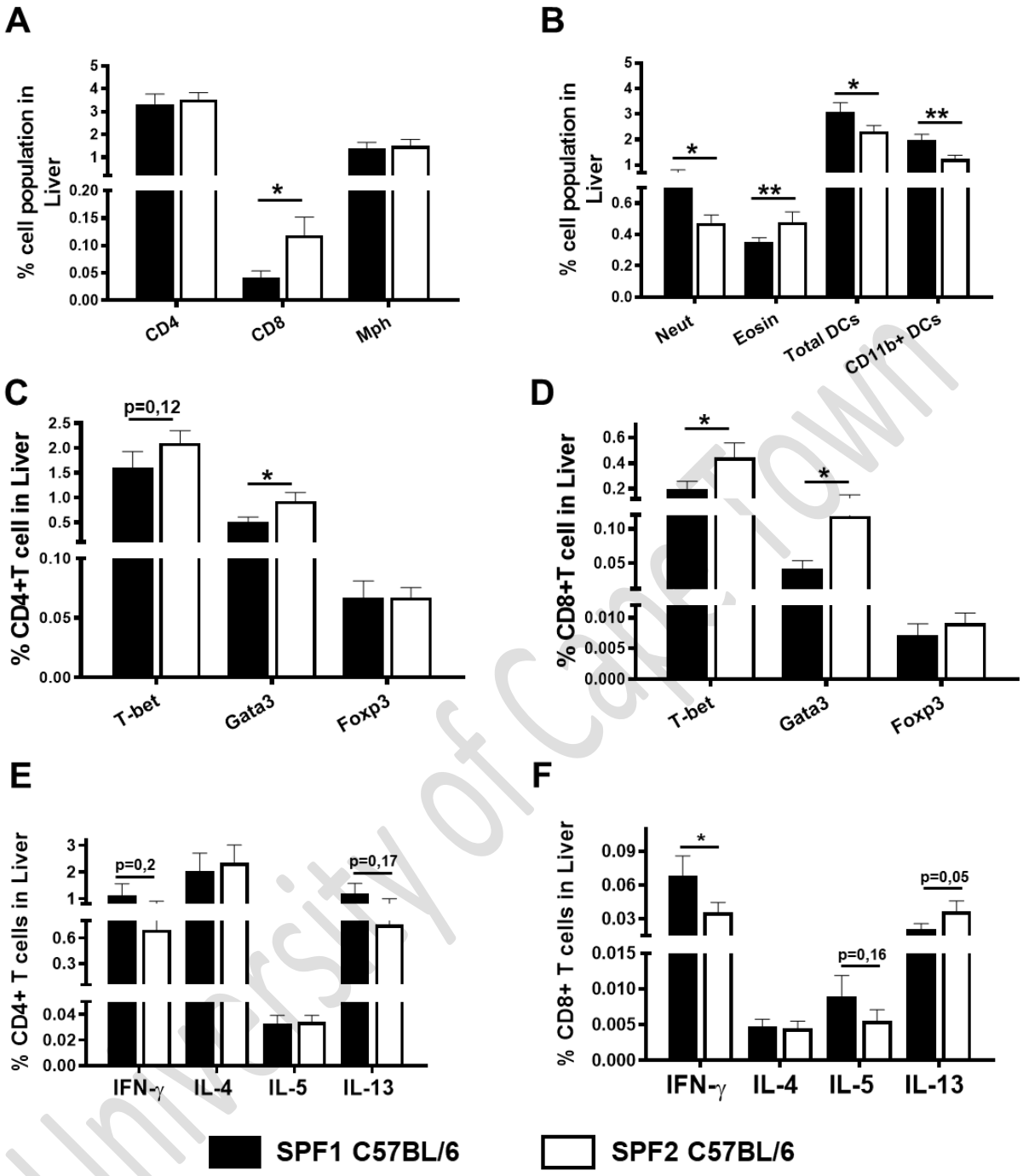

Figure 34: Altered hepatic immune responses in susceptible SPF2 C57BL/6 mice when compared to the resistant SPF1 C57BL/6 during chronic *S. mansoni* infection.

SPF2 and SPF1 C57BL/6 mice were infected percutaneously with a dose of 35 *S. mansoni* cercariae and the immune responses were analysed in the liver tissue during week 10 post infection. Quantification of immune cellular populations analysed using flow cytometry (A, B). Quantification of CD4+ (C) and CD8+ (D) T lymphocyte polarization during the infection analysed using flow cytometry. Quantification of cytokine producing CD4+ (E) and CD8+ (F) T lymphocytes re-stimulated with PMA/Ionomycin and analysed on flow cytometry. Liver cytokine concentrations per gram of tissue measured using ELISA (G, H). Data represents two experiments conducted independently (n = 7-10). The comparisons of bar graphs were performed by student t test. *p value < 0.05 and **p value < 0.01.

5.2.3.2. Small intestinal immune response

In terms of the immune profile that was associated with small intestinal immunopathology during chronic *S. mansoni* infection, there was a significantly increased recruitment of CD4+, CD8+ T cells in the mesenteric lymph nodes (figure 35A), and small intestinal macrophages, and eosinophils in the susceptible **SPF2 C57BL/6** mice in relation to the resistant **SPF1 C57BL/6** mice during chronic *S. mansoni* infection (figure 35B). The polarization of both CD4+ and CD8+ T cell into Th1 (T-bet) and Th2 (gata3) subsets were significantly increased in these susceptible **SPF2 C57BL/6** mice (figure 35C, D). There was also a significantly increased regulatory subsets (foxp3) of CD4+ T cells (figure 35C) in the susceptible **SPF2 C57BL/6** mice in relation to the resistant **SPF1 C57BL/6** mice, while those of CD8+ T cells were similar (figure 35D). Although the susceptible **SPF2 C57BL/6** mice had increased polarization of the T lymphocytes, their ability to release inflammatory cytokines (IL-4, IL-5, IL-13) were significantly reduced in both CD4+ and CD8+ T cells in relation to those of the resistant **SPF1 C57BL/6** mice (figure 35E, F). However, the overall production of inflammatory cytokines (figure 35G, H) in the small intestinal tissue were not reduced between the mice during chronic *S. mansoni* infection. The levels of IL-4 cytokines were significantly reduced in the susceptible **SPF2 C57BL/6** mice in relation to the resistant **SPF1 C57BL/6** mice (figure 35G). A type 1 inflammatory cytokine such as TNF-α was significantly increased (figure 35G) while the regulatory IL-10 (figure 35H) cytokine was moderately reduced in the tissue of the susceptible **SPF2 C57BL/6** mice in relation to those of the resistant **SPF1 C57BL/6** mice during chronic *S. mansoni* infection. Altogether, the increased immunopathology observed in the small intestinal tissue of **SPF2 C57BL/6** mice was a result of increased inflammatory immune response during the infection.

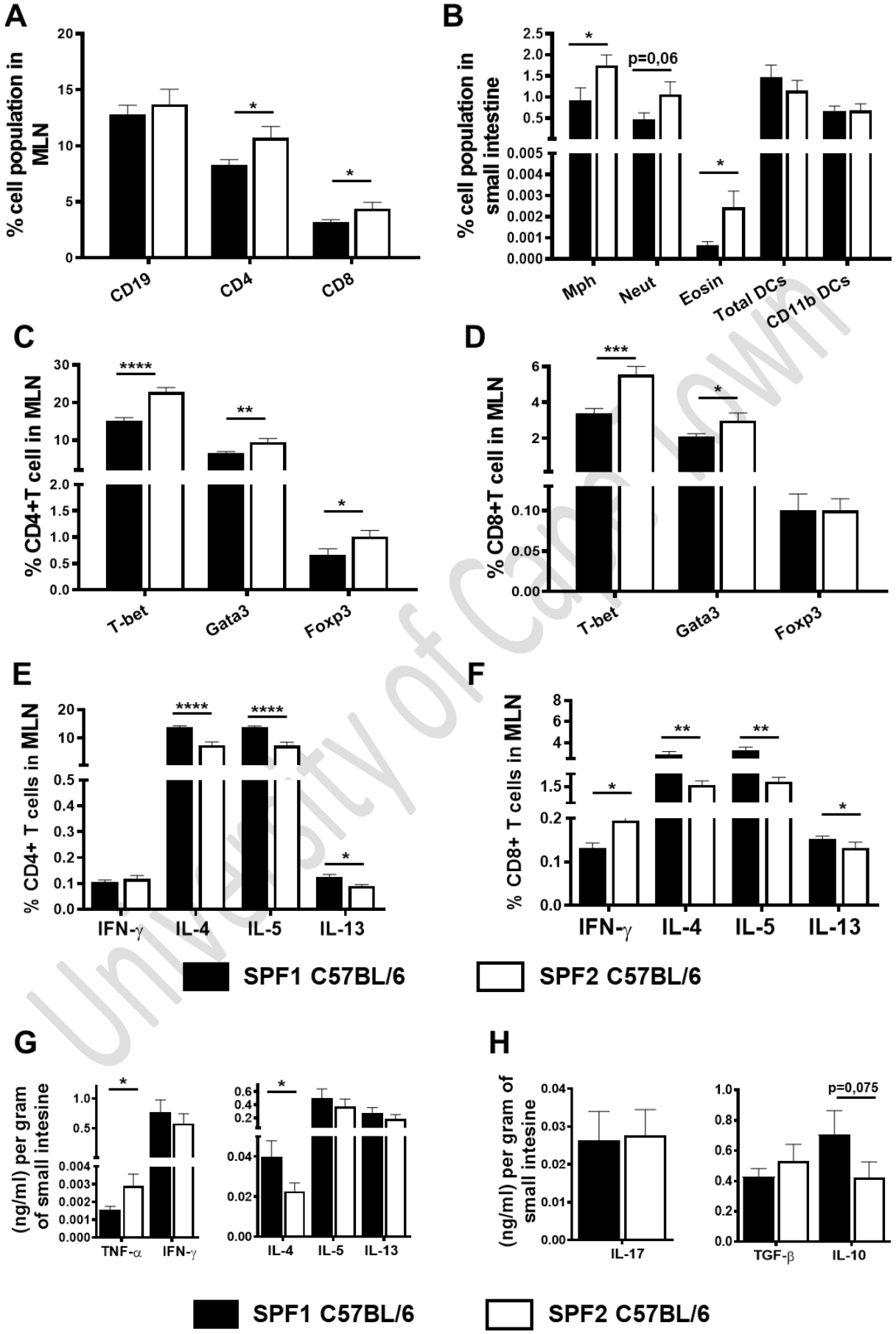

Figure 35: Altered small intestinal immune responses in susceptible SPF2 C57BL/6 mice when compared to the resistant SPF1 C57BL/6 during chronic *S. mansoni* infection.

SPF1 and **SPF2 C57BL/6** mice were infected percutaneously with a dose of 35 *S. mansoni* cercariae and the immune responses were analysed in the small intestinal tissue and mesenteric lymph nodes (MLN) during week 10 post infection. Quantification of MLN lymphocytes (A) and myeloid cellular populations in the small intestine (B) analysed using flow cytometry. Quantification of MLN CD4+ (C) and CD8+ (D) T lymphocyte polarization during the infection analysed using flow cytometry. Quantification of cytokine producing CD4+ (E) and CD8+ (F) T lymphocytes from MLN re-stimulated with PMA/Ionomycin and analysed on flow cytometry. Small intestinal cytokine concentrations per gram of tissue measured using ELISA (G, H). Data represents two experiments conducted independently (n = 7-10). The comparisons of bar graphs were performed by student t test. *p value < 0.05 and **p value < 0.01.

5.2.3.3. Lung immune responses

The immune profile that was associated with the lung immunopathology of the susceptible and resistant **SPF1** and **SPF2 C57Bl/6** mice respectively were analysed during the chronic *S. mansoni* infection. The increased lung cellular count in the susceptible **SPF2 C57Bl/6** mice was linked with increased recruitment of CD8+ T populations, macrophages, immature and as well as mature neutrophils in the lung tissue during the infection (figure 36A, B). Further analysis on polarization of the lymphocytes revealed that the CD4+ T cells in the susceptible **SPF2 C57Bl/6** mice was comparable to those of the resistant **SPF1 C57Bl/6** mice during the infection (figure 36C). Conversely, the polarization of CD8+ T cells into Th1 (T-bet) and Th2 (gata-3) subsets were significantly increased in the susceptible **SPF2 C57Bl/6** mice in relation to resistant **SPF1 C57Bl/6** mice (figure 36D). However, the regulatory subset of the CD8+ T cells in **SPF2 C57Bl/6** mice were significantly reduced in relation to those of **SPF1 C57B/6** mice (figure 36D). In terms of the effector function of the T lymphocytes in the lung tissue, both CD4+ and CD8+ T cells had moderately increased IFN-γ, and reduced IL-13 producing T lymphocytes in the susceptible **SPF2 C57Bl/6** mice in relation to the resistant **SPF1 C57Bl/6** mice during the infection (figure 36E, F). Furthermore, the IL-5 producing CD8+ T cells were moderately increased in the susceptible **SPF2 C57Bl/6** mice in relation to the resistant **SPF1 C57Bl/6** mice during the infection (figure 36F). Although the effector function of the T lymphocytes was not highly affected, the recruitment of immune cells which contribute inflammatory immune responses were significantly increased in the susceptible **SPF2 C57Bl/6** mice in relation to the **SPF2 C57Bl/6** mice during chronic *S. mansoni* infection. Therefore, the susceptibility of **SPF2 C57Bl/6** mice was linked with increased lung inflammatory immune responses during chronic Schistosomiasis.

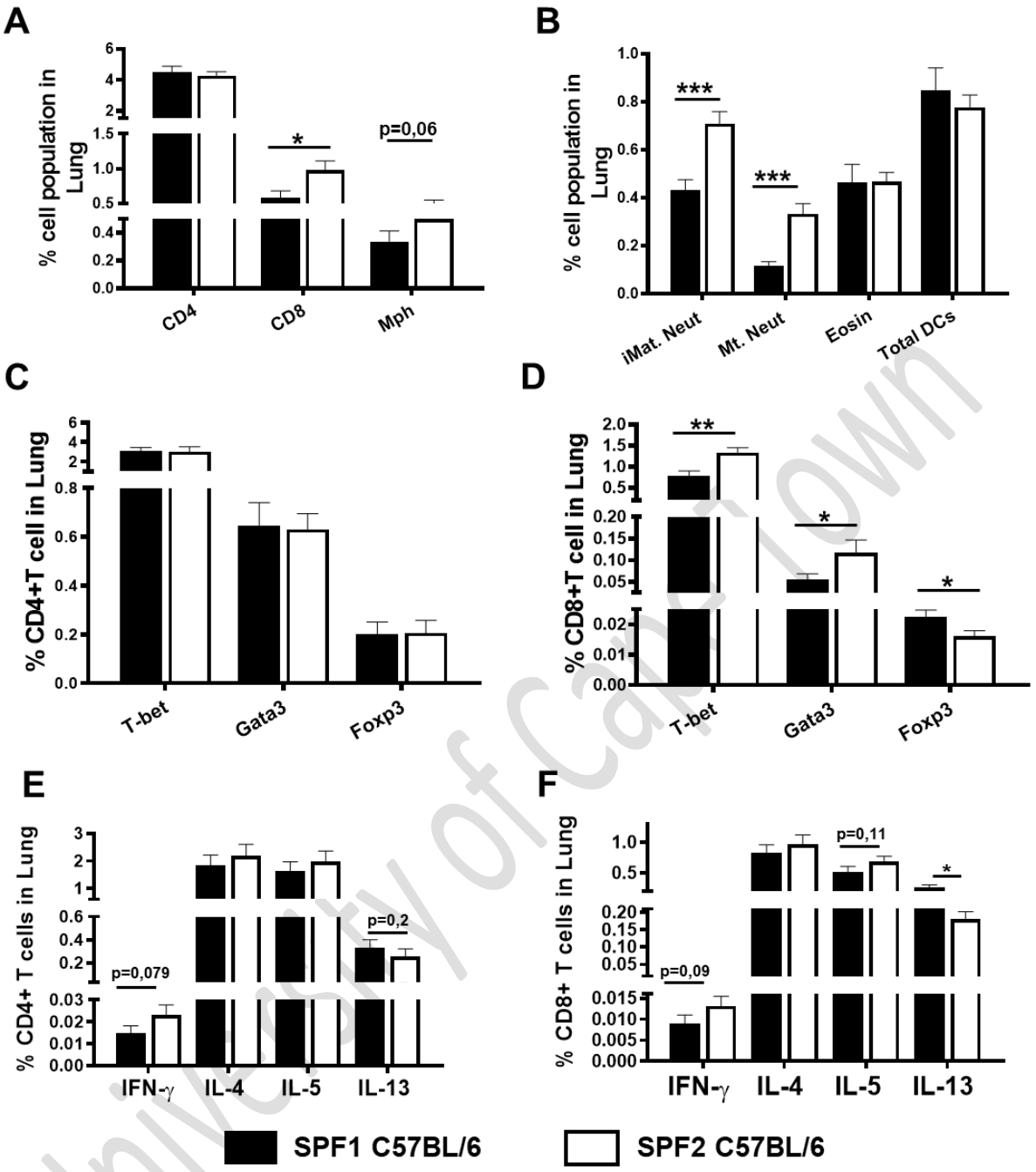

Figure 36: Altered lung immune responses in susceptible SPF2 C57BL/6 mice when compared to the resistant SPF1 C57BL/6 during chronic *S. mansoni* infection.

SPF1 and **SPF2 C57BL/6** mice were infected percutaneously with a dose of 35 *S. mansoni* cercariae and the immune responses in the lung tissue were analysed during week 10 post infection. Quantification of immune cellular populations analysed using flow cytometry (A, B). Quantification of CD4+ (C) and CD8+ (D) T cell polarization measured using flow cytometry. Quantification of cytokine producing CD4+ (E) and CD8+ (F) T lymphocytes re-stimulated with PMA/Ionomycin and analysed on flow cytometry. Data represents two experiments conducted independently (n = 7-10). The comparisons of bar graphs were performed by student t test. *p value < 0.05 and **p value < 0.01.

5.3. The role of the intestinal microbiota in the differential susceptibility of genetically identical mice housed under different specific-pathogen-free facilities during chronic *S. mansoni* infection.

Given that the genetically identical resistant (**SPF1 C57Bl/6)** and susceptible (**SPF2 C57Bl/6)** mice were responding different to chronic Schistosomiasis and had altered immune responses which also affected the immunopathology, the study therefore, aimed to address and show the potential role of intestinal microbiota on the pathogenesis of these mice during the infection. The **SPF1** and **SPF2 C57Bl/6** mice were co-housed together to allow the transfer of intestinal microbiota between the resistant **SPF1 C57Bl/6** and the susceptible **SPF2 C57Bl/6** mice during chronic *S. mansoni* infection. The model resulted in four groups including the **SP1, SP2, SP1-CH (CH = Co-housing)** and **SP2-CH C57Bl/6** mice (figure 37). The mice were then percutaneously infected with a low dose of 35 *S. mansoni* cercariae to induce chronic Schistosomiasis.

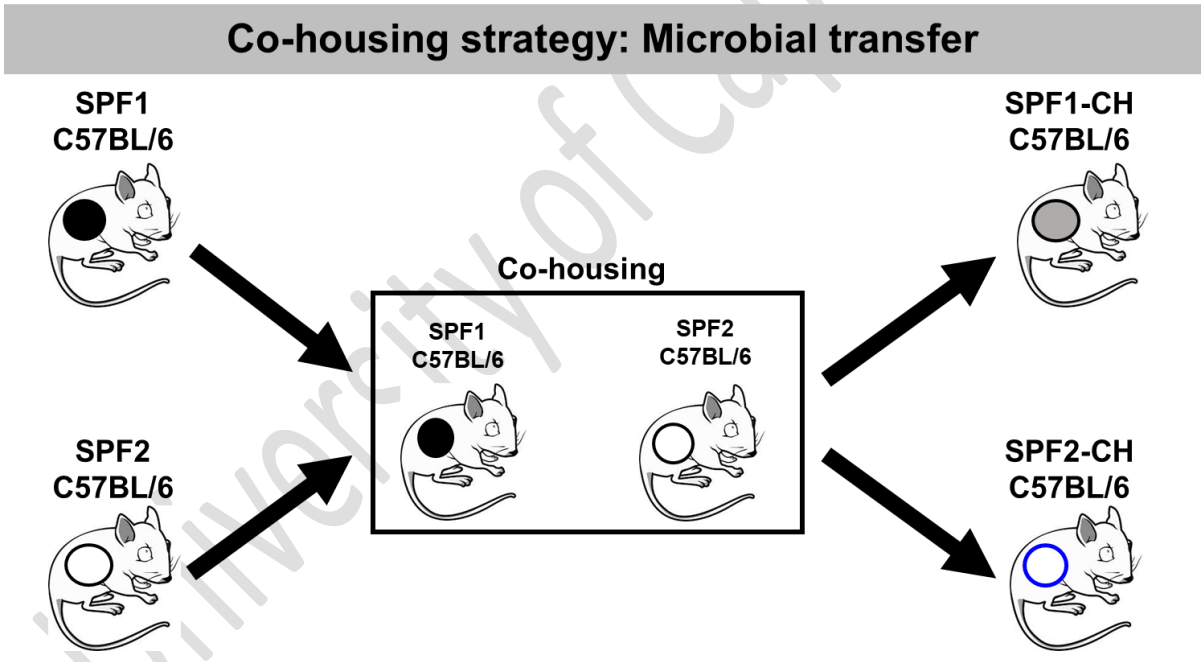

Figure 37: Diagram illustrating the co-housing strategy used to allow the transfer of microbiota between SPF1 and SPF2 C57BL/6 mice during chronic *S. mansoni* infection.

The **SPF1** and **SPF2 C57BL/6** mice were co-housed together 7 days prior to *S. mansoni* infection to allow gut microbial reprogramming within the mice. Using this model, four groups were generated i.e. (i) **SPF1 C57BL/6** (ii) **SPF2 C57BL/6** (iii) **SPF1-CH C57BL/6** (iv) **SPF2-CH C57BL/6** Mice.

5.3.1. Immune alterations as a result of intestinal microbiota transfer from genetically identical resistant to the susceptible mice during chronic *S. mansoni* infection

The immune profile of the **SP1, SP2, SP1-CH (CH = Co-housing)** and **SP2-CH C57Bl/6** mice were analysed in order to assess whether the intestinal microbiota do contribute to the altered immune responses during chronic Schistosomiasis.

5.3.1.1. Alterations in liver immune responses following co-housing of genetically identical resistant and susceptible mice during chronic S. mansoni infection.

The immune profile that was associated with the liver immunopathology of the **SPF2-CH C57Bl/6** mice during chronic *S. mansoni* infection was explored. The susceptible **SPF2 C57Bl/6** mice were characterized by dysregulated recruitment of myeloid populations as evidenced by significantly increased recruitment of eosinophils, and significant reduction in dendritic cells as well as neutrophils in relation to the resistant **SPF1 C57Bl/6** mice (figure 38A - D). However, the recruitment of these myeloid populations was changed in the **SPF2-CH C57Bl/6** mice resulting in reduced recruitment of eosinophils, and significantly increased populations of total DCs, CD11b+ DCs, and moderate increase of the neutrophils which then resembled the profile of the resistant **SPF1 C57Bl/6** mice during the infection (figure 38A - D).

The recruitment of the CD4+ T cells was not different between groups (figure 38E). However, the CD4+ T cells in the susceptible **SPF2 C57Bl/6** mice were significantly more polarized into Th2 (gata3) subsets and moderately more polarised into Th1 (T-bet) subsets in relation to the resistant **SPF1 C57Bl/6** mice (figure 38F, G). The **SPF2-CH C57Bl/6** mice still maintained the increased polarization of the CD4+ T cells into Th2 and Th1 subsets indicating that the microbiota from **SPF1-CH C57Bl/6** mice did not affect these CD4+ T cell subsets during the chronic infection (figure 38F, G). Furthermore, polarization of the CD4+ T cells into regulatory subsets was not majorly affected between the susceptible **SPF2 C57Bl/6** and the resistant **SPF1 C57Bl/6** mice, however the **SPF2-CH C57Bl/6** mice resulted in moderately increased CD4+ T regulatory cells during the infection (figure 38H).

In terms of the effector function of the CD4+ T cells, the data showed no significant influence on the IL-4 and IL-5 producing CD4+ T cells in either the resistant or the susceptible mice, but the **SPF2-CH C57Bl/6** mice resulted in significantly increased IL-5 producing CD4+ T cells in relation to the susceptible **SPF2 C57Bl/6** mice (figure 38I, J). There was also a moderate

increase in IFN-γ and IL-13 producing CD4+ T cells in the **SPF2-CH C57Bl/6** mice in relation to the susceptible **SPF2 C57Bl/6** mice during the infection (figure 38K, L).

The recruitment of the CD8+ T cells were significantly increased in the susceptible **SPF2 C57Bl/6** mice in relation to the resistant **SPF1 C57Bl/6** mice (figure 38M). Following the microbial transfer, these cells were then moderately reduced in the **SPF2-CH C57Bl/6** mice in relation to the susceptible **SPF2 C57Bl/6** mice (figure 38M). Although the polarization of the CD8+ T cells into Th1 (T-bet) and Th2 (Gata3) subsets were significantly increased in the susceptible **SPF2 C57Bl/6** mice in relation to the resistant **SPF1 C57Bl/6** mice, only the Th2 CD8+ T cell subsets were moderately reduced in the **SPF2-CH C57Bl/6** mice while the Th1 CD8+ T cell subsets remained the same in relation to the susceptible **SPF2 C57Bl/6** mice (figure 38N, O). This indicated that the microbiota from the resistant **SPF1 C57Bl/6** mice were enough to reduce the inflammatory Th2 and increase anti-inflammatory Th1 responses mediated by the CD8+ T cells during chronic *S. mansoni* infection. Furthermore, the regulatory CD8+ T cells were also not significantly affected between the resistant **SPF1**, susceptible **SPF2 C57Bl/6** and the **SPF2-CH C57Bl/6** mice during the infection (figure 38P).

In terms of the effector function of the CD8+ T cells, the IL-4 producing CD8+ T cells were not affected (figure 38Q), however, other Th2 mediators were interchanged, where the IL-5 producing CD8+ T cells were moderately increased while the IL-13 producing CD8+ T cells were moderately reduced in the **SPF2-CH C57Bl/6** mice in relation to the susceptible **SPF2 C57Bl/6** mice during the infection (figure 38R, S). On other hand, the IFN-γ producing CD8+ T cells which were significantly low in the susceptible **SPF2 C57Bl/6** mice in relation to the resistant **SPF1 C57Bl/6** mice, were significantly increased in the **SPF2-CH C57Bl/6** mice in relation to the susceptible **SPF2 C57Bl/6** mice (figure 38T). Altogether, the data indicated that the commensal microbiota of the resistant **SPF1 C57Bl/6** mice contributed altered immune responses which potentially may be contributing to the Schistosomiasis-induced liver immunopathology.

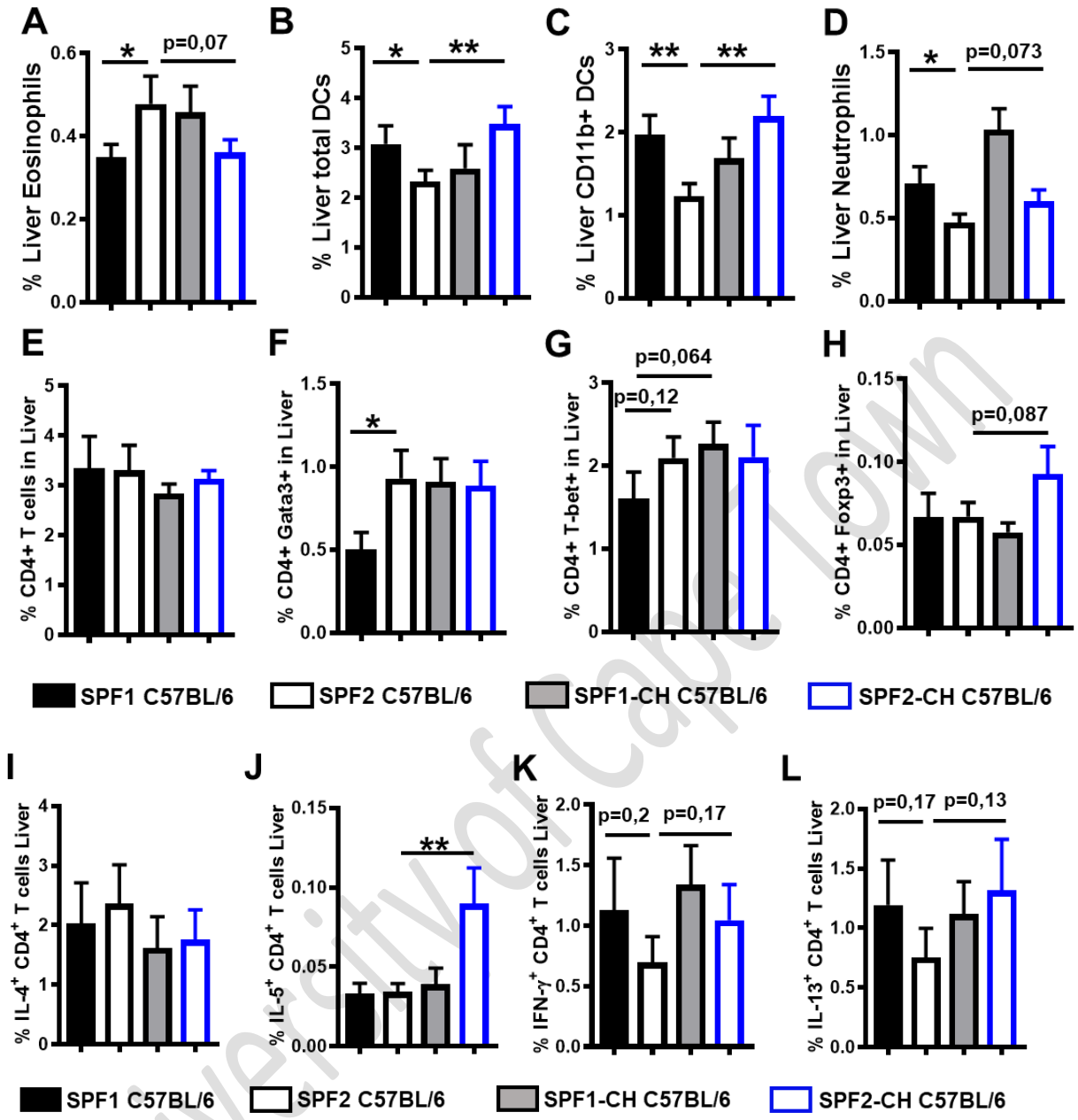

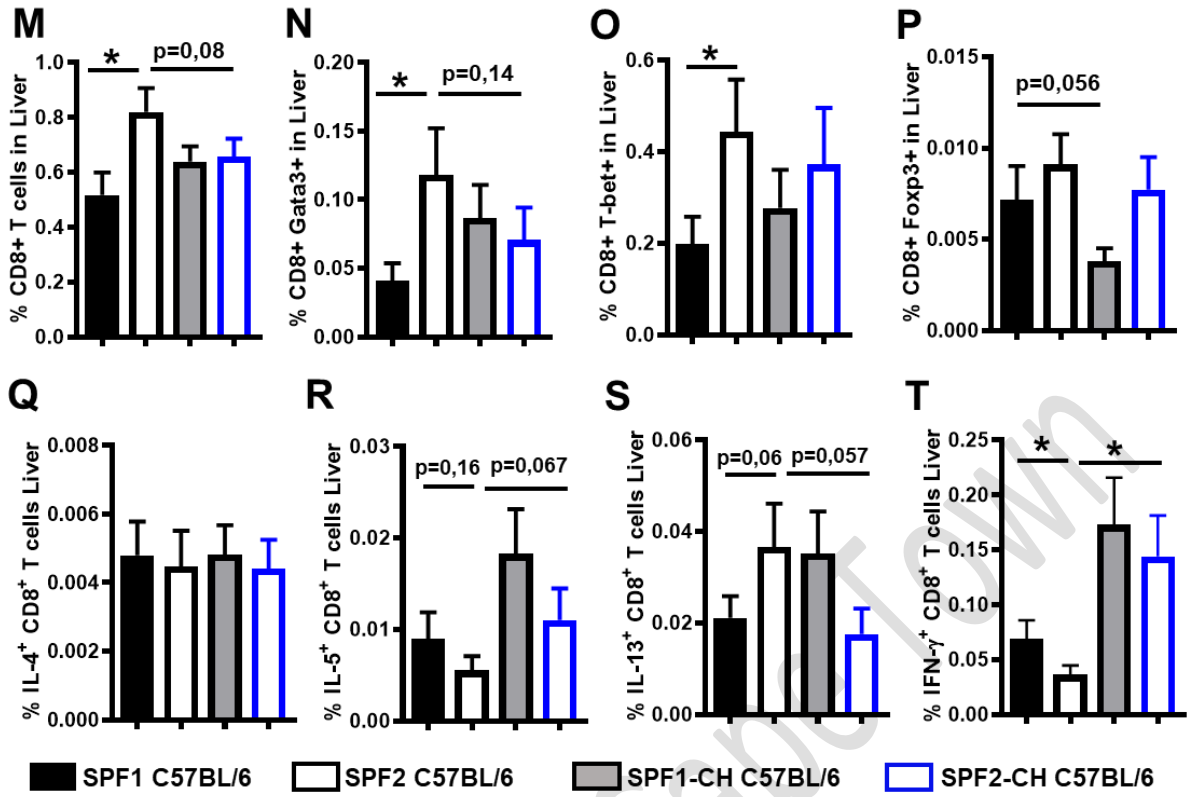

Figure 38: Altered liver immune responses following co-housing of genetically identical resistant and susceptible mice during chronic *S. mansoni* infection.

SPF1-CH, SPF2, SPF1 and **SPF2-CH C57Bl/6** mice were percutaneously infected with a dose of 35 *S. mansoni* cercariae and the immune responses were analysed in the liver tissue during week 10 post infection. Quantification of myeloid cellular populations analysed using flow cytometry (A - D). Quantification of liver CD4+ T cells (E) and their polarization (F - H) during the infection analysed using flow cytometry. Quantification of cytokine producing CD4+ T lymphocytes from liver tissue re-stimulated with PMA/Ionomycin and analysed on flow cytometry (I - L). Quantification of liver CD8+ T cells (M) and their polarization (N - P) during the infection analysed using flow cytometry. Quantification of cytokine producing CD4+ T lymphocytes from liver tissue re-stimulated with PMA/Ionomycin and analysed on flow cytometry (Q - T). Data represents two experiments conducted independently (n = 7-10). The comparisons of bar graphs were performed by student t test. *p value < 0.05 and **p value < 0.01.

The liver tissue was analysed further and the concentrations of IL-4, IL-5 and IL-17 cytokines in the liver were found not to be significantly affected in the **SPF2-CH C57Bl/6** mice in relation to the susceptible **SPF2 C57Bl/6** mice during the chronic *S. mansoni* infection (figure 39A - C). In terms of the concentrations of IL-13 and IFN-γ cytokines, their levels were similar between the susceptible **SPF2 C57Bl/6** and the resistant **SPF1 C57Bl/6** mice, and in both the mice following the microbial transfer, the concentration of these tissue cytokines were significantly increased indicating that the alteration in intestinal microbiota was the cause of

the observed increase of the two cytokines during the infection (figure 39D, E). On the other hand, the liver TNF-α levels which were increased in the susceptible **SPF2 C57Bl/6** mice in relation to the resistant **SPF1 C57Bl/6** mice, were reduced in the **SPF2-CH C57Bl/6** mice in relation to the susceptible **SPF2 C57Bl/6** mice during the infection and this indicated a reduction in type 1 inflammatory immune response in the **SPF2-CH C57Bl/6** mice (figure 39F). The transfer of the microbiota from **SPF1-CH** to **SPF2-CH C57Bl/6** mice also resulted in significantly reduced levels of IL-10 and TGF-β in the **SPF2-CH C57Bl/6** mice in relation to the susceptible **SPF2 C57Bl/6** mice (figure 39G, H). The observed reduction in IL-10 and TGF-β was indicative of reduced type 2 and 17 immune regulatory mediators during the chronic *S. mansoni* infection.

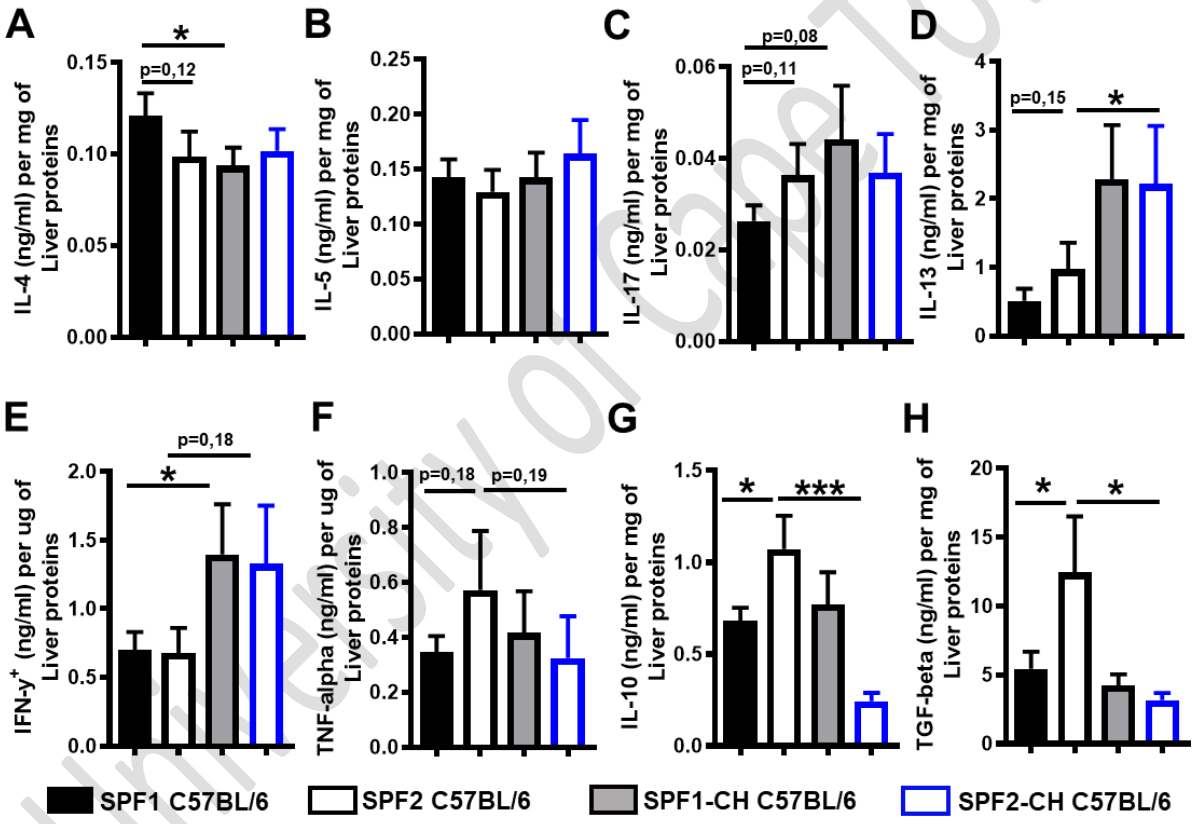

Figure 39: Altered liver cytokine responses following co-housing of genetically identical resistant and susceptible mice during chronic *S. mansoni* infection.

Liver cytokine concentrations per gram of tissue measured using ELISA (A - H). Data represents two experiments conducted independently (n = 7-10). The comparisons of bar graphs were performed by student t test. *p value < 0.05 and **p value < 0.01.

5.3.1.2. Alterations in intestinal immune responses following co-housing of genetically identical resistant and susceptible mice during chronic S. mansoni infection.

The immune profile that was associated with the small intestinal tissue potentially driven by the microbiota from the **SPF1-CH C57Bl/6** mice were analysed. Interestingly the susceptibility of the **SPF2 C57Bl/6** mice was associated with significantly increased recruitment of CD4+, CD8+ T lymphocytes in MLN, as well as small intestinal macrophages, eosinophils, and neutrophils during the infection. The intestinal microbiota from **SPF1-CH C57Bl/6** mice did not affect the recruitment of lymphocyte populations in MLN (figure 40A, B), they however, resulted in significantly reduced recruitment of the myeloid populations including the macrophages, eosinophils, and neutrophils in the **SPF2-CH C57Bl/6** mice in relation to the susceptible **SPF2 C57Bl/6** mice during the chronic infection (figure 40C - E).

Although the recruitment of the lymphocytes remained higher, the polarization of both the CD4+ and CD8+ T cells into Th1 (T-bet), and Th2 (Gata3) subsets, including the regulatory CD4+ T subsets (Foxp3+ CD4+ T cells) were all significantly reduced in the **SPF2-CH C57Bl/6** mice in relation to the susceptible **SPF2 C57Bl/6** mice during the chronic *S. mansoni* infection (figure 40F - J). Interestingly, unlike the regulatory CD4+ T cells which were significantly reduced, the regulatory CD8+ T cells (CD8+ Foxp3+ T cells) were rather increased in the **SPF2-CH C57Bl/6** mice in relation to the susceptible **SPF2 C57Bl/6** mice (figure 40K).

The effector functions of CD4 and CD8+ T cells were further analysed, and as already demonstrated, the susceptibility of the **SPF2 C57Bl/6** mice was associated with significantly reduced production of IL-4, IL-5, and IL-13 by both the CD4+ and CD8+ T cells in relation to those of the resistant **SPF1 C57Bl/6** mice during the infection while the while IFN-γ producing CD4+ and CD8+ T cells were the same (figure 40L - S). However, IFN-γ, IL-4, and IL-5 producing CD4+ and CD8+ T cells of **SPF2-CH C57Bl/6** mice were increased following the transfer of intestinal microbiota from **SPF1 C57Bl/6** mice during the infection (figure 40M - R). Only the IL-13 producing CD4+ T cells were significantly increased while the IL-13 producing CD8+ T cells were not affected in the **SPF2-CH C57Bl/6** mice in relation to those of the susceptible **SPF2 C57Bl/6** mice during chronic *S. mansoni* infection (figure 40O, S).

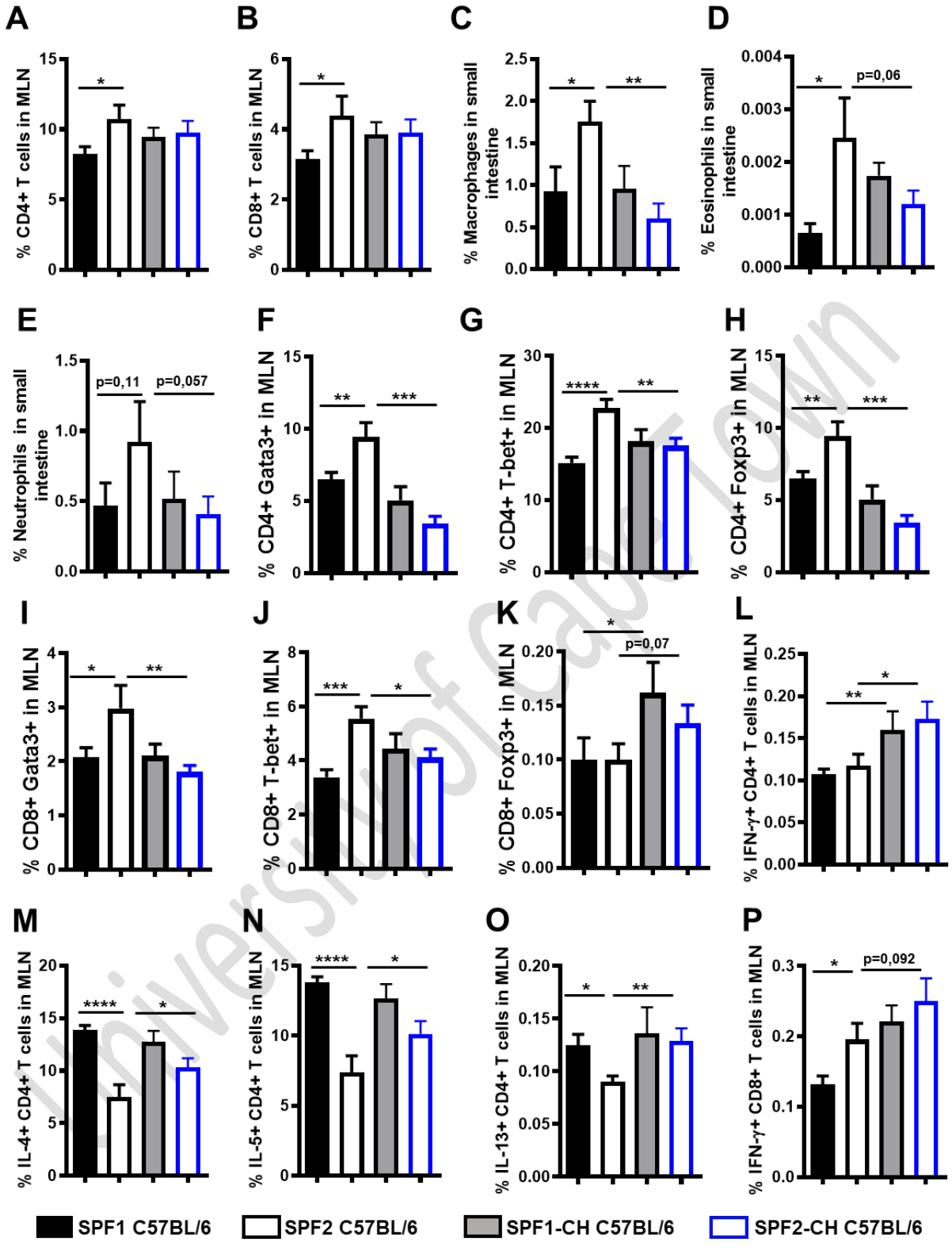

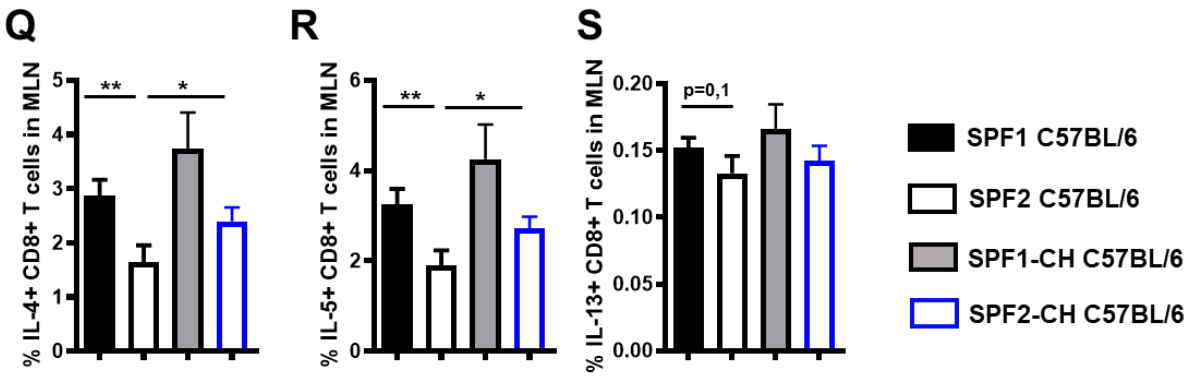

Figure 40: Altered small intestinal immune responses following co-housing of genetically identical resistant and susceptible mice during chronic *S. mansoni* infection.

SPF1, SPF2, SPF1-CH and **SPF2-CH C57Bl/6** mice were percutaneously infected with a dose of 35 *S. mansoni* cercariae and the immune responses were analysed in the small intestinal tissue and mesenteric lymph nodes (MLN) during week 10 post infection. Quantification of MLN CD4+ (A) and CD8+ (B) T lymphocytes, as well as small intestinal myeloid cellular populations (C - E) analysed using flow cytometry. Quantification of MLN CD4+ (F- H) and CD8+ (I - K) T lymphocyte polarization during the infection analysed using flow cytometry. Quantification of cytokine producing CD4+ (L - O) and CD8+ (P - S) T lymphocytes from MLN re-stimulated with PMA/Ionomycin and analysed on flow cytometry. Data represents two experiments conducted independently (n = 7-10). The comparisons of bar graphs were performed by student t test. *p value < 0.05 and **p value < 0.01.

The small intestinal tissue was analysed further to explore the tissue cytokine responses associated with the observed altered immune responses during chronic *S. mansoni* infection. The production of IFN-γ, IL-13, TGF-β and IL-5 cytokines were comparable between the susceptible **SPF2 C57Bl/6** and the **SPF1, SPF1-CH** and **SPF2-CH C57Bl/6** mice during the chronic infection (figure 41A - E). Conversely, the level of IL-17 cytokines which contributes type 17 inflammatory response, were increased in both the **SPF1-CH** and **SPF2-CH C57Bl/6** mice (figure 41F). The levels of TNF-α which contributes to type 1 inflammatory immune response, were significantly reduced in the **SPF2-CH C57Bl/6** mice in relation to the susceptible **SPF2 C57Bl/6** mice during the infection (figure 41G).

Interestingly, the levels of IL-4 cytokines were significantly increased in the **SPF2-CH C57Bl/6** mice in relation to the susceptible **SPF2 C57Bl/6** mice during the infection (figure 41H). Given that IL-4 is a key cytokine that mediates a type 2 dependent immune response against the *S. mansoni* infection, the observed increase of this key cytokine was also linked with increased levels of regulatory IL-10 cytokine in the **SPF2-CH C57Bl/6** mice in relation to the susceptible **SPF2 C57Bl/6** mice (figure 41I). The data, therefore, meant that the

microbiota from **SPF1-CH C57Bl/6** mice were responsible for the altered intestinal immune response during the infection.

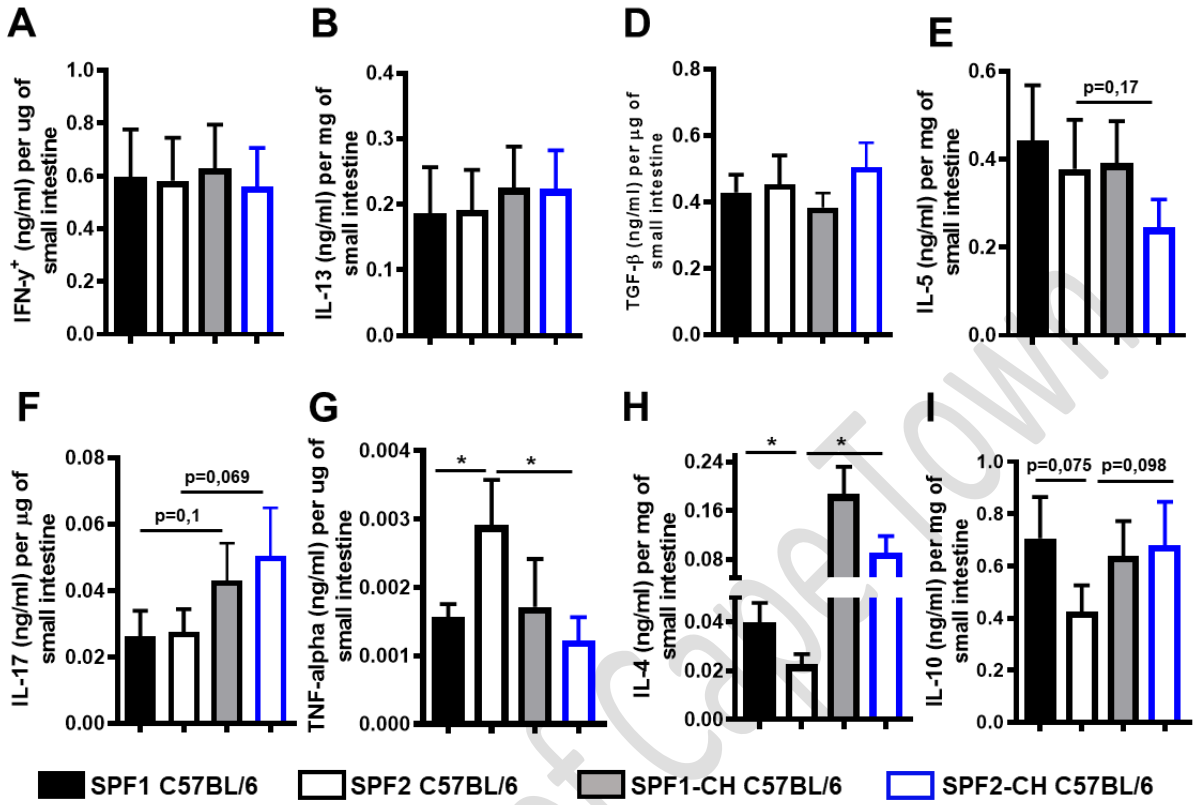

Figure 41: Altered small intestinal cytokine responses following co-housing of genetically identical resistant and susceptible mice during chronic *S. mansoni* infection.

Small intestinal cytokine concentrations per gram of tissue measured using ELISA (A - I). Data represents two experiments conducted independently (n = 7-10). The comparisons of bar graphs were performed by student t test. *p value < 0.05 and **p value < 0.01.

5.3.1.3. Alterations in lung immune responses following co-housing of genetically identical resistant and susceptible mice during chronic S. mansoni infection.

The immune profile associated with the lung tissue revealed the tissue had significantly reduced recruitment of macrophages, immature and mature neutrophils in the **SPF2-CH C57Bl/6** mice in relation to the susceptible **SPF2 C57Bl/6** mice (figure 42A – C). Although the CD8+ T cells were moderately reduced in the **SPF2-CH C57Bl/6** mice during the infection, their polarization into Th1 (T-bet) and regulatory (foxp3+) subsets were significantly increased while the Th2 (Gata3) subsets were moderately reduced in relation to the susceptible **SPF2 C57Bl/6** mice (figure 42D - G). In the case of the CD4+ T cells which were not majorly affected during the infection, their effector function was however affected following the microbial transfer. The IFN-γ and IL-13 producing CD4+ T cells which were increased in the susceptible **SPF2**

C57Bl/6 mice, were further potentiated in the **SPF2-CH C57Bl/6** mice during the infection while the IL-5 producing CD4+ T cells remained the same (figure 42H - J). Similarly, the IFN-γ and IL-13 producing CD8+ T cells were also potentiated further in the **SPF2-CH C57Bl/6** mice in relation to the susceptible **SPF2 C57Bl/6** mice during the infection (figure 42K - M). Altogether, the data showed that the microbiota from **SPF1-CH C57Bl/6** mice were able to alter the lung immune during chronic *S. mansoni* infection.

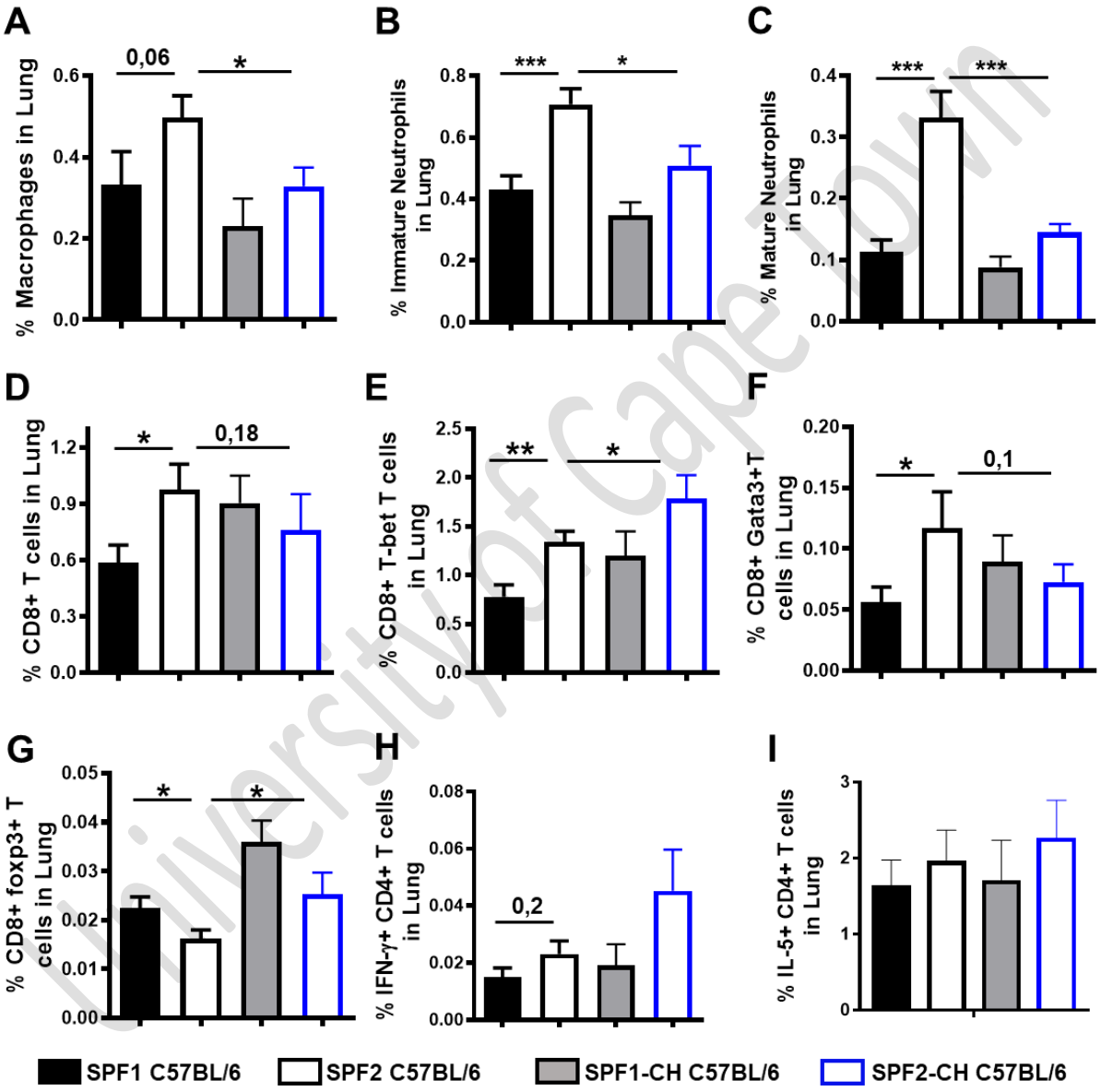

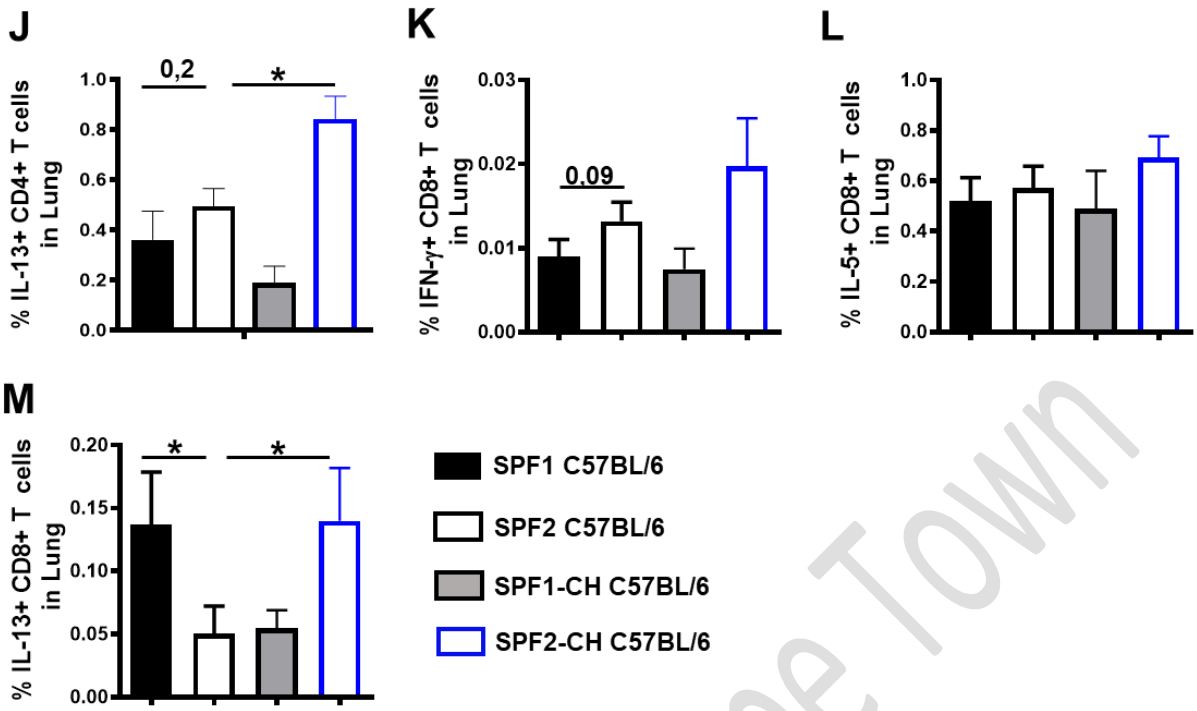

Figure 42: Altered lung immune responses following co-housing of genetically identical resistant and susceptible mice during chronic *S. mansoni* infection.

SPF1, SPF2, SPF1-CH and **SPF2-CH C57Bl/6** mice were percutaneously infected with a dose of 35 *S. mansoni* cercariae and the immune responses in the lung tissue were analysed during week 10 post infection. Quantification of immune cellular populations recruited to the tissue analysed using flow cytometry (A- D). Quantification of CD8+ T cell polarization measured using flow cytometry (E - G). Quantification of cytokine producing CD4+ (H - J) and CD8+ (K- M) T lymphocytes re-stimulated with PMA/Ionomycin and analysed on flow cytometry. Data represents two experiments conducted independently (n = 7-10). The comparisons of bar graphs were performed by student t test. *p value < 0.05 and **p value < 0.01.

Interestingly, the immune responses of the affected tissues of the **SPF1-CH C57Bl/6** mice were also altered following the microbial transfer, and this resulted in immune profile that resembled that of the susceptible **SPF2 C57Bl/6** mice. This, therefore, demonstrated a bidirectional transfer of causal microbiota between the resistant **SPF1 C57Bl/6** and susceptible **SPF2 C57Bl/6** mice during chronic Schistosomiasis.

5.3.2. Transfer of the intestinal microbiota from resistant to susceptible mice result in ameliorated tissue immunopathology during chronic *S. mansoni* infection.

5.3.2.1. The intestinal microbiota of resistant mice drives reduced hepatic immunopathology during chronic S. mansoni infection.

Following the observed altered immune responses in the target tissues of **SPF2-CH C57Bl/6** mice driven by the intestinal microbiota, the immunopathological features associated with these changes were analysed to find out if the changes were enough to also alter the Schistosomiasis-induced immunopathology of infected mice. Analysis of the liver pathology showed that the immune responses in the **SPF2 C57Bl/6** mice were associated with increased liver granulomatous immunopathology (figure 43A, B), which was then reversed or significantly reduced following the microbial transfer that altered the immune responses in liver of the **SPF2-CH C57Bl/6** mice in relation to the susceptible **SPF2 C57Bl/6** mice during the infection (figure 43A, B). However, the **SPF1-CH C57Bl/6** mice also resulted in significantly increased liver granulomatous immunopathology the infection further confirming a bidirectional transfer of causal microbiota across the two groups of mice (figure 43A, B). Although the altered immune responses affected the development of granulomatous immunopathology around the trapped *S. mansoni* eggs, they however did not have a significant influence on the production of fibrosis as it remained higher in the liver tissue of the **SPF2-CH C57Bl/6** mice and remained lower for the **SPF1-CH C57Bl/6** mice during the infection (figure 43C, D). The data, therefore, shows that the intestinal microbiota from **SPF1-CH C57Bl/6** mice alters the tissue immune response which in turn results in reduced liver granulomatous immunopathology while the microbiota from the **SPF2-CH C57Bl/6** mice resulted in altered immune responses that causes exacerbated liver granulomatous immunopathology during chronic *S. mansoni* infection.

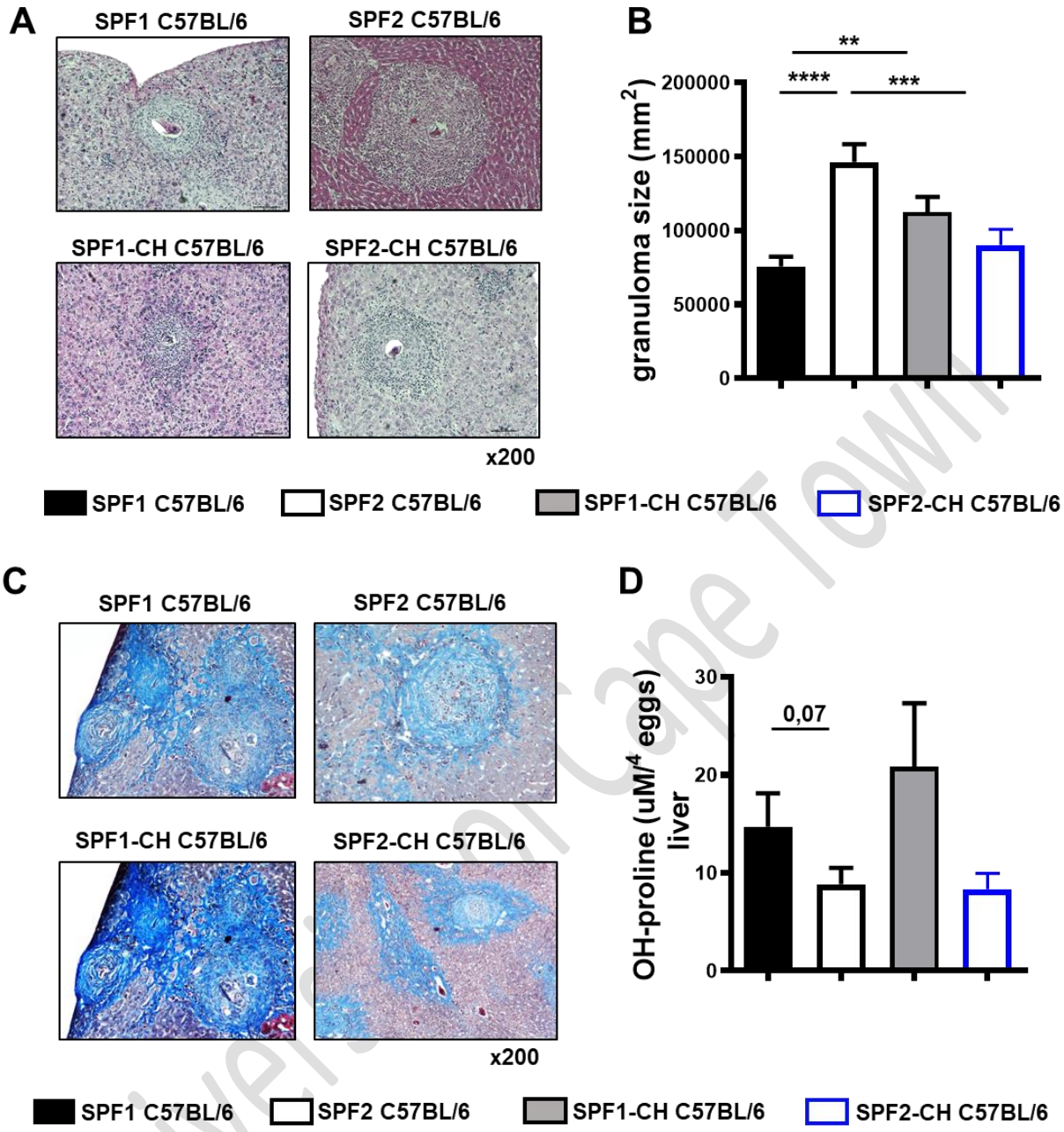

Figure 43: The intestinal microbiota of resistant mice drives reduced hepatic immunopathology during chronic *S. mansoni* infection.

Liver sections fixed in formalin were stained with H&E for morphological analysis of the egg-surrounding granuloma (200x) (A). Granuloma measurements quantified using microscopic analysis from H&E-stained sections (B). Liver sections fixed in formalin were stained with CAB staining for morphological analysis of fibrosis development in the liver of infected mice (200x) (C). Fibrosis measurements quantified using hydroxyproline assay on liver tissues (D). Comparison of survival curves was made using Logrank test. The comparisons of bar graphs were performed by student t test. *p value < 0.05 and **p value < 0.01. (n = 7-12).

5.3.2.2. The intestinal microbiota of resistant mice drives increased small intestinal tissue immunopathology during chronic S. mansoni infection.

The small intestinal tissue was then analysed to understand how the altered immune responses influenced tissue immunopathogenesis of the **SPF2-CH C57Bl/6** mice during chronic *S. mansoni* infection. The susceptibility of **SPF2 C57Bl/6** mice was linked with significantly increased small intestinal immunopathology in relation to the resistant **SPF1 C57Bl/6** mice during the chronic *S. mansoni* infection (figure 44A, B). But the transfer of intestinal microbiota from the resistant **SPF1-CH C57Bl/6** mice to the **SPF2-CH C57Bl/6** mice which resulted in altered immune responses, did not influence, or result in reduced small intestinal immunopathology, however, the altered immune responses in **SPF1-CH C57Bl/6** mice resulted in significantly increased intestinal immunopathology (figure 44A, B). Furthermore, both the **SPF1-CH** and the **SPF2-CH C57Bl/6** mice resulted in similar levels of small intestinal fibrosis which were higher than the **SPF1** and **SPF2 C57BL/6** mice that were not co-housed during chronic *S. mansoni* infection (figure 44C, D) indicating that the altered microbiota (dysbiosis) was responsible for the observed increase in the tissue fibrosis. To confirm the influence of the altered immune response on the tissue inflammation, the mesenteric lymph node (MLN) cells were also quantified. Interestingly, the MLN cell count of **SPF2-CH C57Bl/6** mice was reduced in relation to the susceptible **SPF2 C57Bl/6** mice during chronic *S. mansoni* infection (figure 44E). This, therefore, indicated that the altered immune responses in **SPF2-CH C57BL/6** mice did influence a reduced intestinal immunopathology during chronic *S. mansoni* infection even though it was not strong enough to reverse the pathology.

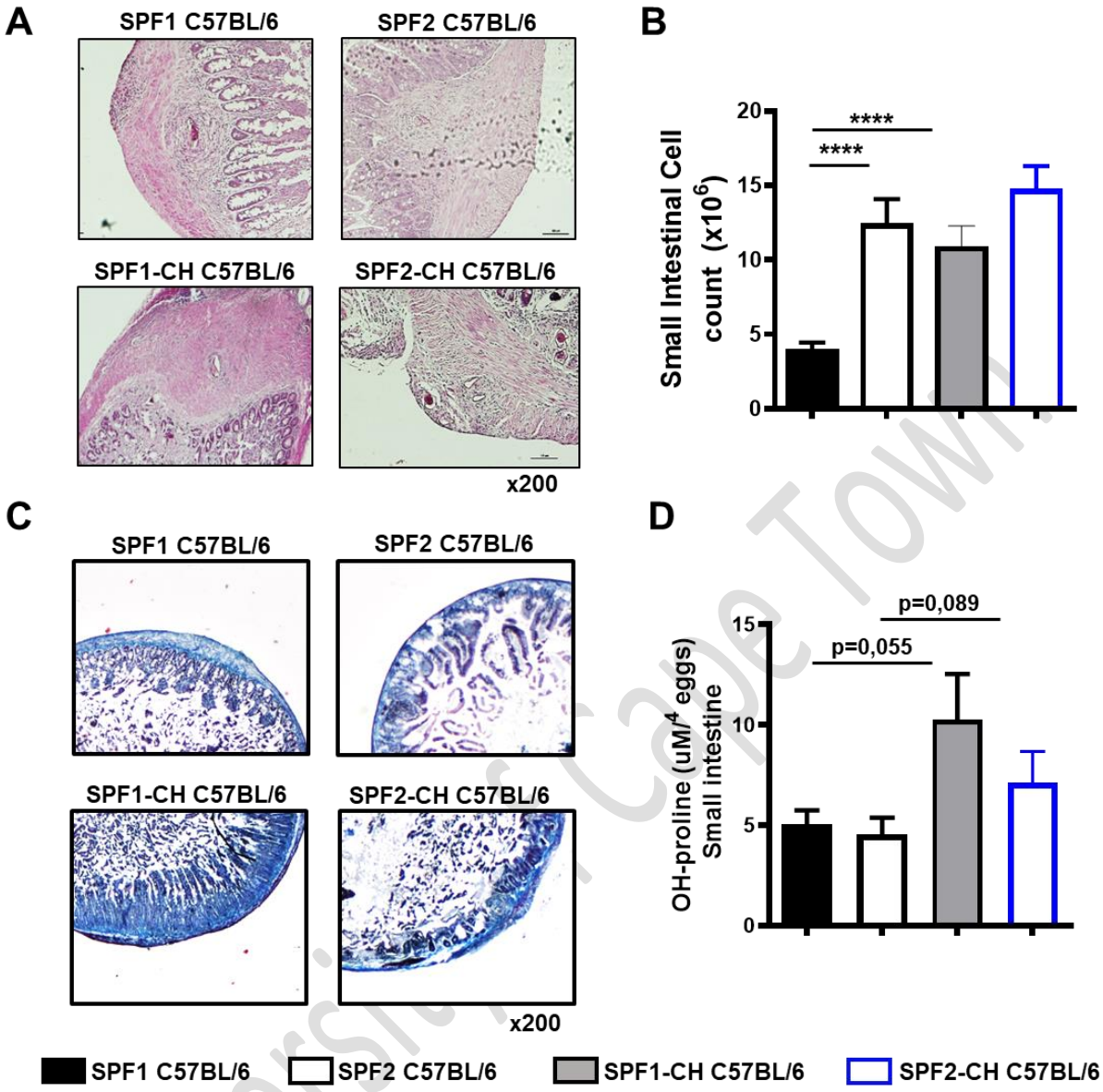

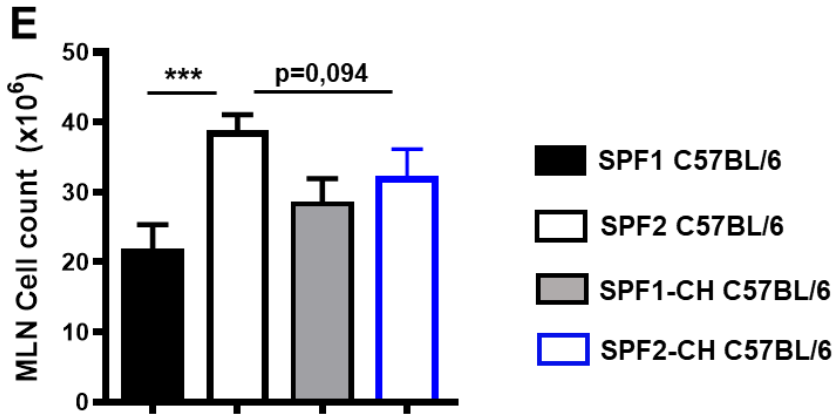

Figure 44: The intestinal microbiota of resistant mice drives increased small intestinal immunopathology during chronic *S. mansoni* infection.

Formalin-fixed small intestinal sections stained with H&E for morphological analysis of the cellular recruitment around the trapped *S. mansoni* eggs (100x) (A). Quantification of small intestinal cell counts (B). Formalin fixed small intestinal sections stained with CAB staining for morphological analysis of fibrosis development in the small intestinal of infected mice (200x) (C). Fibrosis measurements quantified using hydroxyproline assay on liver tissues (D). Quantification of MLN cell counts (E). Data represents two experiments conducted independently (n = 7-10). The comparisons of bar graphs were performed by student t test. *p value < 0.05 and **p value < 0.01.

5.3.2.3. The intestinal microbiota of resistant mice drives increased lung weight that is associated with reduced cellular count during chronic S. mansoni infection.

Further analysis on tissue immunopathology associated with chronic Schistosomiasis that were potentially affected by the intestinal microbiota revealed that there were no observable differences in the organ weight indices which included the liver, spleen as well as the heart (figure 45A – C). However, the lung index which was significantly reduced in the susceptible **SPF2 C57Bl/6** mice in relation to the resistant **SPF1 C57Bl/6** mice, was then increased in the **SPF2-CH C57Bl/6** mice in relation to the susceptible **SPF2 C57Bl/6** mice during the infection (figure 45D). Despite the increased lung index, the cellular count of the tissue in **SPF2-CH C57Bl/6** was reduced in relation to the susceptible **SPF2 C57Bl/6** mice indicating a reduction in inflammation during chronic Schistosomiasis (figure 45E). This, therefore, shows that the altered immune response in the lung contributed to reduced inflammation in the lung of **SPF2-CH C57Bl/6** mice during chronic Schistosomiasis.

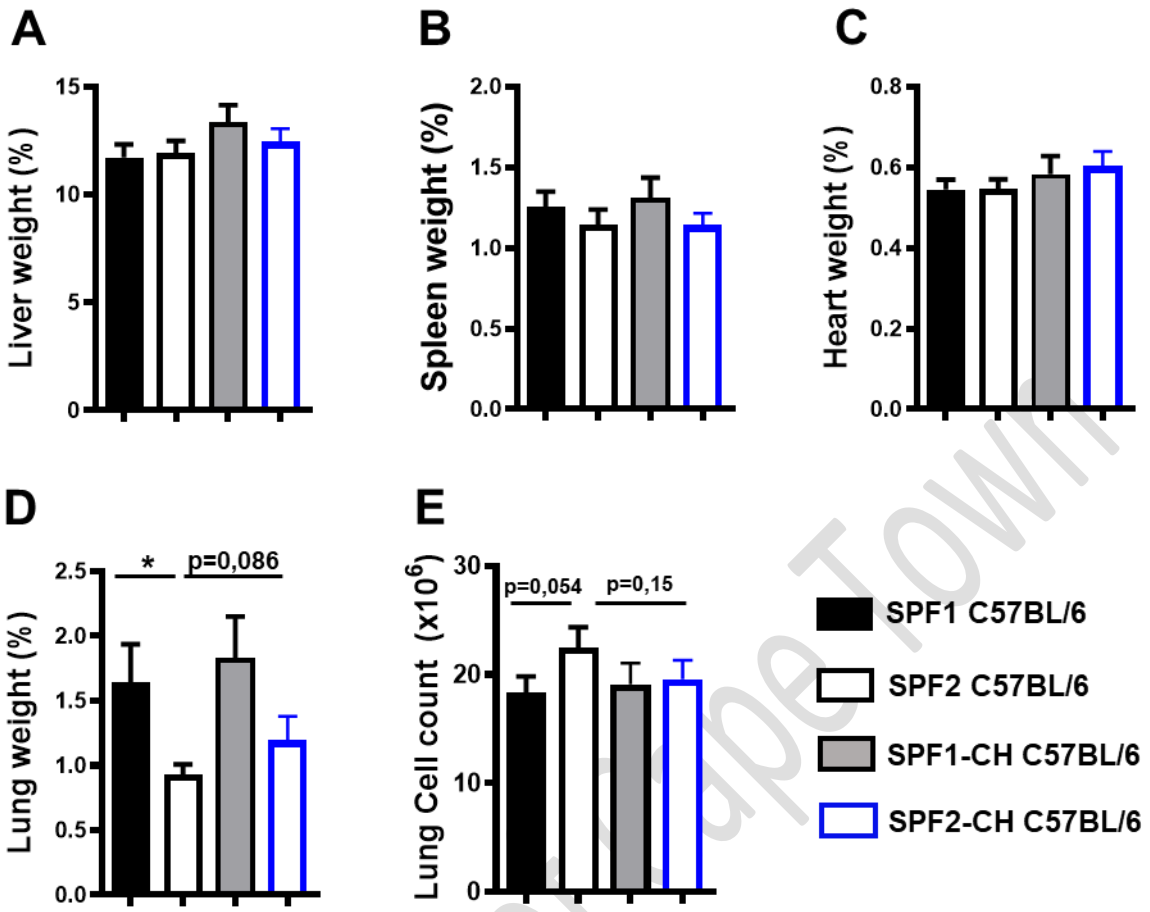

Figure 45: The intestinal microbiota of resistant mice drives increased lung weight that is associated with reduced cellular count during chronic *S. mansoni* infection.

SPF1, SPF2, SPF1-CH and **SPF2-CH C57Bl/6** mice were percutaneously infected with a dose of 35 *S. mansoni* cercariae and analysed at week 10 post infection. Liver (A), heart (B), spleen (C), and lung (D) weights were measured during chronic *S. mansoni* infection. Quantification of MLN cellular count (E) were measured during chronic schistosomiasis. Data represents two experiments conducted independently (n = 7-10). The comparisons of bar graphs were performed by student t test. *p value < 0.05 and **p value < 0.01.

Altogether, the data shows that the intestinal microbiota of **SPF1-CH C57Bl/6** mice result in altered immune responses in target tissue (liver, small intestine, and lung) which in turn contribute to regulated immunopathology in infected **C57Bl/6** mice.

5.3.3. Transfer of the intestinal microbiota from resistant to susceptible mice result in prolonged survival of the susceptible mice during chronic *S. mansoni* infection.

Considering the controlled immunopathology observed in **SPF1** and **SPF2-CH C57Bl/6** mice, and exacerbated immunopathology observed in **SPF2** and **SPF1-CH C57Bl/6** mice, the next objective was to explore how those changes translated in terms of the mice' susceptibility

during chronic Schistosomiasis. Interestingly the controlled tissue immunopathology in **SPF2-CH C57BL/6** mice was enough to rescue the mice from premature mortality in relation to **SPF2 C57Bl/6** mice (figure 46A: blue and white line graphs respectively), while the increased immunopathological changes observed in **SPF1-CH C57Bl/6** mice resulted increased susceptibility of the mice in relation to the **SPF1 C57Bl/6** mice during the infection (figure 46A: grey and black line graphs respectively). The worm burden was similar across all the groups indicating that the observed differences in susceptibility were a result of the intestinal microbiota through priming of the immune responses that mediated Schistosomiasis-induced immunopathology in the mice (figure 46B and C). Given that both the **SPF1-CH** and **SPF2-CH C57Bl/6** mice' susceptibility were affected during the infection, this therefore, demonstrates a bidirectional transfer of causal microbiota, with the intestinal microbiota of **SPF1 C57Bl/6** mice driving a protective phenotype while the intestinal microbiota of **SPF2 C57Bl/6** mice drive a more pathogenic phenotype against chronic Schistosomiasis.

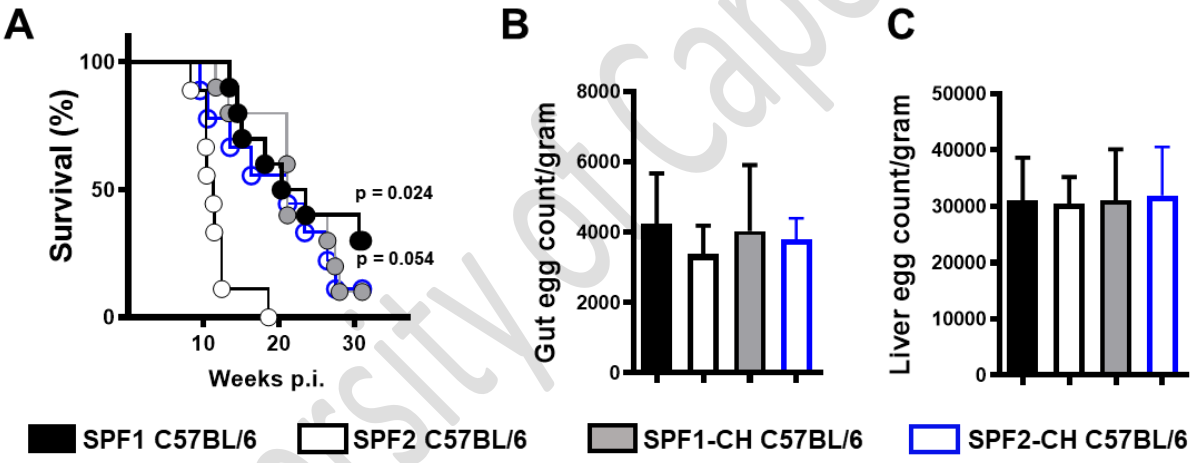

Figure 46: Intestinal microbiota of resistant mice result in prolonged survival of the mice during chronic *S. mansoni* infection.

The survival **of SPF1, SPF1-CH, SPF2** and **SPF1-CH C57BL/6** mice during chronic *S. mansoni* infection were compared(A). Quantification of *S. mansoni* eggs comparing the worm burden in the small intestinal tissue (B) as well the liver (C) during the infection. Data represents two experiments conducted independently (n = 7-10). Comparison of survival curves was made using Logrank test. The comparisons of bar graphs were performed by student t test. *p value < 0.05 and **p value < 0.01.

5.3.4. Antibiotic treatment does not abrogate the protective potential of the intestinal microbiota of resistant mice.

Given that the bacteria constitute a large number compared to other microbes in the intestine and have been shown to play crucial roles in diseases that are also caused by helminth infections (Rapin and Harris, 2018; Tlaskalová-Hogenová et al., 2011; Sender, R. et al. 2016), the next

step of the study was to confirm whether the observed changes in Schistosomiasis-induced pathogenesis was driven by the intestinal bacteria. For this, the **SPF1 C57Bl/6** mice were orally administered with a broad-spectrum antibiotic (Abx) cocktail containing 0.8mg of Amoxicillin, 1.7mg of Enrofloxacin, 0.2mg neomycin, and 0.2mg ampicillin dissolved in sterile water, for each **SPF1 C57Bl/6** mouse to disrupt and reduce the number of bacterial populations. Following the treatment, these mice were then co-housed with the **SPF2 C57Bl/6** mice to generate two new groups for the study. The antibiotic treated **SPF1 C57Bl/6** mice were termed **Abx+ SPF1-CH C57Bl/6** mice while the untreated **SPF2 C57Bl/6** mice were termed **Abx- SPF2-CH C57Bl/6** mice. The mice together with their controls (**SPF1-CH** and **SPF2-CH C57Bl/6** mice) were percutaneously infected with a low dose of 35 *S. mansoni* cercariae to induce chronic Schistosomiasis. The antibiotic cocktail was administered every 3 days for the duration of the experiment. Over the course of infection, the antibiotic cocktail was demonstrated to be sufficient to significantly reduce both aerobic and anaerobic populations of bacteria in the **Abx+ SPF1-CH C57Bl/6** mice (figure 47A - D: grey and blue bar graphs), while the levels of aerobic and anaerobic bacterial populations in **Abx- SPF2-CH C57Bl/6** mice remained unaffected throughout the infection (figure 47A - D: brown and red bar graphs). This experiment was performed to reprogram the intestinal microbiota so to disrupt the transfer of protective microbiota which would prevent the rescue of **Abx- SPF2-CH C57Bl/6** mice during chronic Schistosomiasis. Surprisingly, this was not the case as the transfer of microbiota following the antibiotic treatment was still enough to rescue the **Abx- SPF2-CH C57Bl/6** mice during the infection (figure 47E). This, therefore, demonstrated that the suspected bacteria were not dominantly contributing to increased protection against chronic Schistosomiasis.

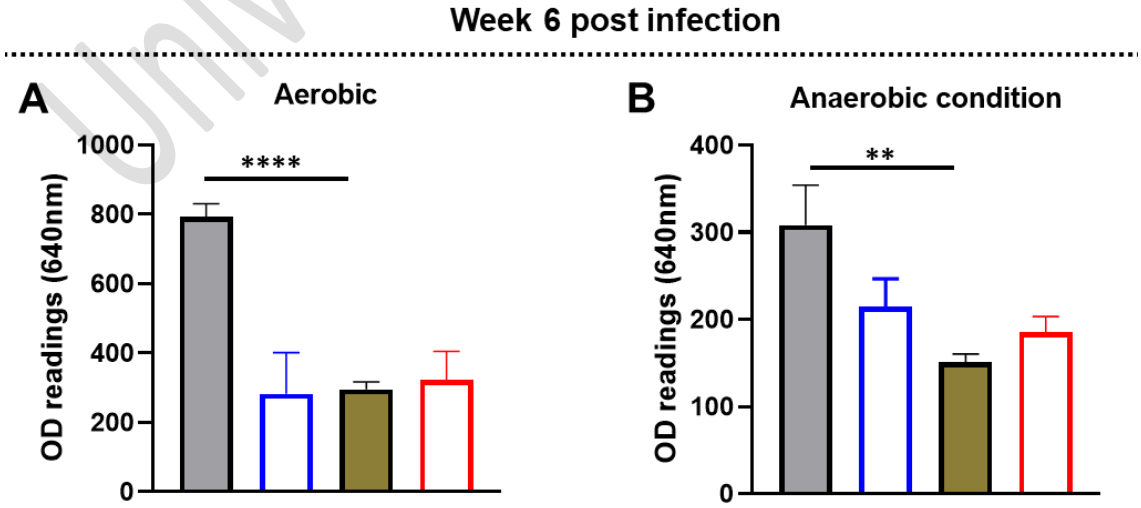

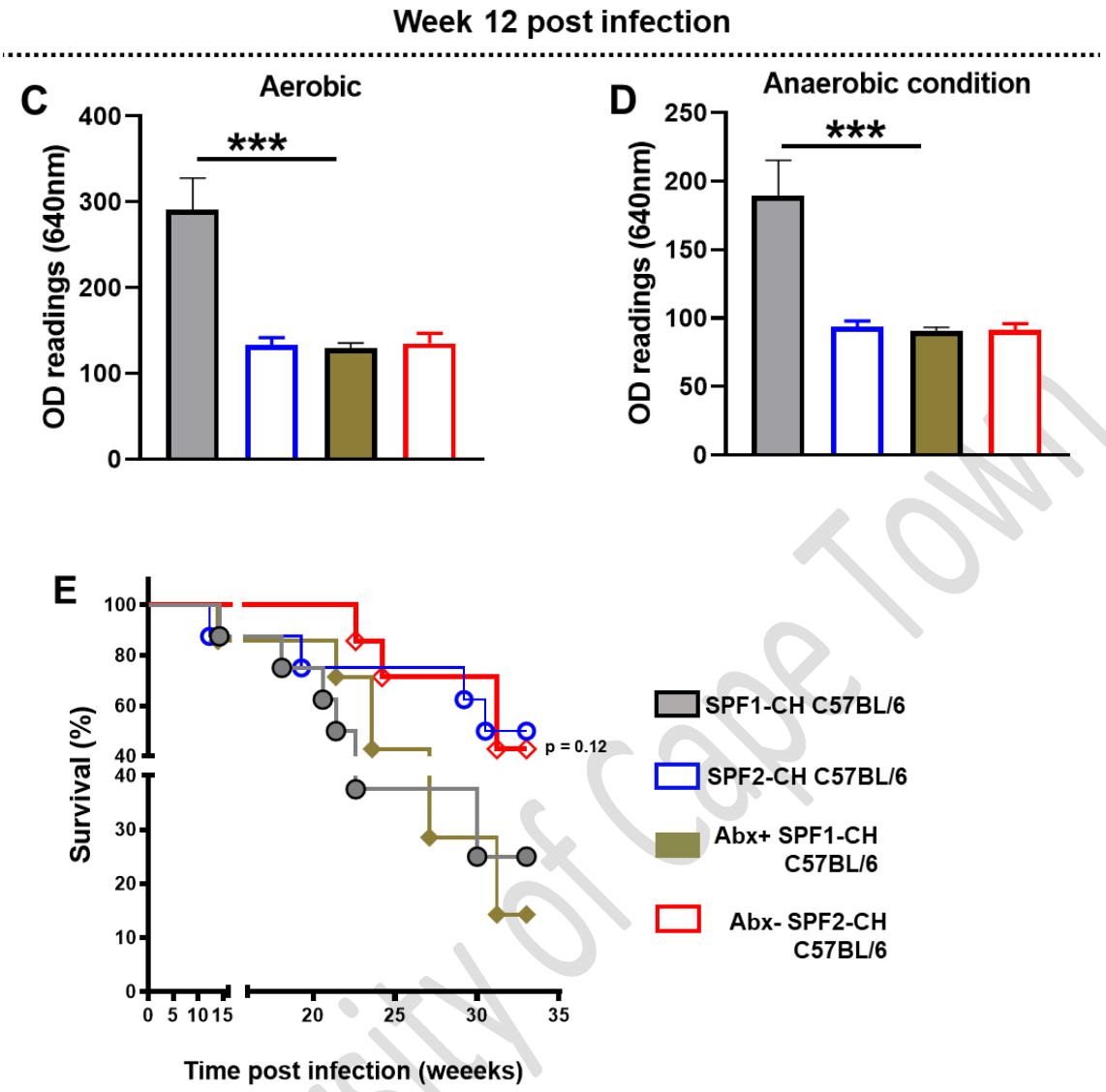

Figure 47: Antibiotic treatment does not abrogate the protective potential of the intestinal microbiota of resistant mice.

Quantification of aerobic (A) and anaerobic (B) bacteria using TSA broth media during week 6 post *S. mansoni* infection. Quantification of aerobic (C) and anaerobic (D) bacteria using TSA broth media during week 12 post *S. mansoni* infection. The survival of **SPF1-CH, SPF2-CH, Abx+ SPF1-CH** and **Abx- SPF1-CH C57BL/6** mice during chronic *S. mansoni* infection were compared (E). Data represents two experiments conducted independently (n = 7-10). Comparison of survival curves were performed by Logrank test. The comparisons of bar graphs were performed by student t test. *p value < 0.05 and **p value < 0.01.

5.3.5. Comparative analysis of the intestinal microbiota profiles of the genetically identical susceptible and resistant mice

Since it was still unclear which organisms were contributing to prolonged survival of the mice during chronic Schistosomiasis, the **SPF1** and **SPF2 C57BL/6** mice were screened to identify and compare intestinal microbes between these groups of mice. For this, serum and faecal

samples were collected from both the **SPF1** and **SPF2 C57BL/6** mice and were analysed using PCR, Indirect Immunofluorescence (IFA), and ELISA. The microbiological profiles were analysed by Biomedical Diagnostics (BioDoc, Germany) (Mr Jabu Magagula). According to the report that was provided the **SPF2 C57BL/6** mice were found to be free of FELASA listed organisms including the *Helicobacter sp*, *Murine norovirus* (*MNV*) and *Pasteurella pneumotropica*, which are three organisms that were found to be present in the **SPF1 C57BL/6** mice that are more resistant to chronic Schistosomiasis (table 1). It can be suggested that one of these organisms if not all, were responsible for the prolonged survival of the **SPF1 C57BL/6** mice during the infection. Nevertheless, the study has therefore, extensively demonstrated the influence of intestinal microbiota on the pathogenesis of mice during chronic Schistosomiasis.

Table 1: Screening of serum and faecal samples for detection and profiling of intestinal microorganisms in SPF1 and SPF2 C57BL/6 mice.

		SPF1 C57BL/6				SPF2				
Microbe	**Method**	**S1**	**S2**	**S3**	**S4**	**S1**	**S2**	**S3**	**S4**	**S5**
MHV	IFA	-	-	-	-	-	-	-	-	-
Reo3	IFA									
Theiler (GDVII)	IFA	-	-	-	-	-	-	-	-	-
PVM	IFA	-	-	-	-	-	-	-	-	-
Sendai	IFA	-	-	-	-	-	-	-	-	-
MVM	IFA	-	-	-	-	-	-	-	-	-
MPV	IFA	-	-	-	-	-	-	-	-	-
Ektromelie	IFA	-	-	-	-	-	-	-	-	-
LCMV	IFA	-	-	-	-	-	-	-	-	-
Adeno (MAd K87)	IFA	-	-	-	-	-	-	-	-	-
Polyoma	IFA	-	-	-	-	-	-	-	-	-
MTV	IFA	-	-	-	-	-	-	-	-	-
Hanta	IFA	-	-	-	-	-	-	-	-	-
MCMV	IFA	-	-	-	-	-	-	-	-	-
Rota (EDIM)	IFA	-	-	-	-	-	-	-	-	-
MNV	**IFA**	**++**	**+++**	**++**	**+++**	-	-	-	-	-
LDV	ELISA	-	-	-	-	-	-	-	-	-
Mycopl. Pulmonis	IFA	-	-	-	-	-	-	-	-	-
Tyzzer (Cl. Piliforme)	IFA	-	-	-	-	-	-	-	-	-
Past. Pneumotropica	**IFA**	**+**	**+**	**+**	**+**	-	-	-	-	-
Toxoplasma gondil	IFA	-	-	-	-	-	-	-	-	-
Encephalitozoon cun.	IFA	-	-	-	-	-	-	-	-	-
Helicobacter sp.	**PCR**	**pos.**	**pos.**	**pos.**		-	-	-	-	-

IFA	Indirect Immunofluorescence
ELISA	enzyme-linked immunosorbent assay
PCR	Polymerase chain reaction
S	**Sample**

+	**weak reaction**
++	**medium reaction**
+++	**strong reaction**

6. **Discussions**:

The aim of the current study was to explore the interrelationship that exist between commensal microbiota, host genetic factor (Batf2), and the immune system to control disease complications such as chronic Schistosomiasis. And in so doing, the study has proved for the first time beyond association the presence of causal microbiota which contribute to the pathogenesis of *S. mansoni* infected mice leading to either increased or decreased susceptibility to the infection.

6.1. Gene deletion and resistance to chronic Schistosomiasis

The study initially explored the differential expression dynamics of Batf2 and its influence in mice if disrupted. Although removal of the transcription factor as previously demonstrated, does not induce any major physiological and immune cellular changes in the lung and liver tissues, it however has been demonstrated to alter immune cellular responses in small intestinal tissue of naïve mice (Guler et al 2018; Mpotje, 2017). The current study has demonstrated further that the removal of Batf2 alters the intestinal microbiota which potentially contributes to the altered immune responses even though the overall fitness of the mice was not affected during homeostasis. Considering all these, it stands to reason that the transcription factor has a direct link with the composition of the intestinal microbiota and thus help maintain homeostasis.

Upon acute Schistosomiasis, the host maintains expression of Batf2 in small intestinal tissue and this helps regulate the type 2 and type 17 inflammatory responses mediated by both inflammatory T cells, which in turn also regulate the intestinal fibro-granulomatous immunopathology leading to prolonged survival of the infected mice (Guler et al, 2017). This, therefore, demonstrates that the Batf2 is an important regulator which allows for a well-controlled type 2 and type 17 inflammatory immune responses in the intestine protecting the host against toxic pathogens, and in turn minimizes autoimmune-induced tissue damage during acute Schistosomiasis.

Furthermore, the role of Batf2 is demonstrated to be tissue specific since it did not influence other tissue organs such as the liver despite the observed increase in expression during acute Schistosomiasis. Although the host still maintains increased expression of Batf2 in the liver during chronic Schistosomiasis, it was unclear how that translated into the tissue

immunopathology and ultimately the survival of the mice. Intriguingly, unlike with acute schistosomiasis, the absence of Batf2 during the chronic Schistosomiasis resulted in significantly prolonged survival of the mice.

6.2. Immunity, immunopathology, and resistance to chronic Schistosomiasis

Previous studies have demonstrated that the core of the pathology during schistosomiasis is primarily driven by excessive or unregulated inflammatory immune response to eggs rather than the cytotoxic action of the eggs themselves (Hams et al., 2013). Therefore, given that the removal of Batf2 in this current study resulted in significantly reduced type 2 inflammatory immune response (Figure 16), this might explain the reduced pathology observed in batf2$^{-/-}$ mice when compared to the WT mice despite similar levels of parasite egg loads. Additionally, the immunopathology of other tissue organs that are normally affected by the infection such as the lung, the small intestine, and the spleen, were also regulated.

Interestingly, the reduced immunopathology was associated with increased tissue fibrosis which is known to be a wound healing factor that helps restore damaged tissue following an injury from autoimmune responses, mechanical stress, or infection (Kamden et al., 2018). However, *S. mansoni* infection causes an immune response that induces exacerbated liver fibrosis which in turn becomes pathogenic to the infected host (Kamdem et al., 2018; Andrade, 2009; Hams et al., 2013). In the current study, we observed an increase in fibrosis in the resistant Batf2$^{-/-}$ mice which was also associated with reduced granulomatous pathology highlighting the potential need for increased fibrosis during chronic Schistosomiasis. It is not fully clear how this increase in fibrosis would affect the long-term tissue function. So far, the study further highlights the significance of finding an appropriate balance in the levels of fibrosis which would enable adequate wound healing ability while also being sufficient to keep the tissue integrity to prevent long term loss of tissue function. Importantly, as of yet, mice prone to develop such an elevated fibrosis in the midst of reduced granulomatous response tended to survive longer arguing in favour of the protective advantage of the pathophysiological display (elevated fibrosis + low granulomatous inflammation) during chronic schistosomiasis.

Furthermore, there was also a reduction in inflammatory immune cell mediators such as inflammatory myeloid populations (neutrophils, eosinophils, and dendritic cells) as well as reduced type 2 adaptive T lymphocytes in the absence of Batf2. Additionally, the regulatory IL-10 also contributed to the observed immunopathology given that it was increased in the

knockout mice. Despite this immune profile, it was not surprising to see an increase in inflammatory IL-17 cytokine response in the liver of Batf2 deficient mice during the infection. This is because the transcription factor was previously reported to be an important inhibitor of immunopathological Th17 responses during helminth infection, *Trypanosoma cruzi* (Kitada, 2017). However, this increase in inflammatory hepatic IL-17 and other inflammatory cytokines such as IFN-γ, IL-4, and IL-5 which were increased in the tissue, did not have major observable influence on the tissue immunopathology. Contrary to the liver, the IL-17 response was significantly reduced in the small intestine which contributed to reduced immunopathology. The differences in IL-17 responses between the liver and the small intestine suggest differential tissue specific role for Batf2.

Furthermore, the lung immunopathology in the resistant Batf2 deficient mice was mainly attributed to significantly reduced recruitment of neutrophil populations given that the type 2 immune response was not significantly affected, or rather was moderately increased suggesting a different regulatory role in the tissue compared to other target tissues such as the liver, the small intestine, and the spleen that were mainly influenced by reduced type 2 immune responses in the absence of Batf2. The findings from the current study revealed tissue-specific cytokine patterns as well as immune infiltrate in the lung vs liver, vs small intestine. This demonstrate differences in regulation of the host-pathogen interaction for each tissue type which can be attributed to differences in tissue cellular and molecular mechanisms, as well as tissue specific microbiota composition which are all capable of modulating host immune responses (Pestka et al., 2004; Wu et al., 2012; Turnbaugh et al., 2006). Based on the findings from the current study and by Guler et al. 2019, there appears to be a differential need for Batf2 in the liver, lung and small intestine depending on the disease context. In the previous study, it was demonstrated that Batf2 did not have any observable influence in the lung and liver, while it was shown to be crucial in regulating against exacerbated intestinal inflammation during acute Schistosomiasis (Guler et al., 2019; Mpotje, 2017). This was also shown in a study by Kayama et al., (2019) where they demonstrated Batf2 to be crucial in preventing T cell mediated inflammation in the intestine through regulation of the IL-23/IL-17 pathway (Kayama et al., 2019).

In the current study, there is a significant reduction in intestinal IL-17 mediated inflammation in the protected mice of Batf2 model (Batf2$^{-/-}$, WT-CH, and Batf2$^{-/-}$ CH) during chronic Schistosomiasis. This indicates that the control of inflammation in the intestine is mediated mainly through the suppression of IL-17 mediated signaling that is independent of Batf2.

Therefore, Batf2$^{-/-}$-induce microbiota helps keep in check IL-17 mediated responses in the intestine during infection. In the case of other organs such as the liver, regulation of inflammatory immune responses by the absence of Batf2 during chronic Schistosomiasis, appears to be mediated through type 1 CD8+ T cell signaling and reduced recruitment of myeloid populations which led to reduced Th2 inflammatory immune response that was independent of IL-17 signaling (Figure 21 and 22). This can be attributed to the different composition of microbiota that the liver harbors which are not sufficient to induce exacerbated IL-17 responses.

Overall, the observed reduction in inflammatory immunopathology of the Batf2 deficient mice suggested a different role for the Batf2 that is detrimental to the mice during chronic Schistosomiasis unlike its previously reported protective role during acute Schistosomiasis (Guler *et al*, 2017). The findings from this study regarding the hepatic immunopathology observed in the Batf2 deficient mice, are like those in a previous study by Layland *et al*. (2005) where they also showed that the absence of MyD88 in mice during Schistosomiasis results in reduced hepatic granulomatous inflammation that is associated with increased fibrosis in the tissue. However, the immunopathology was reported to be associated with a Th2 dominated phenotype as well as reduced percentages of eosinophils (Layland *et al*., 2005). Among the Th2 dominant phenotype were the T regulatory subsets (IL-10 producing T cells), which they reported to be responsible for the lack of antigen specific Th1 responses such as the IFN-γ producing T cells (Layland *et al*., 2005). Suppression of the Th1 responses were further reported to contribute to reduced liver immunopathology (Rezende et al., 1997; Layland *et al*., 2005).

Although it may be true that the lack of Th1 responses do contribute to reduced immunopathology, the current study however, point towards a more complicated role for the type 1 responses during chronic Schistosomiasis. This is because the absence of Batf2 did not affect the Th1 (IFN-γ producing CD4+ T cells) response, but rather resulted in increased type 1 responses such as IFN-γ producing CD8+ T cells as well as overall tissue-specific cytokine, IFN-γ. Given that other reported regulatory mediators such as CD4+ foxp3+ T cells and the CD19 B cells (Hogan, 2002; Jankovic, 1998) were not affected or rather reduced in the absence of Batf2, it was therefore suggested that the reduced immunopathology in the absence of Batf2 was also driven by the increase in type 1 responses especially those driven by the CD8+ T cells in the liver. This hypothesis is further supported by Pedras-Vasconcelos *et al*., (1996) and Pancreâ et al., (1999) where they demonstrated that the type 1 CD8+ T cells were contributing

to regulated liver granulomatous immunopathology during *S. mansoni* infection. Drawing from these observations, it was hypothesised that the role of type 1 responses on tissue immunopathology was either inflammatory or anti-inflammatory, and this was dependent on specific T cell subset. As shown in the study by Hernandez et al., (1998), the inflammatory Th1 response was driven by the CD4+ T lymphocytes. Even though Hoffmann et al., (2000) and Layland *et al*., (2005) only demonstrated the effect to be induced by total T lymphocytes. It was not well understood how the CD8+ T lymphocytes were contributing to the immunopathology in these studies. On the other hand, the type 1 responses mediated by IFN-γ+ CD8+ T lymphocytes have also been reported to drive regulation of liver immunopathology (Pedras-Vasconcelos *et al*., 1996; Pancreâ et al., 1999). Given that the role of the CD8+ T cells is still poorly understood in the context of *S. mansoni* infection, the current study, therefore suggests a crucial role of the CD8+ T cells in regulating the liver granulomatous immunopathology in the absence of Batf2 during chronic *S. mansoni* infection.

To confirm the suggested regulatory role of the CD8+ T cells, soluble anti-CD8 antibodies were used to neutralize the CD8+ expressing cells in Batf2 deficient mice during chronic *S. mansoni* infection. Interestingly, neutralization of the CD8+ expressing cells in the absence of Batf2, led to exacerbated hepatic granulomatous inflammation as well as premature mortality during chronic Schistosomiasis. This was consistent with what was reported in a study by Chensue et al., (1993). Since both, the T cell and dendritic cell populations can express the CD8 marker, it therefore, stands to reason that treatment with anti-CD8 antibody results in neutralization of both the CD8 expressing T lymphocytes as well as the CD8 expressing dendritic cells making it difficult to assess whether the CD8 T lymphocytes were responsible for the observed immunopathology. However, the CD8+ dendritic cells, which have a direct link with Batf2 during infections (Tussiwand et al., 2012), have been reported to play a significant role of cross priming with the CD8+ T cells through MHCI molecule, therefore highlighting a direct link between the cells (Fu and Jiang, 2018; Schnorrer et al, 2006). Altogether, the data demonstrates a poorly understood role of the CD8+ T cells, potentially through the CD8+ dendritic cells, in regulating chronic Schistosomiasis-induced immunopathology. Since the type 1 CD8+ T cells were more prominent in the resistant mice (Batf2 deficient mice) that were not treated with anti-CD8 antibodies during the infection, it can be suggested that these are the key immune cells driving improved protection of the Batf2 deficient mice during chronic schistosomiasis.

Furthermore, previous studies have also demonstrated that schistosome egg antigens (SEA) are able to induce a type 1 CD8+ T cell response that plays a significant immunoregulatory role leading to a dampened immunopathologic type 2 responses and ultimately reduced granulomatous inflammation (Pancré et al., 1999, Pedras-Vasconcelo et al., 1996) as evidenced also in the current study. These studies suggested a potential use of schistosomiasis-induced type 1 CD8+ T cells as potential targets for immunization against the Schistosomiasis (Pancré et al., 1999). However, it was not clear whether the CD8+ T cell response was SEA specific or was a result of other potential antigens such as microbiota that may have led to the priming of the response during the infection. This was interesting since the absence of Batf2 was already shown to alter the composition of the intestinal microbiota. Additionally, the CD8+ T cells were more prominent in the Batf2 deficient mice suggesting that the response was potentially not SEA specific, but rather Batf2 mediated. This, therefore, meant that the absence of Batf2 resulted in altered microbiota with the potential to prime for CD8+ T cell responses during the infection.

Although the study shows that the CD8+ T cells do contribute to prolonged survival of Batf2$^{-/-}$ mice; however, the prolonged survival can also be a result of CD4+ T cells which in the absence of Batf2, their inflammatory response was significantly reduced as demonstrated in Figure 16C and D. Furthermore, the reduced pathology was also a result of reduced recruitment of myeloid cells i.e. neutrophils, eosinophils, and dendritic cells (Figure 16B) which contribute to formation of granulomatous inflammation during schistosomiasis (Hams et al., 2013)

According to recent studies, it appears that Batf2 drives regulation T cell recruitment during inflammation through the activity of myeloid populations such as macrophages and dendritic cells (Kitada et al., 2017; Kayama et al., 2019). This was demonstrated by the studies where Batf2 inhibited expression of IL-23 in both macrophages and DCs which led to reduced Th17 responses during T. cruzi infection (Kitada et la., 2017) and in a colitis model (Kayama et al., 2019). In our previous work, we demonstrated the role of Batf2 to be crucial in differentially regulating inflammatory immune responses depending on the disease context (Guler et al., 2019). The study demonstrated the transcription factor to be crucial in regulating against exacerbated type 2 inflammation that was associated with reduced recruitment of inflammatory T cells during acute Schistosomiasis (Guler et al., 2019). However, in the current study, I have demonstrated an alternative role of Batf2 in driving increased type 2 inflammation that is associated with increased recruitment of myeloid and T cells during chronic Schistosomiasis. The differences in recruitment of T cells during acute and chronic Schistosomiasis can be

attributed to altered Dendritic cell (DC) populations between the two phases of infection. This is because, during acute Schistosomiasis, there was an increase in DC populations in the absence of Batf2 which was also associated with increased T cell recruitment (Guler et al., 2019), while during chronic Schistosomiasis, I observed a reduction in DC populations which was associated with reduced recruitment of T cells.

6.3. Microbiota and resistance to chronic Schistosomiasis

To address the role of the commensal microbiota on the pathogenesis of mice in the absence of Batf2 during chronic Schistosomiasis, the susceptible WT and resistant Batf2 deficient mice were co-housed together and were percutaneously infected with a low dose of 35 *S. mansoni* cercariae to induce chronic Schistosomiasis.

Following the microbial transfer through co-housing, the Wildtype Co-housed (**WT-CH**) mice became more resistant to the infection while the Batf2 deficient Cohoused (**Batf2$^{-/-}$-CH**) mice were not majorly affected by the microbiota suggesting a unidirectional transfer of the causal microbiota. The increased resistance of the **WT-CH** mice was also associated with significantly reduced tissue immunopathology of the target tissues (spleen, liver, small intestine, and the lung), as well as increased fibrosis. The **WT-CH** mice resulted in immunopathogenesis that resembled that of the resistant **Batf2** deficient mice during the chronic infection. These results, therefore, prove that the commensal microbiota from **Batf2** deficient mice were contributing to the reduced susceptibility of the mice during chronic Schistosomiasis.

Furthermore, the prolonged survival was associated with reduced tissue immunopathology which was mediated by reduced type 2 inflammatory immune response driven by both myeloid and T lymphocytes in the major target tissues which include the liver and the small intestine. It is not clear what would happen in Batf2$^{-/-}$ mice treated with antibiotic or germ-free mice. This is because antibiotic treatment is diverse in its composition and scope of activity. The use of the presently reported cocktail might result in a similar phenotype for Batf2$^{-/-}$ mice than that of antibiotic treated SPF1 C57BL/6 mice, provided the protective microbe (s) is the same in both systems. This does not rule out a possible effect from our antibiotic treatment on this Batf2$^{-/-}$ system which would uncover another protective microbiota disposition than that of SPF1 C57BL/6 mice. Whatever the case, empirical assessment of the outcome of antibiotic treatment of Batf2$^{-/-}$ mice would be informative and is warranted.

The current study has demonstrated that Batf2$^{-/-}$-induced microbiota are responsible for driving reduced survival of the mice through exacerbated inflammatory immune responses during chronic Schistosomiasis. Furthermore, the data revealed that the intestinal microbiota from **Batf2** deficient mice is responsible for the reduction in liver immunopathology, through the type 1 CD8+ T cells (IFN-γ producing CD8+ T cells). However, the exact mechanism of protection by the Batf2-induced microbiota has not been explored. The hypothesis from the observed current data and that from Kayamaya et al, (2019) is that the Batf2-induced microbiota lack factors/microbes that can recognize antigen presenting cells (APC) such as the CD8+ dendritic cells, which through MHCI molecules would activate the CD8+ T cells leading to expansion of protective type 1 CD8+ T cells during chronic Schistosomiasis (Wieczorek et al., 2017).

It is not clear what the mechanism of reduced accumulation of immune cells in the liver of Batf2$^{-/-}$ mice is, however, it can be hypothesized that it is through priming of immune cells by the intestinal microbiota that is influenced by Batf2. This is based on the observation in my thesis that removal of Batf2 resulted in altered intestinal microbiota. Moreover, I also reported a reduced accumulation of immune cells in the livers of WT that had intact Batf2, following acquisition of microbiota from Batf2$^{-/-}$ mice.

Interestingly, the microbiotas have a selective impact on the immune response during chronic Schistosomiasis having more effect on some cytokines such as IL-5, IL-10, IL-17, and IFN-γ, but no observable effect on IL-4 cytokine. This could be attributed to the fact that most of the mentioned cytokines (IL-5, IL-10, IL-17, and IFN-γ) are mainly T cell-mediated during Schistosomiasis (Yoshimoto, 2018, Hams et al., 2013; Pearce, 2002), while IL-4 is unique in that it plays a central role of priming naïve CD4+ T cells into Th2 phenotype that is required during Schistosomiasis, and the cytokine is primarily produced by eosinophils and basophils (Tang et al., 2018; Yoshimoto, 2018, Pearce, 2002). The Batf2$^{-/-}$ protective microbiotas are, therefore, hypothesized to regulate the T cell mediated responses, hence the IL-4 was not majorly affected during chronic Schistosomiasis. This is a very crucial finding given that IL-4 deficient mice were observed to have impaired granuloma formation and developed acute fatal cachexia (Brunet et al., 1997; Pearce, 2002). The findings provide an IL-4 independent regulation of granulomatous inflammation which potentially prevents impaired granuloma formation and development of acute fatal cachexia during Schistosomiasis and thus providing a potential target for the development of a host-directed therapy during the disease (Brunet et al., 1997).

The influence of commensal microbiota on Schistosomiasis-induced pathogenesis was further demonstrated using **C57BL/6** mice that were housed from two different facilities. This came about following an observation that the mice which were housed in Specific Pathogen Free 2 (SPF2) facility were, surprisingly more susceptible to chronic Schistosomiasis even with a low dose of infection. This observation was further demonstrated when the susceptibility of these mice was then compared to that of genetically similar **C57BL/6** mice that were housed in Specific Pathogen Free 1 (SPF1) facility. The **SPF1 C57BL/6** mice were more resistant to the infection in relation to the **SPF2 C57BL/6** mice. Furthermore, the susceptibility of the **SPF2 C57BL/6** mice was associated with increased tissue immunopathology in the liver, the small intestine as well as the lung, which were all driven by altered immune responses that favoured increased inflammation and hepatic eosinophilia during chronic Schistosomiasis. This, therefore, indicated that the mice coming from SPF2 facility were more susceptible to the infection in relation to the mice from SPF1 facility.

To confirm whether the commensal microbiota was responsible for compromising the resistance of the **SPF2 C57BL/6** mice during chronic Schistosomiasis, the susceptible **SPF2 C57BL/6** and resistant **SPF1 C57BL/6** mice were co-housed together. This was done to understand if the commensal microbiota were responsible for the altered immune responses that were mediated during the infection leading to the observed pathogenesis. Interestingly, the intestinal microbiota following their transfer, did induce altered immune responses in tissues (liver, small intestine, lung) affected by the infection in both the groups of mice. Although the inflammatory immune responses were reduced in the resistant and rescued **SPF1** and **SPF2-CH C57BL/6** mice respectively for both the small intestine and the lung, the liver on the other hand presented a more complex altered immune responses which included reduction in eosinophilia, type 2 CD8+ T cell, IL-4 & TNF-α tissue cytokine responses, and increased IL-13 cytokine response which all support regulation of the liver pathology. Interestingly, the regulatory cytokines (IL-10 and TGF-β) were significantly reduced in the liver of **SPF1** and **SPF2-CH C57BL/6** mice, which potentially may have contributed to increased type 1 CD8+ T cell (IFN-γ+ CD8+ T cell) response which as reported above in Batf2 model, were hypothesised to also contribute to regulation of liver granulomatous immunopathology during chronic Schistosomiasis. This further demonstrated the link that exist between the CD8+ T cell response and the intestinal microbiota in response to chronic Schistosomiasis.

The altered immune responses in the affected tissues of the resistant **SPF1** and rescued **SPF2-CH C57BL/6** mice respectively, resulted in reduced tissue immunopathology of the liver and

the lung, while the tissue immunopathology of the small intestine was significantly reduced. Despite the observed small intestinal pathology, there was a reduction in tissue inflammatory response while the tissue repairing mediators were increased in these. The resolved tissue immunopathology of the mice translated into prolonged survival of the mice during chronic Schistosomiasis. This, therefore, proved further that the intestinal microbiota from **SPF1 C57BL/6** mice drive increased protection, while the intestinal microbiota from **SPF2 C57BL/6** mice drive reduced protection during chronic Schistosomiasis. On the other hand, the transfer of intestinal microbiota from **SPF2-CH C57BL/6** mice also induced altered immune responses which resulted in increased tissue immunopathology of the liver and the small intestinal tissue in **SPF1-CH C57BL/6** mice which ultimately led to premature mortality in relation to **SPF1 C57BL/6** mice. This demonstrated that the **SPF2 C57BL/6** mice were harbouring intestinal microbiota that compromised the susceptibility of the **C57BL/6** mice during chronic Schistosomiasis.

Among the intestinal microbiota, the commensal bacteria constitute a larger number of microbiotas in the intestine compared to other microbes (Rapin and Harris, 2018; Tlaskalová-Hogenová et al., 2011; Sender et al. 2016), and for this reason most microbiome wide association studies have mainly focused on these microbes and have demonstrated their association with disease complications (Surana and Kasper, 2017; Lynch and Pedersen, 2016). It was, therefore, hypothesised that the commensal bacteria were potentially responsible for driving the observed pathogenesis in **C57BL/6** mice during chronic Schistosomiasis. To test this, the **SPF1 C57BL/6** mice were treated with a broad-spectrum antibiotic cocktail which allowed for the suppression of intestinal bacteria from a composition of protective microbiota. This was done to disrupt the transfer of protective commensal microbiota to the susceptible **SPF2 C57BL/6** mice during chronic Schistosomiasis. Interestingly, however, the transfer of intestinal microbiota from the antibiotic treated **SPF1-CH C57BL/6** mice was still enough to rescue the **SPF2-CH C57BL/6** mice during the infection. This, therefore, ruled out the influence of commensal bacteria on the pathogenesis of **C57BL/6** mice during chronic Schistosomiasis.

The antibiotic cocktail was a large spectrum acting combo selected based on previous data which have demonstrated the ability of each compound to effectively reduce broad spectrum of bacteria (Marx, et al., 2014; Bayer et al., 2019; Slate et al., 2014; Andes and Craig, 1998; Kennedy et al., 2018). Furthermore, in the experiments conducted with the antibiotic treatment (Figure 47), there was no complete abrogation of the bacteria since the antibiotic treated SPF1

C57BL/6 mice were cohoused with SPF2 C57BL/6 mice which were not antibiotic treated. Therefore, even though the antibiotic cocktail were reducing the bacteria, the mice were constantly receiving microbiota from the untreated SPF2 C57BL/6 mice. Fortunately, the antibiotic treatment was effective enough to keep the bacterial load lower as demonstrated in figure 47. But rightfully, the Antibiotic treatment did not effectively limit the protective microbe pointing at the need for more diverse depletion approaches (other antibiotic cocktails, anti-fungi, anti-viral agents et...)

Of note, the SPF2 C57BL/6 mice were not treated with antibiotic cocktail since the transfer of microbiota from SPF2 C57BL/6 mice did not change or increase the susceptibility of the protected SPF1 C57BL/6 mice. This, therefore, indicated that there is a transfer of causal microbiota (protection) from SPF1 C57BL/6 mice while there was no observable transfer of causal microbiota (susceptibility) from SPF2 C57BL/6 mice

Since it was still unclear which organisms were contributing to improved protection of the **SPF1** and **SPF2 C57BL/6** mice, the intestinal microbiota and serum samples from **SPF1** and **SPF2 C57BL/6** mice were comparatively analysed to identify the differences in commensal microbiota compositions that may be contributing to the observed protection. According to the report that was generated, organisms including the *Helicobacter sp*, *Murine norovirus* (*MNV*) and *Pasteurella pneumotropica* were found to be present in the resistant **SPF1 C57BL/6** mice and were not detected in the susceptible **SPF2 C57BL/6** mice. Interestingly, one of these identified organisms is a virus (*Murine norovirus*) which has previously been reported to form part of commensal microbiota with the potential role of replacing the commensal bacteria for their beneficial functions and restoring immune responsiveness in the host they inhabit (Kernbauer et al., 2014). Furthermore, they also compensate for the deleterious effects that are caused by antibiotic treatment, and therefore play significant compensatory role like that of commensal bacteria (Kernbauer et al., 2014). Furthermore, the *Murine norovirus* were demonstrated to drive expansion of IFN-γ+ CD8+ T cell responses among others, which is consistent with what is observed in the current study. Given the reported role of the *Murine norovirus*, it therefore, stands to reason that they were potentially contributing to increased resistance of **SPF2 C57BL/6** mice during chronic Schistosomiasis. However, more studies will be needed to explore further and identify the exact roles of these microbes (*Murine norovirus*)

during chronic Schistosomiasis. This will help in strategies employed to generate potential therapeutic inventions.

Even through the study clearly demonstrates the influence of intestinal microbiota on the pathogenesis *Schistosoma mansoni* infected mice, it is still unclear which microbes are contributing the protective phenotype. Furthermore, it is only speculated that the microbes may potentially be interacting with CD8 expressing populations to induce a protective immune response during chronic Schistosomiasis. However, the exact mechanism that the microbes use to mediate a protective immune response is still poorly understood and warrants more research to explore these mechanisms. The two mouse models used in the study suggest the protective phenotype to be driven by causal microbiota that are distinct and potentially unique to each model. To fully understand and explore which microbes constitute a protective phenotype in both models, a more inclusive approach such whole genome sequencing will be required to explore all the microbiota to differentiate between the bacteria, virus, and fungi.

It is also important to note that all microbiota transfer studies were performed using inbred C57BL/6 mice. The use of inbred mice makes our observations less translatable to the human situation when compared to the use of outbred mice. However, the use of such a limited microbiota as the ones in inbred mice enable might enable a quicker identification of the disease regulating microbes from the pool of known commensals. An outbred setting would certainly require more power and more experiment to narrow down the observation to a given / group of microbe (s). Nevertheless, the validation of our findings in outbred mice is a clear next logical step to generalize the proposed concept given their increased genetic and microbiota diversity more closely mimicking the elevated diversity in the human population (Tuttle et al., 2018) than inbred mice.

Interactome and resistance to chronic Schistosomiasis

Among the host's protective mechanisms that are induced during Schistosomiasis there exist CD8+ T cell-driven mechanism which is still poorly understood; however, it appears that different subsets of the population induce varying roles with the type 1 CD8+ T cells being demonstrated to contribute to regulated liver granulomatous immunopathology during *S. mansoni* infection through the production of IFN-γ (Pedras-Vasconcelos et al., 1996; Pancreâ et al., 1999). Interestingly, the studies have demonstrated that the SEA favours induction of the CD8+ T cell subsets than other cell types (Fallon et a., 1998; Pancreâ et al., 1999; Pedras-Vasconcelos et al., 1996). On the other hand, the role of other subsets of CD8+ T cells such

type 2 CD8+ T cells, during Schistosomiasis is poorly understood. The type 2 CD8+ T cells are responsible for the production of inflammatory type 2 cytokines such IL-4, 5, and 13 (Fallon et a., 1998). Our data demonstrate that these type 2 subsets of CD8+ T cells may be contributing to increased inflammatory immune response as we have evidenced an increase type 2 CD8+ T cells in the susceptible SPF2 C57BL/6 mice during chronic Schistosomiasis (Figure 38). These would need to be further explored and may not be SEA specific but rather a result of altered intestinal microbiota. Therefore, the CD8+ T cells are either good or potentially bad during chronic Schistosomiasis depending on the subset they polarize into upon their activation during the infection. This is similar to what is observed with the CD4+ T cell polarization during infection. When the CD4+ T cells polarize into Th2 subsets during Schistosomiasis, they drive increased granulomatous inflammatory immune responses that help neutralize the pathogenic schistosomiasis eggs, and such a response can be pathogenic to host if not controlled (Hams et al., 2013). To prevent this, the host also induces Foxp3+ CD4+ T cells which help regulate against exacerbated Th2 immune responses during Schistosomiasis (Baumgart et al., 2006). Therefore, similar to CD4+ T cells taking different phenotypes to control the infection, the CD8+ T cells also follow the same polarization diversity resulting in different subsets with varying roles during the infection.

In line with this, the foxp3+ CD8+ T cells were also explored during chronic Schistosomiasis. These cells are a unique population in that they can recognize antigens presented by cells with both MHC-I and MHC-II molecules, (Flippe et al., 2019). This gives them the advantage of being able to have suppressive effects on all cells, unlike the Foxp3-expressing CD4+ T cells which only have suppressive effects on cells expressing MHC-II molecules (Flippe et al., 2019). Therefore, the recruitment of Foxp3-expressing CD8+ T cells is vital in the current study in that they can induce their suppressive effects on all inflammatory immune populations that expresses both MHC-I and MHC-II molecules which may have potentially been activated by the intestinal microbiota. The resistant mice (Baft2$^{-/-}$, WT-CH, SPF1 C57BL/6, SPF2-CH C57BL/6 mice) all maintained increased recruitment of these cells which potentially have also contributed to their survival during chronic Schistosomiasis.

The data presented in the current study demonstrated the ability of the host genetic factor (Batf2) to influence the intestinal microbiota composition which in turn also influences the host immune responses. The changes in these components resulted in regulated immunopathology and ultimately improved survival of mice during chronic Schistosomiasis. This highlighted an important interrelationship that exist between host genetic factor (Batf2), microbiota, and the

immune system during Schistosomiasis. Considering this, it therefore, stands to reason that, the use of microbiota together with host components such as IL-4 or Batf2, as well as key immune populations that might have a direct link with the microbes (i.e., CD8 expressing cells) could provide a strong approach for the control of infections and their resultant immunopathology. The present work is a proof of concept of this existing tripartite regulation of chronic schistosomiasis progression and calls for more multilevel considerations in future investigations of the regulation of this debilitating disease.

7. References

Aagaard, K., Ma, J., Antony, K.M., Ganu, R., Petrosino, J., Versalovic, J. 2014. The placenta harbors a unique microbiome. *Science Translational Medicine*. **6**: 237ra65.

Adams, J., Follett, D., Hamilton, H., & Czuprynski, C. 1993. Effects of administration of anti-CD4 and anti-CD8 monoclonal antibodies on *Mycobacterium paratuberculosis* infection in intragastrically challenged mice. *Immunology Letters*. **35** (2): 183 – 189. doi:10.1016/0165-2478(93)90089-k.

Alexander H. Tuttle, Vivek M. Philip, Elissa J. Chesler and Jeffrey S. Mogil. 2018. Comparing phenotypic variation between inbred and outbred mice. *Nature methods*. **15**: 994 – 996.

Anderson, R. M. 1982. Population dynamics of infectious diseases: theory and applications. *Chapman and Hall. London, United Kingdom*. **1:** 368 - 380.

Andes, D., Craig, W. A. 1998. In Vivo Activities of Amoxicillin and Amoxicillin-Clavulanate against Streptococcus pneumoniae: Application to Breakpoint Determinations. *Antimicrobial Agents and Chemotherapy*. **42** (9): 2375–2379

Andrade, Z. A. 2009. Schistosomiasis and liver fibrosis. *Parasite Immunology*. 31, 656 – 663.

Andrews, A., Holloway, J. W., Holgate, S. T., Davies, D. E. 2006. IL-4 Receptor α Is an Important Modulator of IL-4 and IL-13 Receptor Binding: Implications for the Development of Therapeutic Targets. *J Immunol*. **176**: 7456 - 7461; DOI: https://doi.org/10.4049/jimmunol.176.12.7456.

Arrieta, M., Finlay, B. B., 2012. The commensal microbiota drives immune homeostasis. *Frontiers in Immunology*. **3**:1 – 6. doi: 10.3389/fimmu.2012.00033.

Babu, S., Nutman, T. B. 2016. Helminth-Tuberculosis Co-infection: An Immunologic Perspective. *Trends in Immunology: Review*. **37**: 597 – 607.

Bayer, F., Ascher, S., Pontarollo, G., Reinhardt, C. 2019. Antibiotic Treatment Protocols and Germ-Free Mouse Models in Vascular Research. *Frontiers in Immunology*. **10** (2174). doi: 10.3389/fimmu.2019.02174

Bearfield, C., Davenport, E. S., Sivapathasundaram, V., Allaker, R. P. 2002. Possible association between amniotic fluid micro-organism infection and microflora in the mouth. *British Journal of Obstetrics and Gynaecology*. **109**: 52733.

Belkaid, Y., Hand, T. W. 2014. Role of the Microbiota in Immunity and Inflammation. *Cell*. **157**: 121 – 141.

Björkholm, B., Bok, C. M., Lundin, A., Rafter, J., Hibberd, M. L., et al. 2009. Intestinal Microbiota Regulate Xenobiotic Metabolism in the Liver. *PLoS ONE*. **4** (9): e6958. doi:10.1371/journal.pone.0006958.

Blanton, L. V., Charbonneau, M. R., Salih, T., Barratt, M. J., Venkatesh, S., Ilkaveya, O., Subramanian, S., Manary, M. J., Trehan, I., Jorgensen, J. M., Fan, Y., Henrissat, B., Leyn, S. A., Rodionov, D. A., Osterman, A. L., Maleta, K. M., Newgard, C. B., Ashorn, P., Dewey, K. G., Gordon, J. I. 2016. Gut bacteria that prevent growth impairments transmitted by microbiota from malnourished children. *Science*. **351**: (6275), aad3311. DOI: 10.1126/science.aad3311.

Brindley, P. J., Sher, A. 1987. The chemotherapeutic effect of praziquantel against *Schistosoma mansoni* is dependent on host antibody response. *J Immunol*. **139:** 215 – 20.

Brunet, L. R., Finkelman, F. D., Cheever, A. W., Kopf, M. A., Pearce, E. J. 1997. IL-4 protects against TNF-alpha-mediated cachexia and death during acute schistosomiasis. *J Immunol*. **159** (2): 777-85.

Caldas, I. R., Campi-Azevedo, A. C., Oliveira, L. F. A., Silveira, A. M. S., Oliveira, R. C., Gazzinelli, G. 2008. Human *schistosomiasis mansoni*: immune responses during acute and chronic phases of the infection. *Acta Trop*. **108**: 109 –117.

Cano, L. E., Singer-Vermes, L. M., Costa, T. A., Mengel, J. O., Xidieh, C. F., Arruda, C., André, D. C., Vaz, C. A. C., Burger, E., Calich, V. L. G. 2000. Depletion of CD8+ T Cells In Vivo Impairs Host Defense of Mice Resistant and Susceptible to Pulmonary Paracoccidioidomycosis. *Infection and Immunity*. **68** (1): 352 – 359. doi: 10.1128/IAI.68.1.352-359.2000.

Cardin, S., Verbek, K., Vipon, D. T., Corf, B. M., Owen, L. J. 2015. Dysbiosis of the gut microbiota in disease. *Microbial Ecology in Health & Disease*. **26**: 26191.

Castro, G.A. 1996. Helminths: Structure, Classification, Growth, and Development. In: *Baron S, editor. Medical Microbiology. 4th edition. Galveston (TX): University of Texas Medical Branch at Galveston.* Chapter 86. Available from: https://www.ncbi.nlm.nih.gov/books/NBK8282/.

Centers for Disease Control and Prevention. 2016. Parasites. Obtained on 07/05/2020. https://www.cdc.gov/parasites/about.html#worms.

Centers for Disease Control and Prevention. 2019. Parasites – Schistosomiasis. Obtained on 27/09/2020. https://www.cdc.gov/parasites/schistosomiasis/biology.html.

Chensue, S. W., Warmington, K. S., Hershey, S. D., Terebuh, P. D., Othman, M., Kunkel, S. L. 1993. Evolving T cell responses in murine schistosomiasis. Th2 cells mediate secondary granulomatous hypersensitivity and are regulated by CD8+ T cells in vivo. *J Immunol*. **151** (3): 1391-400.

Chirac, P., and Torreele, E. 2006. Global framework on essential health R&D. *Lancet*. **367**: 1560 – 1561.

Christian, P., Khatry, S. K., West, J. P. 2004. Antenatal anthelminthic treatment, Birth weight, and infant survival in rural Nepal. *Lancet*. **364**: 981 – 983.

Cox, F. E. G. 2002. History of human parasitology. *Clinical Microbiology Review*. **15**: 595 – 612.

Crompton, D. W., Nesheim, M. C. 2002. Nutritional impact of intestinal helminthiasis during the human life cycle. *Ann. Rev. Nutr*. **22**: 35 – 59.

Czuprynski, C. J., Brown, J. F. 1990. Effects of purified anti-Lyt-2 mAb treatment on murine listeriosis: comparative roles of Lyt-2^+ and L3T4^+ cells in resistance to primary and secondary infection, delayed-type hypersensitivity and adoptive transfer of resistance. *Immunology*. **71**: 107-112.

D'Elia, R., DeSchoolmeester, M. L., Zeef, L. A., Wright, S. H., Pemberton, A. D., Else, K. J. 2009. Expulsion of Trichuris muris is associated with increased expression of angiogenin 4 in the gut and increased acidity of mucins within the goblet cell. *BMC Genomics*. **10**: 492.

Dea-Ayuela, M. A., Rama-In˜iguez, S., Bola´s-Fernandez, F. 2008. Enhanced susceptibility to Trichuris muris infection of B10Br mice treated with the probiotic Lactobacillus casei. *Int. Immunopharmacol*. **8**: 28 – 35.

Dillon, S. R., Sprecher, C., Hammond, A., Bilsborough, J., Rosenfeld-Franklin, M., Presnell, S. R., Haugen, H. S., Maurer, M., Harder, B., Johnston, J., Bort, S., Mudri, S., Kuijper, J. L., Bukowski, T., Shea, P., Dong, D. L., Dasovich, M., Grant, F. J., Lockwood, L., Levin, S. D., LeCiel, C., Waggie, K., Day, H., Topouzis, S., Kramer, J., Kuestner, R., Chen, Z., Foster, D., Parrish-Novak, J., Gross, J. A. 2004. Interleukin 31, a cytokine produced by activated T cells, induces dermatitis in mice. *Nat. Immunol*. **5**: 752–760.

Doughty, B. L. 1996. Schistosomes and Other Trematodes. In: *Baron S, editor. Medical Microbiology. 4th edition. Galveston (TX): University of Texas Medical Branch at Galveston.* Chapter 86. Available from: https://www.ncbi.nlm.nih.gov/books/NBK8037/.

Dunne, D. W., Cooke, A. 2005. A worm's eye view of the immune system: consequences for evolution of human autoimmune disease. *Nature Reviews Immunology*. **5**(5): 420 – 426. doi:10.1038/nri1601.

Fallon, P. G., Smith, P., Dunne, D. W. 1998. Type 1 and type 2 cytokine-producing mouse CD4+and CD8+T cells in acute *Schistosoma mansoni* infection. *Eur. J. Immunol*. **28**: 1408–1416.

Filbey, K. J., Camberis, M., Chandler, J., Turner, R., Kettle, A. J., Eichenberger, R. M., Giacomin, P., Le Gros, G. 2018. Intestinal helminth infection promotes IL-5- and CD4+ T cell dependent immunity in the lung against migrating parasites. *Mucosal Immunology*. **12**: 352–362. https://doi.org/10.1038/s41385-018-0102-8.

Finkelman, F. D., Shea-Donohue, T., Morris, S. C., Gildea, L., Strait, R., Madden, K. B., Schopf, L., Urban Jr, J. F. 2004. Interleukin-4- and interleukin-13-mediated host protection against intestinal nematode parasites. *Immunol. Rev*. **201**: 139–155.

Flippe, L., Bézie, S., Anegon, I., Guillonneau, C. 2019. Future prospects for CD8+ regulatory T cells in immune tolerance. *Immunology Reviews*. **292** (1): 209–224.

Fort, M. M., Cheung, J., Yen, D., Li, J., Zurawski, S. M., Lo, S., Menon, S., Clifford, T., Hunte, B., Lesley, R., Muchamuel, T., Hurst, S. D., Zurawski, G., Leach, M. W., Gorman, D. M., Rennick, D. M. 2001. IL-25 induces IL-4, IL-5, and IL-13 and Th2-associated pathologies in vivo. *Immunity*. **15**: 985–995.

Fu, C., Jiang, A. 2018. Dendritic Cells and CD8 T Cell Immunity in Tumor Microenvironment. *Frontiers in Immunology*. **9**: 3059.

Geuking, M. B., Cahenzli, J., Lawson, M. A., Ng, D. C., Slack, E., Hapfelmeier, S., McCoy, K. D., Macpherson, A. J. 2011. Intestinal bacterial colonization induces mutualistic regulatory T cell responses. *Immunity*. **34**: 794 – 806.

Goodrich, J. K., Davenport, E. R., Beaumont, M., Jackson, M. A., Knight, R., Ober, C., Spector, T. D., Bell, J. T., Clark, A. G., Ley, R. E. 2016. Genetic determinants of the gut microbiome in UK twins. *Cell Host Microbe*. **19**: 731 - 743.

Grove, D. I. 1986. Replicating Helminth Parasites of Man. *Parasitology Today*. **2:** 4.

Guler, R., Mpotje, T., Ozturk, M., Nono, J. K., Parihar, S. P., Chia, J. E., Aziz, N. A., Hlaka, L., Kumar, S., Roy, S., Penn-Nicholson, A., Hanekom, W. A., Zak, D. E., Scriba, T. J., Suzuki, H., Brombacher, F. Batf2 differentially regulates tissue immunopathology in Type 1 and Type 2 diseases. *Mucosal Immunology*. **12**: 390–402.

Hams, E., Aviello, G., Fallon, P. G. 2013. The Schistosoma granuloma: friend or foe? *Frontier in Immunology: Review article*. **4**: 1 – 7. doi: 10.3389/fimmu.2013.00089.

Hayes, K. S., Bancroft, A. J., Goldrick, M., Portsmouth, C., Roberts, I. S., Grencis, R. K. 2010. Exploitation of the intestinal microflora by the parasitic nematode Trichuris muris. Science **328**: 1391–1394.

Helmby, H., and Grencis, R. K. 2003. Essential role for TLR4 and MyD88 in the development of chronic intestinal nematode infection. *Eur. J. Immunol*. **33**: 2974–2979.

Herbert, D. R., Hölscher, C., Mohrs, M., Arendse, B., Schwegmann, A., Radwanska, M., Leeto, M., Kirsch, Hall, R., Mossmann, H., Claussen, B., Förster, I., Brombacher, F. 2004. Alternative macrophage activation is essential for survival during schistosomiasis and downmodulates T helper 1 responses and immunopathology. *Immunity*. **20**: 623 – 635.

Hernandez, H. J., Edson, C. M., Harn, D. A., Ianelli, C. J. 1998. *Schistosoma mansoni*: Genetic Restriction and Cytokine Profile of theCD41T Helper Cell Response to Dominant Epitope Peptide of Major Egg Antigen Sm-p40. *Experimental Parasitology*. **90**: 122 – 130.

Hewitson, J. P., Grainger, J. R., Maizels, R. M. 2009. Helminth immunoregulation: The role of parasite secreted proteins in modulating host immunity. *Molecular & Biochemical Parasitology*. **167**: 1–11.

Hoffmann, K.F., Cheever, A. W., Wynn, T. A. 2000. IL-10 and the Dangers of Immune Polarization: Excessive Type 1 and Type 2 Cytokine Responses Induce Distinct Forms of Lethal Immunopathology in Murine Schistosomiasis. *The Journal of Immunology*. **164**: 6406-6416.

Hogan, L. H., Wang, M., Suresh, M., Co, D. O., Weinstock, J. V., Sandor, M. 2002. CD4+ TCR Repertoire Heterogeneity *in Schistosoma mansoni*-Induced Granulomas. *The Journal of Immunology*. **169**: 6386-6393.

Holm, J. B., Sorobetea, D., Kiilerich, P., Ramayo-Caldas, Y., Estelle´, J., Ma, T., Madsen, L., Kristiansen, K., and Svensson-Frej, M. 2015. Chronic Trichuris muris Infection Decreases Diversity of the Intestinal Microbiota and Concomitantly Increases the Abundance of Lactobacilli. *PLoS One*. **10**: e0125495.

Holzscheiter, M., Layland, L. E., Loffredo-Verde, E., Mair, K., Vogelmann, R., Langer, R., Wagner, H., Prazeres da Costa, C. 2014. Lack of host gut microbiota alters immune responses and intestinal granuloma formation during schistosomiasis. *Clin Exp Immunol*. **175** (2): 246 - 57. doi: 10.1111/cei.12230.

Hooper, L. V., Littman, D. R., Macpherson, A. J. 2012. Interactions between the microbiota and the immune system. *Science*. **336**: 1268 – 1273.

Hotez P. J., Brindley, P. J., Bethony, J. M., King, C. H., Pearce, E. J., Jacobson, J. 2008. Helminth infections: The great neglected tropical diseases. *The Journal of Clinical Investigation*. **118**: 4.

Hotez, P. J. 2008. Forgotten people and forgotten diseases, the neglected tropical diseases and their impact on global health and development. *ASM Press*. **27**: 292.

Hotez, P. J., Molyneux, D. H., Fenwick, A., Ottesen, E., Sachs, S. E., Sachs, J. D. 2006. Incorporating a rapid-impact package for neglected tropical diseases with programs for HIV/AIDS, tuberculosis, and malaria. *PLoS Med*. **3**: e102.

Houlden, A., Hayes, K. S., Bancroft, A. J., Worthington, J. J., Wang, P., Grencis, R. K., Roberts, I. S. 2015. Chronic Trichuris muris infection in C57BL/6 mice causes significant changes in host microbiota and metabolome: effects reversed by pathogen clearance. *PLoS One*. **10**: e0125945.

Ismail, M., Botros, S., Metwally, A., William, S., Farghally, A., Tao, L. F., et al. 1999. Resistance to praziquantel: direct evidence from *Schistosoma mansoni* isolated from Egyptian villagers. *Am J Trop Med Hyg*. **60**: 932 – 5.

Jankovic, D., Cheever, A. W., Kullberg, M. C., Wynn, T. A., Yap, G., Caspar, P., Lewis, F. A., Clynes, R., Ravetch, J. V., Alan Sher, A. 1998. CD4+ T Cell–mediated Granulomatous Pathology in Schistosomiasis Is Downregulated by a B Cell–dependent Mechanism Requiring Fc Receptor Signalling. *The Journal of Experimental Medicine*. **187**: 619 – 629.

Jime´nez E, Ferna´ndez L, Marı´n ML, Martı´n R, Odriozola JM, Nueno-Palop C, et al. (2005). Isolation of commensal bacteria from umbilical cord blood of healthy neonates born by cesarean section. *Current Microbiology*. **51**: 2704.

Jime´nez, E, Marı´n, M. L., Martı´n, R., Odriozola, J. M., Olivares, M., Xaus, J., Ferna´ndez, L., Rodrı´guez, J. M. 2008. Is meconium from healthy newborns actually sterile? *Research in Microbiology*. **159**: 187 - 193.

Jiménez, E., Fernández, L., Marín, M. L., Martín, R., Odriozola, J. M., Nueno-Palop, C., Narbad, A., Olivares, M., Xaus, J., Rodríguez, J. M. 2005. Isolation of commensal bacteria from umbilical cord blood of healthy neonates born by cesarean section. *Current Microbiology*. **51**: 270 - 4. doi: 10.1007/s00284-005-0020-3.

Jung, S. R., Suprunenko, T., Ashhurst, T. M., King, N. J. C., Hofer, M. J. 2018. Collateral Damage: What Effect Does Anti-CD4 and Anti-CD8α Antibody–Mediated Depletion Have on Leukocyte Populations*? Journal of Immunology*. **201** (7): 2176 - 2186; doi: https://doi.org/10.4049/jimmunol.1800339.

Kamdem, S. D., Moyo-Somo, R., Brombacher, F., Nono, J. K. 2018. Host Regulators of Liver Fibrosis During Human Schistosomiasis. *Frontiers in Immunology: Mini Reviews*. **9**: 2781. doi: 10.3389/fimmu.2018.02781.

Kamdem, S. D., Moyo-Somo, R., Brombacher, F., Nono, J. K. 2018. Host Regulators of Liver Fibrosis During Human Schistosomiasis. *Frontiers in Immunology*. **8**: 1 – 9. https://doi.org/10.3389/fimmu.2018.02781.

Kaufmann, S., Dorhoi, A., Hotchkiss, R. Bartenschlager, R. 2018. Host-directed therapies for bacterial and viral infections. *Nature Reviews, Drug Discovery*. **17:** 35 – 56. https://doi.org/10.1038/nrd.2017.162.

Kay, G. L., Millard, A., Sergeant, M. J., Midzi, N., Gwisai, R., Mduluza, T., Ivens, A., Nausch, N., Mutapi, F., Pallen, M. 2015. Differences in the faecal microbiome in Schistosoma haematobium infected children vs. uninfected children. *PLoS Neglected Tropical Diseases*. **9**: e0003861.

Kayama, H., Tani, H., Kitada, S., Opasawatchai, A., Okumura R., Motooka, D., Nakammura, S., Takeda, K. 2019. BATF2 prevents T-cell-mediated intestinal inflammation through regulation of the IL-23/IL-17 pathway. *International immunology*. **31**(6): 371–383.

Kennedy, E. A., King, K. Y., Baldridge, M. T. 2018. Mouse Microbiota Models: Comparing Germ-Free Mice and Antibiotics Treatment as Tools for Modifying Gut Bacteria. *Frontiers in Immunology*. **9** (1534): doi: 10.3389/fphys.2018.01534.

Kernbauer, E., Ding, Y., Cadwell, K. 2014. Anenteric virus can replace the beneficial function of commensal bacteria. *Nature*. **516**: 94 – 98. doi:10.1038/nature13960.

Kitada, S., Kayama, H., Okuzaki, D., Koga, R., Kobayashi, M., Arima, Y., Kumanogoh, A., Murakami, M., Ikawa, M., Takeda, K. 2017. BATF2 inhibits immunopathological Th17 responses by suppressing Il23a expression during *Trypanosoma cruzi* infection. *The Journal of Experimental Medicine*. **214** (5): 1313–1331. https://doi.org/10.1084/jem.20161076.

Kostic, A. D., Xavier, R. J., Gevers, D. 2014. The microbiome in inflammatory bowel disease: current status and the future ahead. *Gastroenterology*. **146**: 1489 – 1499.

Kumar, P., Monin, L., Castillo, P., Elsegeiney, W., Horne, W., Eddens, T., Vikram, A., Good, M., Schoenborn, A. A., Bibby, K., Montelaro, R. C., Metzger, D. W., Gulati, A. S., Kolls, J. K. 2016. Intestinal interleukin-17 receptor signaling mediates reciprocal control of the gut microbiota and autoimmune inflammation. *Immunity*. **44**(3): 659–671.

Layland, L. E., Wagner, H., Prazeres da Costa, C. U. 2005. Lack of antigen-specific Th1 response alters granuloma formation and composition in *Schistosoma mansoni* infected MyD88$^{-/-}$ mice. *European. Journal of Immunology*. **35**: 3248 – 3257.

Liu, J., Pang, Z., Wang, G., Guan, X., Fang, K., Wang, Z., Wang, F. 2017. Advanced Role of Neutrophils in Common Respiratory Diseases. *Journal of Immunology Research*. **2017**: https://doi.org/10.1155/2017/6710278.

Liu, Z., Wei, P., Yang, Y., Cui, W., Cao, B., Tan, C., Yu, B., Bi, R., Xia, K., Chen, W., Wang, Y., Zhang, W., Du, X., Zhou, X. 2015. BATF2 Deficiency Promotes Progression in Human Colorectal Cancer via Activation of HGF/MET Signaling: A Potential Rationale for Combining MET Inhibitors with IFNs. *Clinical Cancer Research*. **21** (7): 1752–63. DOI: 10.1158/1078-0432.CCR-14-1564.

Loke, P., Gallagher, I., Nair, M. G., Zang, X., Brombacher, F., Mohrs, M., Allison, J. P., Allen, J. E. 2007. Alternative activation is an innate response to injury that requires CD4+ T cells to be sustained during chronic infection. *Journal of Immunology*. **179**: 3926 – 3936.

LoVerde, P. T. 2019. Schistosomiasis. *Digenetic Trematodes, Advances in Experimental Medicine and Biology*. **1154.** https://doi.org/10.1007/978-3-030-18616-6_3.

Lynch, S. V., Pedersen, O. 2016. The human intestinal microbiome in health and disease. *The New England journal of medicine*. **375**: 2369–2379.

Macpherson, A. J., Geuking, M. B., McCoy, K. D. 2012. Homeland security: IgA immunity at the frontiers of the body. *Trends in Immunology*. **33**: 160 – 167.

Maizels, R. M., and Smith, K. A. 2011. Regulatory T cells in infection. Advances in Immunology. **112**: 73 – 136.

Marchesi, J. R., Adams, D. H., Fava, F., Hermes, G. D., Hirschfield, G. M., Hold, G., Quraishi, M. N., Kinross. J., Smidt, H., Tuohy, K. M., Thomas, L. V., Zoetendal, E. G., Hart, A. 2016. The gut microbiota and host health: a new clinical frontier. *Gut*. **65**: 330 – 339.

Marx, J. O., Vudathala, D., Murphy, L., Rankin, S., Hankenson, F. C. 2014. Antibiotic Administration in the Drinking Water of Mice. *Journal of the American Association for Laboratory Animal Science*. **53** (3): 301 – 306.

Mbow, M., Larkin, B. M., Meurs, L., Wammes, L. J., de Jong, S. E., Labuda, L. A., Camara, M., Smits, H. H., Polman, K., Dieye, T. N., Mboup, S., Stadecker, M. J., Yazdanbakhsh, M. 2013. T-helper 17 cells are associated with pathology in human schistosomiasis. *Journal of Infectious Diseases***. 207**: 186 – 195.

McSorley, H. J., Maizels, R. M. 2012. Helminth Infections and Host Immune Regulation. *Clinical Microbiology Reviews*. **25**: 585 – 608.

Mesnil, C., Raulier, S., Paulissen, G., Xiao, X., Birrell, M. A., Pirottin, D., Janss, T., Starkl, P., Ramery, E., Henket, M., Schleich, F. N., Radermecker, M., Thielemans, K., Gillet, L.,

Thiry, M., Belvisi, M. G., Louis, R., Desmet, C., Thomas Marichal, T., and Bureau, F. 2016. Lung-resident eosinophils represent a distinct regulatory eosinophil subset. *Journal of Clinical Investigation*. **126** (9): 3279 – 3295.

Miguel, E.A., and Kremer, M. 2003. Worms: identifying impacts on education and health in the presence of treatment externalities. *Econometrica*. **72**: 159 – 217.

Montresor, A., Crompton, D. W. T., Bundy, D. A. P., Hall, A., Savioli, L. 1998. Guidelines for the evaluation of soil-transmitted helminthiasis and schistosomiasis at community level. http://whqlibdoc.who.int/hq/1998/WHO_CTD_SIP_98.1.pdf.

Mpotje, T. 2017. The role of Batf2 during experimental murine schistosomiasis. Medicine. Corpus ID: 91810696. Master's thesis published in Sematic Scholar: https://www.semanticscholar.org/paper/The-role-of-BATF2-during-of-experimental-murine-Mpotje/6b10d1690c48bc22b24bb5be32d9ce47a4b223fd.

Murphy, T. L., Tussiwand, R., Murphy, K. M. 2013. Specificity through cooperation: BATF–IRF interactions control immune-regulatory networks. *Nature reviews*. **13**: 499 – 509.

Nono, J. K., Fu, K., Mpotje, T., Varrone, G., Aziz, N. A., Mosala, P., Hlaka, L., Kamdem, S. D., Xu, D., Spangenberg, T., Brombacher, F. 2020. Investigating the antifibrotic effect of the antiparasitic drug Praziquantel in in vitro and in vivo preclinical models. *Scientific Reports*. **10**: 10638. https://doi.org/10.1038/s41598-020-67514-4.

Nono, J. K., Ndlovu, H., Aziz N. A., Mpotje, T., Hlaka, L., Brombacher, F. 2017. Interleukin-4 receptor alpha is still required after Th2 polarization for the maintenance and the recall of protective immunity to Nematode infection. *PLOS Neglected Tropical Diseases*. **11**(6): e0005675. https://doi.org/10.1371/journal.pntd.0005675.

Nono, J. K., Ndlovu, H., Aziz, N. A., Mpotje, T., Hlaka, L., Brombacher, F. 2017. Host regulation of liver fibroproliferative pathology during experimental schistosomiasis via interleukin-4 receptor alpha. *PLOS Neglected Tropical Diseases*. **11:** e0005861. https://doi.org/10.1371/journal.

O'Connor, A., Quizon, P. M., Albright, J. E., Lin, F. T., Bennett, B. J. 2014. Responsiveness of cardiometabolic-related microbiota to diet is influenced by host genetics. *Mamm Genome*. **25**: 583 – 599.

Pancreâ, V., Delacre, M., Herno, J., Auriault, C. 1999. Schistosomal egg antigen-responsive CD8 T-cell population in *Schistosoma mansoni*-infected BALB/c mice. *Immunology*. **98**: 525 - 534.

Pearce, E. J., and MacDonald, A. S. 2002. The Immunobiology od Schistosomiasis. *Nature Reviews*. **2**: 499 - 511.

Pedras-Vasconcelos, J. A., Pearce, E. J. 1996. Type 1 CD8+ T cell responses during infection with the helminth *Schistosoma mansoni*. *The Journal of Immunology*. **157**: 3046 – 3053.

Pestka, J. J., Zhou, H., Moon, Y., Chung, Y. J. 2004. Cellular and molecular mechanisms for immune modulation by deoxynivalenol and other trichothecenes: unraveling a paradox. *Toxicology Letters*. **153** (1): 61-73. DOI: 10.1016/j.toxlet.2004.04.023.

Polderman, T. J. C., Benyamin, B., de Leeuw, C. A., Sullivan, P. F., van Bochoven, A., Visscher, P. M., Posthuma, D. 2015. Meta-analysis of the heritability of human traits based on fifty years of twin studies. *Nature Genetics*. **47**:702-709.

Rapin, A., Harris, N. 2018. Helminth–Bacterial Interactions: Cause and Consequence. *Trends in Immunology*. **39**: 9. https://doi.org/10.1016/j.it.2018.06.002.

Rausch, S., Held, J., Fischer, A., Heimesaat, M. M., K€uhl, A. A., Bereswill, S., Hartmann, S. 2013. Small intestinal nematode infection of mice is associated with increased enterobacterial loads alongside the intestinal tract. *PLoS One*. **8**: e74026.

Rautava, S, Collado, M. C., Salminen, S., Isolauri, E. 2012. Probiotics modulate host microbe interaction in the placenta and fetal gut: a randomized, double-blind, placebo-controlled trial. *Neonatology*. **102**: 17884.

Reynolds, L. A., Filbey, K. J., Maizels, R. M. 2012. Immunity to the model intestinal helminth parasite Heligmosomoides polygyrus. *Semin. Immunopathol*. **34**: 829–846.

Reynolds, L. A., Finlay, B. B., Maizels, R. M. 2015. Cohabitation in the Intestine: Interactions among Helminth Parasites, Bacterial Microbiota, and Host Immunity. *The Journal of Immunology*. **195**: 4059 – 4066.

Reynolds, L. A., Harcus, Y., Smith, K. A., Webb, L. M., Hewitson, J. P., Ross, E. A., Brown, S., Uematsu, S., Akira, S., Gray, D., Gray, M., MacDonald, A. S., Cunningham, A. F.,

Maizels, R. M. 2014. MyD88 signaling inhibits protective immunity to the gastrointestinal helminth parasite *Heligmosomoides polygyrus*. *Journal of Immunology*. **193**: 2984 – 2993.

Reynolds, L. A., Smith, K. A., Filbey, K. J., Harcus, Y., Hewitson, J. P., Redpath, S. A., Valdez, Y., Yebra, M. J., Finlay, B. B., Maizels, R. M. 2014. Commensal-pathogen interactions in the intestinal tract: lactobacilli promote infection with, and are promoted by, helminth parasites. *Gut Microbes*. **5**: 522 – 532.

Rezende, S. A., Oliveira, V. R., Silva, A. M., Alves, J. B., Goes, A. M. Reis, L. F. 1997. Mice lacking the gamma interferon receptor have an impaired granulomatous reaction to *Schistosoma mansoni* infection. *Infection and Immunity*. **65**: 3457 – 3461.

Rodrı´guez, J. M., Murphy, K., Stanton, C., Ross, R. P., Kober, O. I., Juge, N., Avershina, E., Rudi, K., Narbad, A., Jenmalm, M. C., Marchesi, J. R., Collado, M. C. 2015. The composition of the gut microbiota throughout life, with an emphasis on early life. *Microbial Ecology in Health & Disease*. **26**: 26050. http://dx.doi.org/10.3402/mehd.v26.26050.

Rolot, M., Dougall, A. M., Chetty, A., Javaux, J., Chen, T., Xiao, X., Machiels, B., Selkirk, M. E., Maizels, R. M., Hokke, C., Denis, O., Brombacher, F., Vanderplasschen, A., Gillet, L., Horsenell, W. G. C., Dewals, B. G. 2018. Helminth-induced IL-4 expands bystander memory CD8+ T cells for early control of viral infection. *Nature Communication*. **9** (4516): https://doi.org/10.1038/s41467-018-06978-5.

Roy, S., Guler, R., Parihar, S. P., Schmeier, S., Kaczkowski, B., Nishimura, H., Shin, J. W., Negishi, Y., Ozturk, M., Hurdayal, R., Kubosaki, A., Kimura, Y., de Hoon, M. J. L., Hayashizaki, Y., Brombacher, F., Suzuki, H. 2020. Batf2/Irf1 Induces Inflammatory Responses in Classically Activated Macrophages, Lipopolysaccharides, and Mycobacterial Infection. *The Journal of Immunology*. **194**: 6035 - 6044.

Rutitzky, L. I., Stadecker, M. J. 2011. Exacerbated egg-induced immunopathology in murine *Schistosoma mansoni* infection is primarily mediated by IL-17 and restrained by IFN-gamma. *Eur. J. Immunol*. **41**: 2677 – 2687.

Sabah, A. A., Fletcher, C., Webbe, G., Doenhoff, M. J. 1985. *Schistosoma mansoni*: reduced efficacy of chemotherapy in infected T-cell-deprived mice. *Experimental Parasitology*. **60**: 348 – 54.

Sadler, C., Rutitzky, L. I., Stadecker, M. J., Wilson, R. A. 2003. IL-10 is crucial for the transition from acute to chronic disease state during infection of mice with *Schistosoma mansoni*. *Eur. J. Immunol*. **33**: 880 – 888.

Schnorrer, P., Behrens, G. M. N., Wilson, N. S., Pooley, J. L., Smith, C. M., El-Sukkari, D., Davey, G., Kupresanin, F., Li. M., Maraskovsky, E., belz, G. T., Carbone, F. R., Shortman, K., Heath, W. R., Villadangos, J. A. 2006. The dominant role of CD8 dendritic cells in cross-presentation is not dictated by antigen capture. *PNAS*. **103**: 10729 – 10734.

Sender, R. Fuchs, S., Milo, R. 2016. Revised estimates for the number of human and bacteria cells in the body. *PLoS Biol*. **14** (8). e1002533.

Singh, K. P., Gerard, H. C., Hudson, A. P., Reddy, T. R., Boros, D. L. 2005. Retroviral Foxp3 gene transfer ameliorates liver granuloma pathology in *Schistosoma mansoni* infected mice. *Immunology*. **114**: 410 – 417.

Slate, A. R., Bandyopadhyay, S., Francis, K. P., Papich, M. G., Karolewski, B., Hod, E. A., Prestia, K. A. 2014. Efficacy of Enrofloxacin in a Mouse Model of Sepsis. *Journal of the American Association for Laboratory Animal Science*. **52** (4): 381 – 386.

Stappenbeck, T. S., Virgin, H. W. 2016. Accounting for reciprocal host–microbiome interactions in experimental science. *Nature*. **534**: 191 – 199.

Steel, J. H., Malatos, S., Kennea, N., Edwards, A. D., Miles, L., Duggan, P., Reynolds, P. R., Feldman, R. G., Sullivan, M. H. F. 2005. Bacteria and inflammatory cells in fetal membranes do not always cause preterm labor. *Pediatric Research*. **57** (3): 404 - 11.

Stelma, F. F., Talla, I., Sow, S., Kongs, A., Niang, M., Polman, K., Deelder, A. M., Gryseels, B. 1995. Efficacy and side effects of praziquantel in an epidemic focus of *Schistosoma mansoni*. *American Journal of Tropical Medicine and Hygiene*. **53 (2)**:167 – 70.

Su, L., Su, C. W., Qi, Y., Yang, G., Zhang, M., Cherayil, B. J., Zhang, X., Shi, H. N. 2014. Coinfection with an intestinal helminth impairs host innate immunity against Salmonella enterica serovar Typhimurium and exacerbates intestinal inflammation in mice. *Infection and Immunity*. **82**: 3855 – 3866.

Su, Z. Z., Lee, S. G., Emdad, L., Lebdeva, I. V., Gupta, P., Valerie, K., Sarkar, D., and Fisher, P. B. 2008. Cloning and characterization of SARI (suppressor of AP-1, regulated by IFN).

Proceedings of the National Academy of Sciences of the United States of America. **105**: 20906 – 20911. http://dx.doi.org/10.1073/pnas .0807975106.

Surana, N. K., Kasper, D. L. 2017. Moving beyond microbiome-wide associations to causal microbe identification. *Nature*. **00**: 1 – 6. doi:10.1038/nature25019.

Tang, C., Liu, Z., Gao, Y. R., Xiong, F. 2018. *Schistosoma* Infection and *Schistosoma*-Derived Products Modulate the Immune Responses Associated with Protection against Type 2 Diabetes. *Frontiers in Immunology*. **8**(1990): https://doi.org/10.3389/fimmu.2017.01990.

Tlaskalová-Hogenová, H., Štěpánková, R., Kozáková, H., Hudcovic, T., Vannucci, L., Tučková, L., Rossmann, P., Hrnčíř, T., Kverka, M., Zákostelská, Z., Klimešová, K., Přibylová, J., Bártová, J., Sanchez, D., Fundová, P., Borovská, D., Šrůtková, D., Zídek, Z., Schwarzer, M., Drastich, P., Funda, D. P. 2011. The role of gut microbiota (commensal bacteria) and the mucosal barrier in the pathogenesis of inflammatory and autoimmune diseases and cancer: contribution of germ-free and gnotobiotic animal models of human diseases. *Cellular and Molecular Immunology*. **8**: 110 – 120.

Turnbaugh, P. J., Ley, R. E., Mahowald, M. A., Magrini, V., Mardis, E. R., Gordon, J. I. 2006. An obesity-associated gut micro-biome with increased capacity for energy harvest. *Nature*. **444**: 1027 – 1131.

Turpin, W., Espin-Garcia, O., Xu, W., Silverberg, M. S., Kevans, D., Smith, M. I., Guttman, D. S., Griffiths, A., Panaccione, R., Otley, A., Xu, L., Shestopaloff, K., Moreno-Hagelsieb, G., GEM Project Research Consortium, Paterson, A. D., Croitoru, K. 2016. Association of host genome with intestinal microbial composition in a large healthy cohort. *Nature Genetics*. **48**:1413 - 1417.

Tussiwand, R., Lee, W., Murphy T. L., Mashayekhi, M., Wumesh, K., Albring, J. C., Satpathy, A. T., Rotondo, J. A., Edelson, B. T., Kretzer, N., Wu, X., Weiss, L. A., Glasmacher, E., Li, P., Liao, W., Behnke, M., Lam, S. S. K., Aurthur, C. T., Leonard, W. J., Singh, H., Stallings, C. L., Sibley, L. D., Schreiber, R. D., Murphy, K. M. 2012. Compensatory dendritic cell development mediated by BATFIRF interactions. *Nature*. **490** (7421): 502–507. doi:10.1038/nature11531.

Tuttle, H., Philip, V. M., Chesler, E. J., Mogil, J. S. 2018. Comparing phenotypic variation between inbred and outbred mice. *Nature methods*. **15**: 994 – 996.

Velazquez, E. M., Nguyen, H., Heasley, K. T., Saechao, C. H., Gil, L. M., Rogers, A. W. L., Miller, B. M., Rolston, M. R., Lopez, C. A., Litvak, Y., Liou, M. J., Faber, F., Bronner, D. N., Tiffany, C. R., Byndloss, M. X., Byndloss, A. J., and Bäumler, A. J. 2019. Endogenous Enterobacteriaceae underlie variation in susceptibility to Salmonella infection. *Nature Microbiology*. **4**(4). 1057 - 1064. https://doi.org/10.1038/s41564-019-0407-8.

Visscher, P. M., Brown, M. A., McCarthy, M. I., Yang, J. 2012. Five years of GWAS discovery. *Am J Hum Genet*. **90**:7-24.

Voehringer, D., Reese, T.A., Huang, X., Shinkai, K., and Locksley, R.M. 2006. Type 2 immunity is controlled by IL-4/IL-13 expression in hematopoietic non-eosinophil cells of the innate immune system. *Journal of Experimental Medicine*. **203**: 1435 – 1446.

Walk, S. T., Blum, A. M., Ewing, S. A., Weinstock, J. V., Young, V. B. 2010. Alteration of the murine gut microbiota during infection with the parasitic helminth Heligmosomoides polygyrus. *Inflammatory bowel disease*. **16:** 1841 – 1849.

Walson, J. L., and John-Stewart, G. 2012. Treatment of helminth co-infection in HIV-1 infected individuals in resource-limited settings. *Cochrane Database Syst Rev*. (1): doi: 10.1002/14651858.CD006419.pub2.

Wang, J., Thingholm, L. B., Skiecevičienė, J., Rausch, P., Kummen, M., Hov, J. R., Degenhardt, F., Heinsen, F. A., Rühlemann, M. C., Szymczak, S., et al. 2016. Genome-wide association analysis identifies variation in vitamin D receptor and other host factors influencing the gut microbiota. *Nature Genetics*. **48**:1396 - 1406.

WebMD, 2019. Praziquantel Tablet. Drugs & Medications. Obtained online 13/08/2020. Website: https://www.webmd.com/drugs/2/drug-8873/praziquantel-oral/details.

Weinstein, P. P., Newton, W. L., Sawyer, T. K., Sommerville, R. I. 1969. Nematospiroides dubius: development and passage in the germfree mouse, and a comparative study of the free-living stages in germfree feces and conventional cultures. *Trans. Am. Microsc. Soc.* **88**: 95–117.

Wen, L., Ley, R. E., Volchkov, P. Y., Stranges, P. B., Avanesyan, L., Stonebraker, A. C., Hu, C., Wong, F. S., Szot, G. L., Bluestone, J. A. Gordon, J. I., Chervonsky, A. V. 2008. Innate

immunity and intestinal microbiota in the development of Type 1 diabetes. *Nature*. **455** (7216): 1109 – 1113.

Wescott, R. B. 1968. Experimental Nematospiroides dubius infection in germfree and conventional mice. *Experimental Parasitology*. **22**: 245–249.

Wieczorek, M., Abualrous, E. T., Sticht, J., Álvaro-Benito, M., Stolzenberg, S., Noé, F., and Freund, C. 2017. Major Histocompatibility Complex (MHC) Class I and MHC Class II Proteins: Conformational Plasticity in Antigen Presentation. *Frontiers in Immunology*. **8** (292): https://doi.org/10.3389/fimmu.2017.00292.

Wilson, M. S., Mentink-Kane, M. M., Pesce, J. T., Ramalingam, T. R. R., Thompson, R., Wynn, T. A. 2007. Immunopathology of schistosomiasis. *Immunology and Cell Biology: Review*. **85**: 148 – 154.

World Health Organization. 2012. Research priorities for helminth infections: technical report of the TDR disease reference group on helminth infections. *WHO Technical Report Series*. ISSN 0512-3054. no. 972: page 1.

World Health Organization. 2020. Accelerating work to overcome the global impact of neglected tropical diseases: A roadmap for implementation. Neglected Tropical Diseases. Website:https://www.who.int/neglected_diseases/NTD_RoadMap_2012_Fullversion.pdf .

World Health Organization. 2020. Soil-transmitted helminth infections. Website: https://www.who.int/news-room/fact-sheets/detail/soil-transmitted-helminth-infections.

Wright, J. E., Werkman, M., Dunn, J. C., Anderson, R. M. 2018. Current epidemiological evidence for predisposition to high or low intensity human helminth infection: a systematic review. *Parasites & Vectors*. **11:** 65.

Wu, H. J., Wu, E. 2012. The role of gut microbiota in immune homeostasis and autoimmunity. *Gut Microbes*. **3**: 4 – 14.

Wynn, T. A., Thompson, R. W., Cheever, A. W., Mentink-Kane, M. M. 2004. Immunopathogenesis of schistosomiasis. *Immunol. Rev*. **201**: 156–167.

Yazdanbakhsh, M., van den Biggelaar, A., Maizels, R. M. 2001. Th2 responses without atopy: immunoregulation in chronic helminth infections and reduced allergic disease. *Trends Immunol*. **22**: 372 – 377.

Yoshimoto. 2018. The Hunt for the Source of Primary Interleukin-4: How We Discovered That Natural Killer T Cells and Basophils Determine T Helper Type 2 Cell Differentiation In Vivo. *Frontiers in Immunology*. **9**(716): doi: 10.3389/fimmu.2018.00716.

Zaiss, M. M., Rapin, A., Lebon, L., Dubey, L. K., Mosconi, I., Sarter, K., Piersigilli, A., Menin, L., Walker, A. W., Rougemont, J., Paerewijck, O., Geldhof, P., McCoy, K. D., Macpherson, A. J., Croese, J., Giacomin, P. R., Loukas, A., Junt, T., Marsland, B. J., Harris, N. L. 2015. The Intestinal Microbiota Contributes to the Ability of Helminths to Modulate Allergic Inflammation. *Immunity*. **43**: 998 – 1010.